Bundesamt für Energie
Office fédéral de l'énergie
Ufficio federale dell'energia
Uffizi federal da l'energia

National Research Programme "Energy Conservation in Buildings"

NEUROBAT
Predictive Neuro-fuzzy Building Control System

Mario El-Khoury, Jens Krauss, CSEM Neuchâtel
Manuel Bauer, Nicolas Morel, LESO-PB / EPF Lausanne

supported by the
Swiss Federal Office of Energy

May 1998

NEUROBAT FINAL REPORT

Title	NEUROBAT	
by	Jens Krauss	CSEM
	Manuel Bauer	LESO-PB/EPFL
	Nicolas Morel	LESO-PB/EPFL
	Mario El-Khoury	CSEM
Project No.	51'565	
Date	15.05.1998	**Class** C

Summary

The control strategy of existing building control systems is based on a set of predefined heating curves which determine the nominal flow temperature of the heating fluid as a function of the external temperature. This open-loop control concept leads to poor energy management and requires considerable commissioning effort during installation and maintenance.

To ensure an intelligent management of the free and solar gains, a predictive neuro-fuzzy building-control-system has been developed and tested by CSEM in collaboration with LESO-PB (Laboratoire d'énergie solaire, EPFL). Like several commercial systems, the new controller is interfaced to four temperature sensors located at: the departure of the heating fluid, its return, in a reference room and outside the building. The former two measurements allow to estimate the heat transfer occurring between the fluid and the building. Thus, a heating strategy based on energy-management is implemented instead of the less efficient but widespread temperature-management one. Furthermore, the new controller is designed to take full advantage of a solar radiation sensor to anticipate solar gains and reduce consumption.

The choice of a predictive control strategy, combined with the non-linear modelling of the building and user's behaviour, and with the weather prediction, allow the NEUROBAT controller to achieve energy savings while ensuring good comfort. Moreover, the commissioning time of the new controller is considerably reduced, thanks to the use of self-learning neuro-fuzzy algorithms.

The NEUROBAT project comprised a simulation work and tests on a real site:

The experimental site corresponds to two thermally isolated offices on the south side of the LESO building. To compare the performances of the NEUROBAT controller with an advanced commercial HVAC controller, the office rooms are equipped with two independent warm water heating circuits. One of the heating circuits is driven by an advanced commercial building controller, while the second heating circuit is controlled by the NEUROBAT system. The experiments have been completed during the heating season '96/'97 and '97/'98. The controller has been developed on a LabView platform and tested under a MATLAB simulation environment.

This simulations are based on a complex linear building model, representing the test sites, chosen for the NEUROBAT project. Based on real data, collected during the test phases, for the climate, the building and the users' behaviour, the performances of the NEUROBAT controller have been simulated and optimized off-line. In order to complete comparative tests, the commercial heating control system has been modelled on a MATLAB simulation environment.

Project Title:

NEUROBAT, Phase I:
Système biomimétique de
gestion énérgétique du bâtiment

Project Duration:

26.01.1996 - 14.05.1998

SFOE Project Representative:

Mark Zimmermann
EMPA
EMPA-KWH
8600 Dübendorf / ZH
Tel.:01 / 823 41 78

Project Representative:

Mario El-Khoury
CSEM
Advanced System Engineering
2000 Neuchâtel / NE
Tel.: 032 / 720 55 96

Project Partner:

Laboratoire d'Energie Solaire
et de Physique du Bâtiment, EPF
Lausanne (LESO-PB/EPFL)

Project Team LESO-PB/EPFL:

Manuel Bauer, Nicola Morel et
Laurent Deschamps
LESO-PB/EPFL
1015 Lausanne / VD

Project Team CSEM:

Jens Krauss, Mario El-Khoury et
Jun Zhao
CSEM/EIC
2000 Neuchâtel / NE

Steering Committee Members:

Markus Brückner
SAUTER S.A
Im Surinam 55
4016 Basel / BS

Jürg Tödtli
LANDIS & STAEFA
Gubelstrasse 22
6301 Zug / ZG

Walter Pfeiffer
HTS - High Technology Systems
Im Langhag 11
8307 Effretikon / ZH

Charles Olivier
SYNETRUM AG
Hallwylstrasse 12
3280 Murten / BE

J.-C. Hadorn
Chef de Programme 'Chaleur Solaire'
Chemin des Fleurettes 5
1007 Lausanne / VD

Charly Cornu
Délégué à l'Energie l'Etat de Vaud
Rue du Valentin 10
1014 Lausanne / VD

Gabriel Guignard
SBS - Service Immobilier
Place St-Francois 16
1002 Lausanne / VD

Contents

1. INTRODUCTION

The control strategy of existing building control systems is essentially based on a set of predefined heating curves which determine the nominal flow temperature of the heating fluid as a function of the external temperature. This open-loop control concept leads to poor energy management and requires considerable commissioning effort during installation and maintenance. Thermostatic valves located on individual radiators allow to take into account the inside air temperature, but only partially and imperfectly. The drawbacks of such systems is not compensated by a continuous adaptation of the control parameters and a detailed description of the state of the art of HVAC systems today in use is shown in sub-chapter 2.2.

To ensure an intelligent management of the free and solar gains, a predictive neuro-fuzzy building-control-system has been developed and tested by CSEM in collaboration with LESO-PB. Like several commercial systems, the new controller is interfaced to four temperature sensors located at: the departure of the heating fluid, its return, in a reference room and outside the building. The former two measurements allow to estimate the heat transfer occurring between the fluid and the building. Thus, a heating strategy based on energy-management is implemented instead of the less efficient but widespread temperature-management one. Furthermore, the new controller is designed to take advantage of a solar sensor to anticipate solar gains and reduce consumption.

The choice of a predictive control strategy, combined with the non-linear modelling of the building and user's behaviour, and with the weather prediction, allow the NEUROBAT controller to achieve energy savings while ensuring good comfort. Moreover, the commissioning time of the new controller is considerably reduced, thanks to the use of self-learning neuro-fuzzy algorithms.

The NEUROBAT project comprised a simulation work and tests on a real site:

The experimental site corresponds to two thermally isolated offices on the south side of the LESO building. To compare the performances of the NEUROBAT controller with an advanced commercial HVAC controller, the office rooms are equipped with two independent warm water heating circuits. One of the heating circuits is driven by an advanced commercial building controller, while the second heating circuit is controlled by the NEUROBAT system. The experiments have been completed during the heating season '96/'97 and '97/'98. The controller has been developed and tested on a LabView environment, the optimal control algorithm being written using the MATLAB language.

These simulations are based on a complex nodal network building model, adjusted and validated to the test building rooms chosen for the NEUROBAT project. Based on real data, collected during the test phases, for the climate, the building and the users' behaviour, the performances of the NEUROBAT controller have been simulated and optimised off-line. In order to complete comparative tests, the commercial heating control system has been modelled on a MATLAB simulation environment.

The NEUROBAT project, phase I, has been funded by the Swiss Federal Office of Energy (SFOE). The project objectives and results have been supervised during the project duration from February 1996 to February 1998 by a steering committee, including representatives of the main Swiss HVAC suppliers. These objectives and results are summarized in the following, with chapter 2 describing the NEUROBAT project background, chapter 3 detailing the NEUROBAT controller concept, chapter 4 and chapter 5 summarizing the simulation results and the experimental test results respectively. Chapter 6 focus on application aspects such as the self-commissioning of the NEUROBAT heating controller and chapter 7 concludes with the project summary and an outlook.

2. PROJECT BACKGROUND

The following sub-chapters describe the background of the NEUROBAT project, such as the description of the problem (sub-chapter 2.1), the summary of the state of the art of HVAC controllers on the market (sub-chapter 2.2) and the objectives of the NEUROBAT project.

2.1 Problem Description

The internal climate of a building is influenced by external and internal disturbances, such as the external temperature, the solar radiation, the free/internal gains and the users. The random nature of these disturbances, especially the solar radiation and the user actions (window openings, manual blind control, room temperature setpoint etc.) makes an optimal control of the delivered heating/cooling power difficult. Therefore the thermal comfort of the user may be sub-optimal (overheating, low room temperatures at the beginning of comfort periods) and the energy consumption excessive. These type of problems can be stated especially for well isolated buildings and buildings with important passive solar gains, as can be seen in Figure 1:

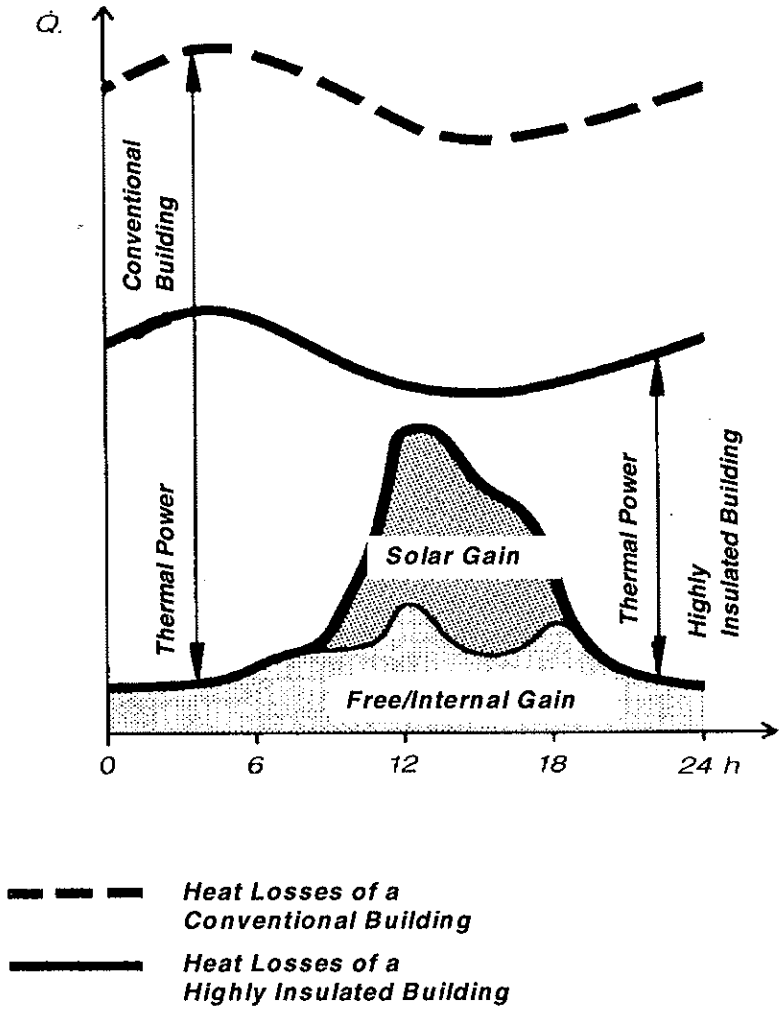

Figure 1: Heat losses and free/internal gains for a conventional and a highly insulated building.

For buildings with important passive solar gains and which are well isolated, an appropriate distribution management of the heating/cooling power becomes therefore mandatory. On the other hand, the internal building climate is strongly influenced by the user setpoint. As a result, an efficient thermal control should not only manage intelligently the distribution of the heating/cooling power, but must be easy to handle to ensure an appropriate application by the user.

In the context of the appropriate use of the heating control system, the so called 'self-commissioning' of the heating control system becomes therefore an important objective. The control concept of the heating control system should be designed in a way a minimum of user and service interactions are required. Such a self-commissioning control concept would reduce the number of the service input parameter considerably and therefore reduce the installation and the maintenance effort of the heating control system. The details concerning the 'self-commissioning'-tasks of the control system, designed and implemented during the NEUROBAT project, Phase I, is detailed in chapter 6 of this document.

2.2 HVAC Controller - State of the Art

Four types of heating control systems are distinguished and shall be introduced in the following:

Closed loop control of the internal temperature:

The closed loop control strategy enables to take into account instantaneously the variations of the solar and internal gains. The heater is switched off/on depending on how the room temperature differs from the comfort temperature setpoint. This closed loop concept on the internal temperature cannot be applied to floor heating systems due to the inertia of such systems.

Open loop control:

The open loop control strategy is based on the measurement of the external temperature. This type of heating control system is independent of the disturbances of the room sensor and can be applied to heating systems with big thermal inertia.

The operation of such systems is based on a static thermal assessment of the building, modelled by so called heating curves. Certain methods have been developed to adapt automatically the parameters of the heating curves. The parameters are difficult to adjust what results in a sub-optimal operation of the heating control system.

Two main problems derive from the fact to base the control action of heating control system on a static thermal assessment of the building. The start-up operation of such systems is not optimal and the principle of static heating curves is not adapted to manage an intermittent operation. Moreover, with regard to the free/internal gains within a building, the parameters of the heating curves should be adapted continuously.

Open loop control combined with the control of the thermostatic valves:

This control approach is applied in most of the buildings, where radiators are used. An open loop control combined with a control of the thermostatic valves, enables the compensation of bad adjusted heating curves. Nevertheless, the principle is based on a static thermal assessment with the same problems of the intermittent operations management as for the previously described open loop control strategy.

Optimal Control:

The control strategy of the optimal control is based on the dynamic behaviour of the building and enables a correct optimisation of the thermal comfort with regard to the user schedule.

In fact the control concept of the NEUROBAT controller references to this optimal control strategy and will be detailed in sub-chapter 3.1.

2.3 NEUROBAT Project - Objectives

With regard to the current situation, described in the previous sub-chapters, the following objectives have been defined for the NEUROBAT controller:

- management of the solar and internal gains on a predefined prediction horizon by means of an optimal control algorithm,
- implementation of a self-commissioning control strategy, such as a continuous adaptation of the control parameters and an efficient optimal start/stop control,
- adaptation to the user's occupation and behaviour.

The management of the solar and internal gains as well as an efficient optimal start/stop algorithm makes the application of an optimal control strategy, as described in the previous sub-chapter, mandatory. Moreover the application of fuzzy logic and neural network technologies enables an adaptation to the user's occupation and behaviour as well as the implementation of a self-commissioning control structure.

The NEUROBAT project objectives and the previous reasoning results into the following basic concept of the NEUROBAT controller, which is detailed in the following chapter.

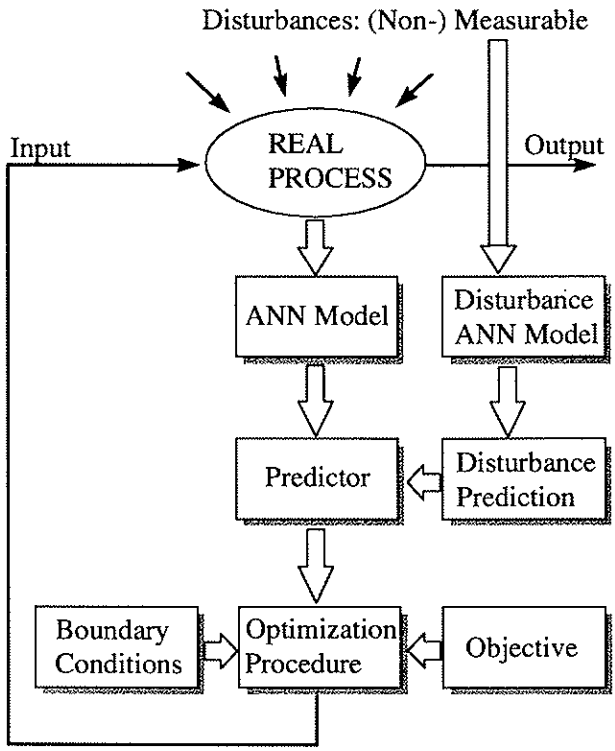

Figure 2: Basic concept of the NEUROBAT controller.

3. NEUROBAT CONTROLLER DESCRIPTION

The following sub-chapters describe the NEUROBAT control concept and details the controller modules. The modules of the solar radiation prediction, the external temperature prediction and the building model are summarized in sub-chapters 3.2, 3.3 and 3.4. These modules are assessed by a comparison with alternative linear and non-linear approaches. Sub-chapter 3.5 introduces the optimal control algorithm, sub-chapter 3.6 summarizes the user block proposal and sub-chapter 3.7 details the cascaded valve control loop.

3.1 Controller Concept

Before detailing the NEUROBAT controller concept, the global objectives for such a building control system are reminded in the following:

- to ensure an optimal comfort of the user with the help of an intelligent management of the solar and internal gains,
- to optimize the commissioning and the maintenance effort and
- to reduce the energy consumption.

The objective of the NEUROBAT controller is the reduction of the energy consumption, while allowing an optimum thermal comfort, adapted to the user's behaviour (occupation schedule, comfort setpoint, management of the free/internal gains, etc.). In addition, a building control system easy to install and to use, provides an underestimated potential to optimize the applied heating power, i.e. reducing the energy consumption.

In order to follow the previously described guidelines of an intelligent, user adaptive and self-commissioning building control system, a predictive optimal neuro-fuzzy NEUROBAT controller has been implemented. In the following the main features of the NEUROBAT control strategy are outlined and shown in Figure 3.

- The prediction of the climate data, such as the solar radiation and the external temperature, enables the anticipation of the solar and heat losses towards outside and optimizes the user comfort on a long-term base.
- Artificial neural networks (ANN) and fuzzy logic (FL) technologies are particularly well adapted to deal with non-linear systems, such as the thermal behaviour of a building, due to the changing solar gains (blind position, operated by the user), the convective heat exchange etc.. In addition, their self-learning features provide a powerful tool to design a self-commissioning heating control system, simplifying the installation and maintenance procedures. With the help of the linguistic description of fuzzy parameters, the user comfort expression can be integrated into the control loop of the heating system.
- In comparison to the widespread temperature-management of commercial building control systems, the NEUROBAT controller distinguishes a predictive energy optimization on a fixed time horizon.
- To be able to interface the NEUROBAT control algorithm with commercial building control systems an cascaded control loop has been implemented. The outer control loop optimizes the heating power, the inner control loop controls the inlet temperature of the heating fluid. The nominal value of the flow temperature of the heating fluid is calculated with the help of the optimal heating power and the measured return temperature of the heating fluid.

Figure 3 shows the concept of the NEUROBAT controller with its sensors and different controller modules, described in the following sub-chapters:

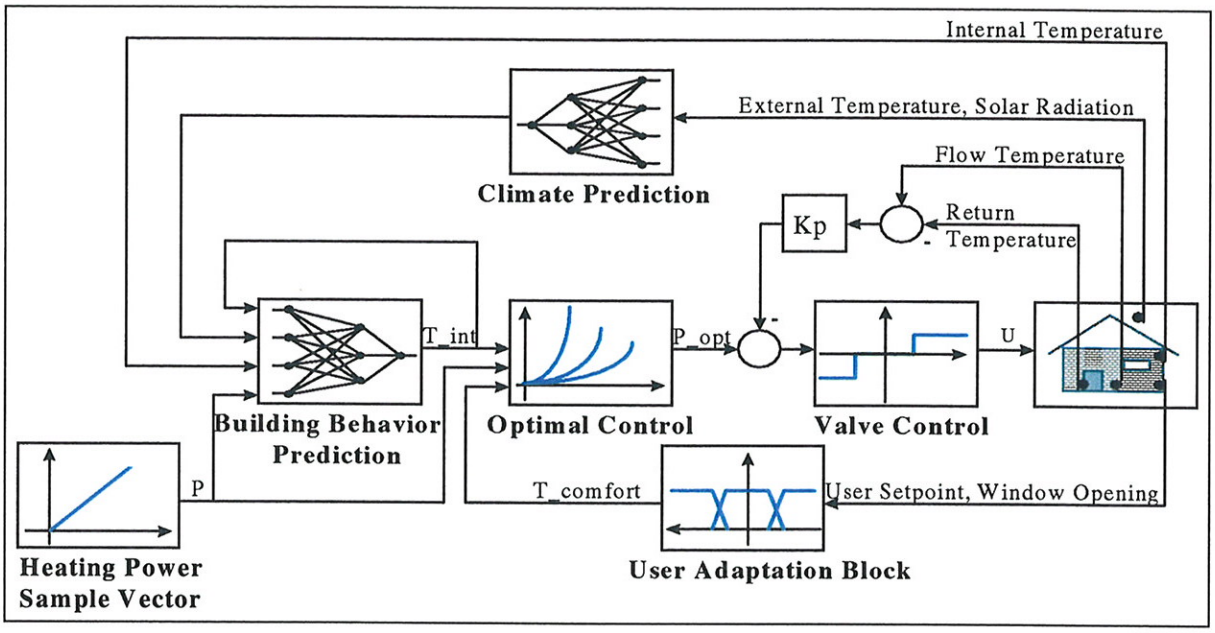

Figure 3: NEUROBAT control concept.

Using artificial neural networks (ANN) and fuzzy logic (FL), an heating controller has been elaborated in the framework of the NEUROBAT project. The command output from the controller is the heating power, which is calculated for a whole timestep (i.e. 15 minutes). The power calculated by the controller is then delivered to the building using a fast loop control of the water circuit, using a 3-way mixing valve. The structure of the whole controller is shown in Figure 3.

The optimization algorithm is detailed in sub-chapter 3.5; it is based on the minimization of a cost function over a fixed time horizon. This cost function is proportional to the energy consumption and to the thermal discomfort, felt by the users. Three main building components allow the function of the optimal control:

Weather Prediction

The climate prediction model is detailed in sub-chapters 3.2 and 3.3. It allows the prediction of the solar radiation on an horizontal plane and the outside air temperature on a 6-hour time horizon. The prediction uses an ANN model and is based on the current and past values of the solar radiation and the outside air temperature.

Building Model

The building model is detailed in the previous sub-chapter. It allows the prediction of the building's behaviour, under the perturbations of the climate data, the users' behaviour and the heating commands. The model uses an ANN and proceeds to a continuous self-adaptation to the building characteristics, at the commissioning stage or during the normal exploitation of the building: it is continuously updated to reflect the modifications of the building characteristics and users' behaviour (for instance, the building characteristics and the users' behaviour differ significantly, depending on the season).

User's Interaction Module

The users can have a direct action on the controller, by changing the optimal comfort temperature. The efficiency of such a control depends on the ability of the controller to follow that constraint during the whole occupation time schedule. We will see in chapter 4 and 5 that a predictive optimal controller is especially efficient on that point, thanks to a precise prediction of the building behaviour.

The saving potential resulting from avoiding an inside air temperature higher than what the user wishes can be estimated from the Table 1 below:

Overheating	*Relative Heating Energy Saving avoiding Overheating*
1 °C	6 %
2 °C	12 %
3 °C	19 %

Table 1: Additional heating energy consumption when temperature is too high relative to the user's wish (base case temperature = 20 °C, average outside air temperature over heating season = 4 °C, no free heat gains).

The users can also decide the time schedule for which thermal comfort will be required. The control system will anticipate the occupation. Nevertheless, during the experimental tests performed at LESO, the optimal temperature has been fixed at 20 °C, and the time schedule at the interval 8 am to 6 pm (no heating during week-ends), in order to be able to compare the NEUROBAT and the conventional controllers on an equal base.

The interaction between the user and the controller has been designed for a maximum ease of use. The user may only express a dissatisfaction by pressing on control buttons "Too Hot" and "Too Cold". The action triggers at the same time a immediate response of the system and a long term adaptation if the action repeats often enough (which means that the user feels systematically too hot or too cold). This algorithm has not been implemented in our experimental test setup, and should be evaluated using a large sample of users.

With reference to the Figure 3, the prediction of the meteorological data, such as the solar radiation and the external temperature is mandatory for the optimal control of the NEUROBAT heating controller. The prediction of the climate data enables to anticipate the external disturbances and to manage the solar gains of the building. The following sub-chapters 3.2 and 3.3 summarize the principles and the results of the climate prediction module.

3.2 Solar Radiation Prediction Model

For the prediction of the horizontal global solar radiation in [W/m^2] on a horizon of 6 hours, data of the ISM-ANETZ (Institut Suisse de Météorolgie) has been used. The data consists of a period of three months during the winter time (December, January and February). The data of the year 1982 is used to train the solar radiation prediction models and the data of the year 1983 is used to evaluate the solar radiation prediction models. The prediction models presented hereafter have been evaluated with the validation data representing as well the results based on the training data. The measurement of the horizontal global solar radiation and the external temperature are regarded as relevant inputs of the solar radiation prediction model. For a more precise and efficient prediction of the horizontal global solar radiation, additional inputs such as the humidity and the wind would be advantageous.

These measurements would require additional sensors and therefore would result into a too complex installation of the heating control system.

Several prediction models have been evaluated. The reference models are very simple and are used as a performance reference for the other prediction models. The linear models (AR and ARX), applied in many other domains for the prediction of time series, are designed, as the artificial neural network models (ANN) with adaptive features. The output of the stochastic prediction models is probability-based and transformed into deterministic values. The transformation enables a performance comparison to other prediction models. The mentioned prediction models are detailed in the following:

Reference Models (REF)

The reference model REF1 uses the current measurement of the horizontal global solar radiation as the prediction value of the six following hours.

The reference model REF2 takes the atmospheric transmittence, i.e. the ratio between the current measurement of the horizontal global solar radiation and the potential maximum value of the horizontal global solar radiation, as the prediction value for the six following hours. During the night the atmospheric transmittence is not defined and therefore the mean value of the horizontal global solar radiation of the last hours of the previous day is assigned as prediction value.

Linear Models (AR/ARX)

The auto-regressive AR and ARX prediction models are linear adaptive models, which parameters are estimated with the least-square method and which equation is listed in the following, with y as the output and u the input variable, a_i and b_{ji} the model parameters and m and o_j the model order:

$$\hat{y}(k) = \sum_{i=1}^{m} a_i \times y(k-i) + \sum_{i=1}^{n} \sum_{j=0}^{o_j} b_{ji} \times u_j(k-i)$$

The AR1 model corresponds to an auto-regressive model of order 2 and uses the horizontal global solar radiation of time step k and k-1 as input. For the prediction up to six hours ahead the estimated values of the previous time steps are used as inputs of the model. The ARX1 model uses in addition to the AR1 model the horizontal global solar radiation of the time step 24 hours ago, taking the periodic characteristic of the meteo into account. The ARX2 model is equal to the ARX1 model with the difference to take the relative horizontal global solar radiation as input (ratio between the measurement of the horizontal global solar radiation and the potential maximum value of the horizontal global solar radiation; the so called atmospheric transmittence).

Stochastic Models (STO)

The applied stochastic models are separated into 4 classes with regard to the daily irradiation fraction (the total received horizontal global solar radiation during one day divided by the potential maximal value [-], see [Sca91]). A Markov matrix (4*4) is assigned to the transition probabilities for the different types of day. The atmospheric transmittence is separated into 10 classes. Every class is assigned to an hourly transition probability for the atmospheric transmittence of the following time step. These probabilities are defined in a Markov matrix (10*10) and there exist one for each type of day. With the measurement of the type of the previous day r(j-1) and the current transmittence value $\tau(k)$ the model enables the calculation of the probability of the transmittence of the following time step.

$$P\left\langle \tau(k+1) \middle| \tau(k), r(j-1) \right\rangle$$

To be able to compare this probabilistic model to the reference, the linear and the neural prediction models, two approaches have been chosen: The model STO1 generates a future transmittence by selecting the most probable:

$$\hat{\tau}(k+1) \longrightarrow P\left\langle \hat{\tau}(k+1) \middle| \tau(k), r(j-1) \right\rangle = \max\Big|_{\tau(k+1)} \left[P\left\langle \tau(k+1) \middle| \tau(k), r(j-1) \right\rangle \right]$$

For the stochastic model STO2, the estimated transmittence is weighed with the probabilities of the corresponding transitions:

$$\hat{\tau}(k+1) = \sum_{\tau(k+1)} \tau(k+1) \times P\left\langle \tau(k+1) \middle| \tau(k), r(j-1) \right\rangle$$

By measuring τ(k) and r(j-1) the estimated value τ(k+1) is calculated. The following tables give an overview of the used model inputs and the model outputs for the reference, the linear and the stochastic models:

Model Input	*REF1*	*REF2*	*AR1*	*ARX1*	*ARX2*	*STO1*	*STO2*
G_h(k)	x		x	x			
G_h(k-1)			x	x			
G_h(k+i-24)				x			
$G_h$max(k+i)		x		x	x	x	x
τ(k)		x			x	x	x
τ(k-1)					x		
τ(k+i-24)					x		
r(j)						x	

Table 2: Used model inputs for the horizontal global solar radiation. G_h(k), G_h(k-1), G_h(k+i-24) correspond to the measurement of the global solar radiation at time step k, k-1 and k+i-24; $G_h$max(k+i) corresponds to the maximal global solar radiation at time step k+i; τ(k), τ(k-1) and τ(k+i-24) correspond to the atmospheric transmittence at different time steps and r(j) corresponds to the daily irradiation fraction of the previous day.

Model Output	*REF1*	*REF2*	*AR1*	*ARX1*	*ARX2*	*STO1*	*STO2*
G_h(k+1)	x		x	x			
τ(k+1)		x			x	x	x

Table 3: Prediction model outputs. G_h(k+1) corresponds to the predicted horizontal global solar radiation at time step k+1; τ(k+1) corresponds to the atmospheric transmittence at time step k+1.

Artificial Neural Network Models (ANN)

Artificial neural networks have been applied for the prediction of the horizontal global solar radiation. For every time step a different network is chosen (6 artificial neural networks). A simple feed-forward network structure is chosen with one hidden layer and all the neurons completely inter-connected. The Levenberg-Marquart training algorithm is applied due to its convergence faculty and as activation function of the neurons the tangent hyperbolic is chosen due to its non-linearity, continuity and derivability. The training data of the ANN has not been pre-processed, e.g. the raw data has been applied to determine the ANN parameters.

Several models with different inputs are applied for the horizontal global solar radiation and with reference to the inputs, described in the previous paragraph the following two additional inputs are used:

1. The maximal external temperature gap of the 6 respectively 24 last hours ($\Delta T_e max(k-i)$) gives an indication of the degree of cloudiness. This information is not characterized by the measurement of the horizontal global solar radiation and the maximal external temperature gap makes the degree of cloudiness available even during the night.
2. A time reference (0: night; 1: day) enables the network to manage the measurements of the atmospheric transmittence during the night.

The following table defines the inputs of the ANN models. The output of the listed models correspond to the atmospheric transmittence. The estimated physical value of the horizontal global solar radiation is calculated afterwards with the help of the potential maximal horizontal global solar radiation.

Model Input	*ANN1*	*ANN2*	*ANN3*	*ANN4*	*ANN5*
$G_h max(k+i)$	x	x	x	x	x
$\tau(k)$	x	x	x	x	x
$\tau(k-1)$	x	x	x	x	x
$\tau(k+i-24)$	x	x	x	x	x
$\Delta T_e max(k-24)$			x		
$\Delta T_e max(k-6)$				x	x
night/day(k)		x	x	x	
night/day(k+i)		x			x

Table 4: ANN model inputs for the prediction of the horizontal global solar radiation; $\tau(k)$, $\tau(k-1)$ and $\tau(k+i-24)$ correspond to the atmospheric transmittence at different time steps; $G_h max(k+i)$ corresponds to the maximal global solar radiation at time step k+i; $\Delta T_e max(k-6)$ and $\Delta T_e max(k-24)$ correspond to the maximal external temperature gap of the last 6 respectively 24 hours; night/day(k) and night/day(k+i) correspond to the time reference.

Comparison of the Prediction Models

Table 5 and Table 6 summarize the results of the prediction of the horizontal global solar radiation for the different prediction models and the different prediction horizon. The list of the mean values and standard deviations of the prediction error refers to the evaluation

during the day (during the night the prediction error is 0, assuming that the predicted value of the horizontal global solar radiation is 0).

Prediction Horizon	*1 hours* [W/m^2]	*2 hours* [W/m^2]	*3 hours* [W/m^2]	*4 hours* [W/m^2]	*5 hours* [W/m^2]	*6 hours* [W/m^2]
REF1	0.4	4.4	14.4	31.0	51.5	72.8
REF2	-5.1	-12.8	-17.4	-19.5	-19.2	-16.5
AR1	12.2	29.4	49.2	70.1	88.2	101.7
ARX1	2.6	5.1	7.6	9.8	10.2	9.4
ARX2	0.95	0.3	0.8	1.6	2.7	4.0
STO1	-8.9	-14.9	-18.9	-21.3	-22.1	-21.1
STO2	0.6	-2.1	-4.7	-7.0	-8.3	-8.1
RNA1	2.4	0.3	1.0	-0.8	2.2	0.3
RNA2	-0.6	0.1	-0.7	-4.4	-5.9	-6.7
RNA3	2.8	1.0	-1.4	-2.2	-8.7	-2.3
RNA4	2.1	-1.2	-2.3	-2.6	-1.7	-2.2
RNA5	-5.1	-5.9	-1.5	-5.8	-0.5	-3.1

Table 5: Mean values of the prediction error of the horizontal global solar radiation on time horizon of 6 hours.

Prediction Horizon	*1 hours* [W/m^2]	*2 hours* [W/m^2]	*3 hours* [W/m^2]	*4 hours* [W/m^2]	*5 hours* [W/m^2]	*6 hours* [W/m^2]
REF1	65.6	113.9	148.9	168.1	171.1	160.6
REF2	42.9	68.0	87.9	102.5	108.9	109.8
AR1	49.5	84.3	108.9	123.0	126.6	124.2
ARX1	46.2	73.0	87.2	93.0	93.5	93.3
ARX2	47.0	64.0	77.0	85.7	90.6	93.4
STO1	48.4	70.0	88.8	103.5	111.4	114.6
STO2	42.7	62.1	76.9	89.2	96.3	99.9
RNA1	43.9	57.8	72.6	78.9	79.8	85.9
RNA2	43.3	57.8	70.6	78.2	82.5	82.6
RNA3	45.2	58.7	71.3	80.3	86.6	87.4
RNA4	44.2	58.4	72.9	80.0	86.0	85.9
RNA5	45.5	60.6	70.7	77.4	81.7	82.1

Table 6: Standard deviations of the prediction error of the horizontal global solar radiation on time horizon of 6 hours.

The following remarks can be made with reference to Table 5 and Table 6:

- The reference model REF1 is the least efficient model (standard deviation on the prediction error of 161 W/m^2 for the 6 hour ahead prediction) with a big bias (mean value on the prediction error of 73 W/m^2 for the 6 hour ahead prediction).
- The performance of the AR1 model is close to the REF1 model (std=124 W/m^2 and moy=102 W/m^2 for the 6 hour ahead prediction). As for the REF1 model the AR1 model is strongly biased due to the under-estimation of the horizontal global solar radiation during the morning period and the over-estimation of the horizontal global solar radiation during the evening period.
- The ARX1 and the ARX2 model result into a good performance due to the use of the maximal potential value of the horizontal global solar radiation.
- Concerning the stochastic models, the calculation method for the atmospheric transmittence of the STO2 model proves as efficient. In comparison to the ARX models, the STO2 model performs better up to the 3 hour ahead prediction but its performance decreases on a long term horizon (3 hours and more).
- The ANN prediction models result into the most precise prediction from the 2 hour ahead prediction step on. The comparison of the ANN models show feeble differences, but it can be said, that the introduction of the night/day information increases the performance of the prediction (ANN2). On the other hand it can be stated that the introduction of the maximal external temperature gap of the previous time period (as an indicator of the degree of cloudiness) does not increase the prediction precision. Figure 4 references to the prediction quality of the ANN model (ANN2) for a period of a week:

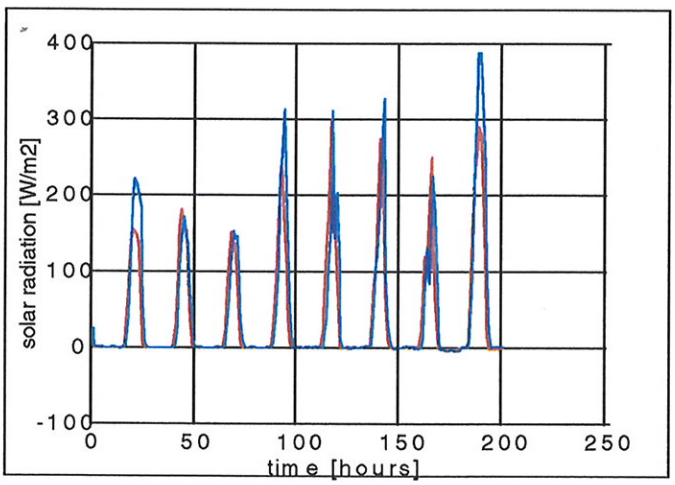

Figure 4: Example of the ANN six hour ahead prediction of the horizontal global solar radiation.

The comparison of the results of the different prediction models show that the auto-regressive, the stochastic and the neural network models perform nearly in the same way concerning the short term prediction (prediction to 3 hours ahead). With reference to the long term prediction (from 3 hours to 6 hours ahead) the auto-regressive and especially the neural network model perform well. In addition, the ARX and the ANN model require a reduced data package for the parameter determination, whereas the stochastic models refer to data of the 10 past years.

With regard to this conclusion an artificial neural network (ANN2) has been chosen for the solar radiation prediction module of the NEUROBAT controller.

3.3 External Temperature Prediction Model

The external temperature is the second important disturbance source of the internal climate of a building. As for the solar radiation prediction models, the external temperature prediction models have been evaluated with the validation data of the year 1983 of the ISM-ANETZ (Institut Suisse de Météorolgie). The behaviour of the external temperature has been modelled to make a prediction on a fixed time horizon of six hours. The following models have been evaluated:

1. A reference model (REF1) considering the current measurement of the external temperature as the prediction value for the following six hours.
2. Two auto-regressive models (ARX1 and ARX2) with the inputs shown in Table 7. The ARX models have been trained on the winter period of the year 1982 and evaluated on the winter period of the year 1983. In addition to the current temperature, the mean temperature of the last 24 hours, the horizontal global solar radiation and its maximal potential value has been taken as input.
3. Two artificial neural network models (ANN1 and ANN2) have been trained and evaluated on the same periods as the ARX and the REF1 models. As for the ANN solar radiation prediction models, the ANN training data has not been pre-processed, e.g. the meteo raw data has been taken to complete the ANN training process.

Model Input	*REF1*	*ARX1*	*ARX2*	*ANN1*	*ANN2*
$T_e(k)$	x	x	x	x	x
$T_e(k-1)$					x
$T_e(k-24)$			x	x	x
$T_h(k-1)$		x	x		
$G_h(k-2)$		x	x		
$G_h max(k+i)$			x	x	x
$G_h(k-24)$				x	

Table 7: Inputs of the external temperature prediction models.

Table 8 summarizes the results of the evaluation of the external temperature prediction models, evaluated with the validation data of the year 1983 of the ISM-ANETZ:

Prediction Horizon	*REF1*	*ARX1*	*ARX2*	*ANN1*	*ANN2*
mean 1 hour	0.00	0.00	0.00	-0.03	-0.02
std 1 hour	0.50	0.45	0.44	0.45	0.46
mean 2 hour	0.01	0.00	0.00	-0.03	-0.04
std 2 hour	0.82	0.69	0.67	0.69	0.71
mean 3 hour	0.01	0.01	0.01	-0.10	-0.05
std 3 hour	1.10	0.89	0.85	0.92	0.88
mean 4 hour	0.01	0.01	0.01	-0.12	-0.09

std 4 hour	1.34	1.06	1.02	1.07	1.02
mean 5 hour	0.01	0.01	0.01	-0.07	-0.10
std 5 hour	1.55	1.21	1.19	1.18	1.14
mean 6 hour	0.01	0.01	0.01	-0.09	-0.11
std 6 hour	1.73	1.35	1.35	1.31	1.32

Table 8: Mean values and standard deviations of the prediction error concerning the external temperature prediction models.

The following statements can be given with reference to the previous tables:

- The ARX and ANN models prove a performance increase concerning the prediction of the external temperature.
- The standard variation of the external temperature for the winter period is small (1.73 °C for the REF1 model). Therefore the information of the prediction of the external temperature as input of the building model is not mandatory. The following paragraph confirms that the mean value of the last 24h of the external temperature as input of the building model proves as sufficient.

Figure 5 shows an example of the chosen ANN external temperature prediction model of the NEUROBAT controller. The graph shows a prediction period of one week for the six hour ahead prediction step.

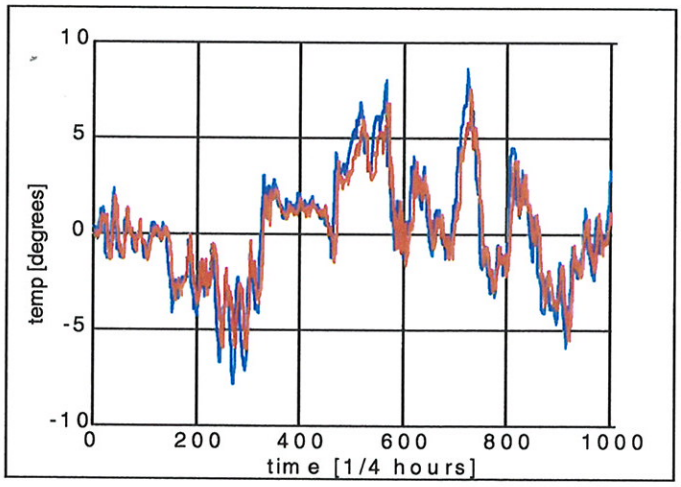

Figure 5: Example of the ANN six hour ahead prediction of the external temperature.

3.4 Building Model

3.4.1 Basic Models and Behavioural Models

Modelling the dynamic behaviour of a building has several applications, for instance:

- numerical simulation of building behaviour relative to time,
- the characterisation of building elements by identification techniques,
- the optimization of technical equipment characteristics (heating, cooling, ventilation, artificial lighting, etc.).

The modelling can either involve a thermo-physical knowledge of the building elements, which parameters are determined or identified, or be a "black box" approach where the model parameters allow the description of the building behaviour without having a physical meaning. The last application quoted above may use both approaches.

The table below shows the advantages of each of the modelling categories:

Model type	*Physical Meaning of the Parameters*	*Ability to describe Thermal Behaviour*	*Effort needed to elaborate Model*
Thermo-Physical Knowledge-Based Model (First Principles Model)	good	depending on the model accuracy, no risk of physically abnormal behaviour	important
Knowledge-Based Model with Identified Parameters	uncertain	good when inside the learning domain, risk of divergence during learning process	medium
Behavioural Model ("black-box")	impossible	good when inside the learning domain, risk of divergence during learning process	normally low, but characterisation of model structure may be difficult

Table 9: Characteristics of various building models.

The models including parameters identified by learning on building measurements allow a good description of the thermal behaviour. They also do not need much effort for the elaboration of the model. On the other hand, they are only valid when they are used inside the learning domain. Several papers ([Nor 94], [Ric 94], [Ham 94] or [Rab 94]) emphasise the fact that the model input must be uncorrelated in order to be able to differentiate the perturbation effects. For instance, a strong correlation between outside air temperature and solar radiation makes the identification of Ho (the heat loss coefficient of the building, in [W/K]) and Ae (the equivalent radiation collection area, in [m2]) difficult.

In order to decorrelate the inputs, one can:

- introduce a random heating of the building (decorrelation of heating power with the other inputs),
- introduce a night setback of the heating equipment (for the same reason) or
- protect the windows from the solar gains (decorrelation of solar radiation and outside air temperature).

These recommendations apply to a knowledge-based model with identified parameters. In the case of a behavioural model, the model is also better, especially the generalisation characteristics, if the inputs used for the learning process cover a large domain and are not correlated.

The artificial neural networks (ANN) can be used for behavioural models (black-box models). They do not need a significant effort for the model elaboration and give an accurate description of the building behaviour. Moreover, due to their inherent non-linearity, they are able to describe thermal behaviours which cannot be described using linear models.

3.4.2 Artificial Neural Network Building Model

Among various structures of ANN's, the multi-layer feed-forward neural network are well suited to the approximation of functions The system modelling being one particular case of such a use. The determination of the network structure (number of layers and neurons in each layer) does not follow any general rule ([Cun 88], [Has 95], [Gom 96). An ad-hoc method has therefore been developed in order to specify the model, which has to fulfil the following requirements:

- describe the building behaviour as accurately as possible, including non-linearities,
- give satisfactory results when starting the control system (before self-learning process),
- getting better when knowledge of parameters is refined through self-learning process,
- integrating easily within the optimal calculation algorithm and
- be feasible in the practice (limited number of sensors and calculation time).

Model Structure: Preliminary Study

A first study has been carried out, using detailed simulation runs on the experimental room described in sub-chapter 5.1. The characteristics of the room are a South orientation, a convective heating, and a large window area (the ratio window area / floor area amounts to 24 %). For the present study, the blind has been left completely open.

The goal of this preliminary study is the determination of the ANN model's inputs and parameters (number of neurons and layers needed, convergence criteria). The following model characteristics have not been studied systematically, because general theoretical results can be applied directly ([Hay 94]):

- ANN Structure: A feed-forward network structure has been chosen due to the extensive calculation of the dynamic programming algorithm.
- Learning algorithm: The Levenberg-Marquart has been used ([Hag 94]), because of its fast and good convergence characteristics.
- Neurone activation functions: The sigmoid function (hyperbolic function) has been chosen for its characteristics of non-linearity, continuity and derivability.
- Input normalization: All inputs have been normalized in the [-1,+1] interval. It allows a comparison of the synaptic weights between the input neurons and the first hidden neuron layer.

The model calculates the evolution of the inside temperature for the next prediction steps (15 minutes or 1 hour) and is based on the current thermal state and the outside and inside excitations. With the inclusion of all possible perturbations, the model structure is represented on the Figure 6.

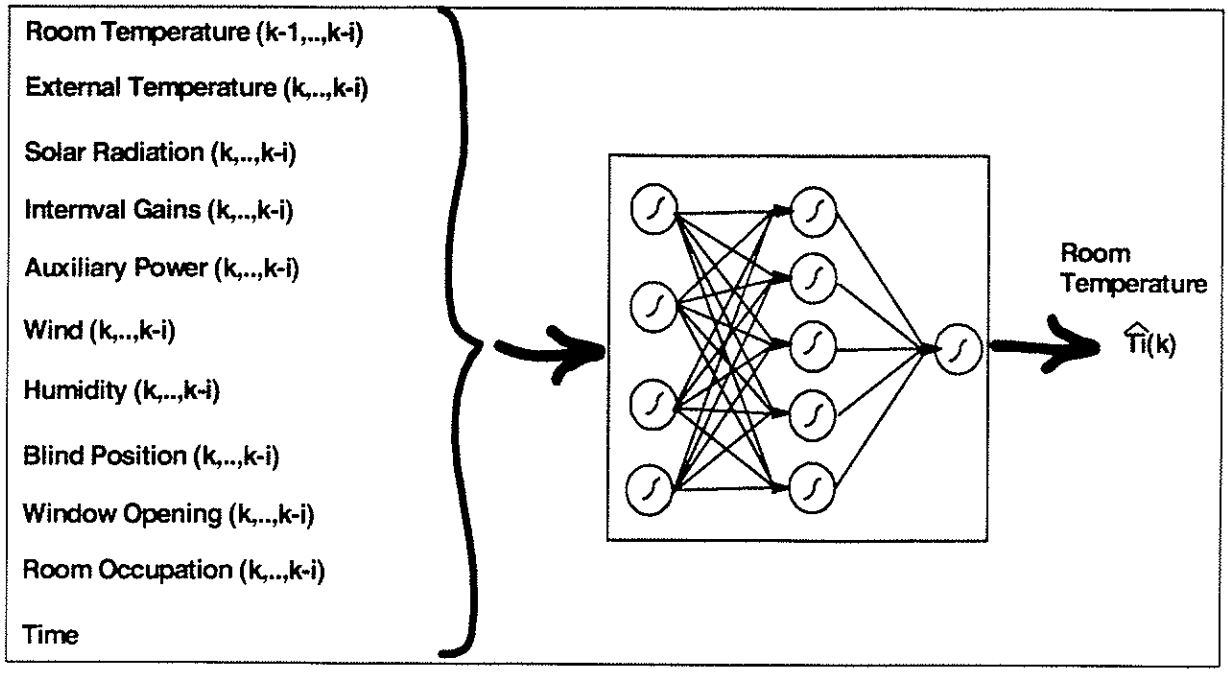

Figure 6: ANN building model.

The thermal state of the building is characterised by the inside air temperature. Another approach would be the use of temperatures of other building elements such as walls or slabs. Using a model such as the one of Figure 6 including all the possible inputs does not give a satisfactory results, for the following reasons:

- Too many sensors are needed in order to measure all the ANN inputs, including some unusual sensors for a heating controller (blind position, window opening).
- The calculation time for the optimal algorithm increases exponentially with the number of characteristic states of the system and heating command levels. Thus the necessary limitation of the input number for the inside temperature and heating power.
- The optimal calculation needs to have all inputs predicted over the time horizon (6 hours in our case), but some inputs are not easily predictable (window opening, blind position).
- The model parameters are identified through the learning algorithm using an example base. The example base must overlap the complete domain, but if there are too many possible inputs, that becomes nearly impossible.
- The initialisation of the ANN is done using a very simple building model (typically a one-node model), and the ANN inputs must correspond to the inputs of that simple building model (typically, inside and outside air temperatures, heating power, and free heat gains).

Therefore, it is necessary to minimise the number of ANN inputs in order to get a good function of the controller. Only the most significant inputs should be kept and correlated inputs may be aggregated.

Finally, a simplified ANN structure has been considered, and the ANN output has been taken as the temperature difference between the current state and the next one, which allows a reduction of the physically possible output and a better definition of the corresponding variable.

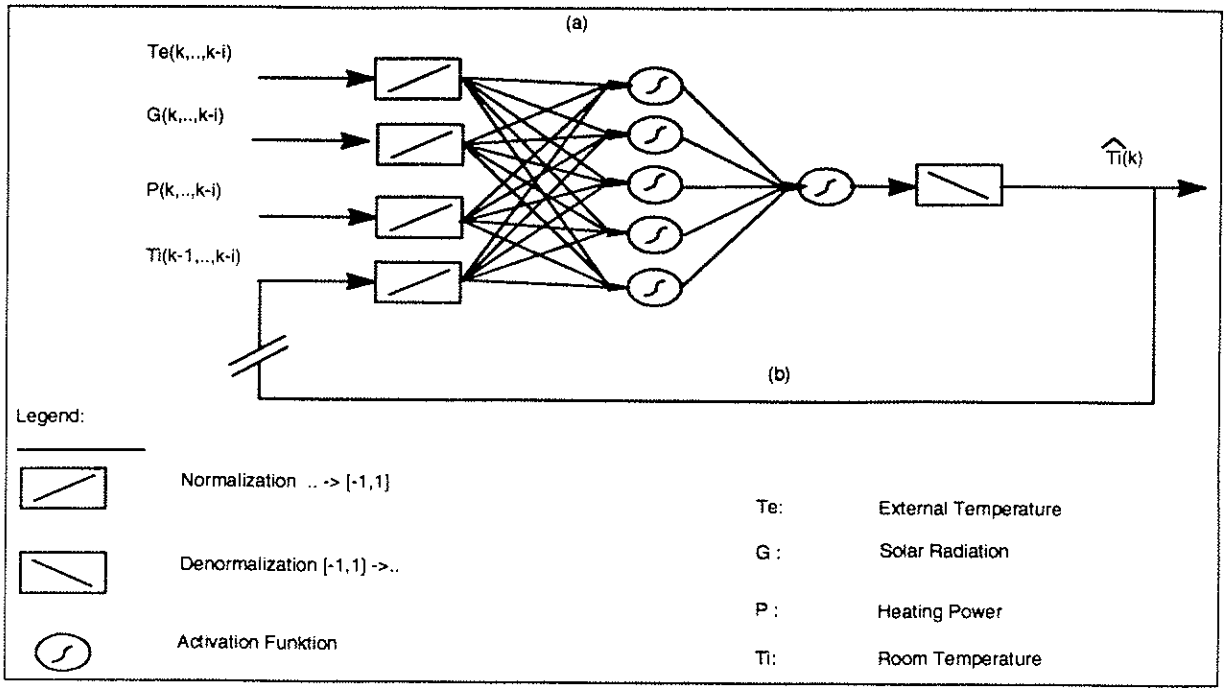

Figure 7: (a) Structure of the ANN building model. (b) For iterative use of the ANN model, the output is fed-back to the ANN input (broken line).

The table below gives a summary of the elaborated ANN model results for the prediction of the inside air temperature (prediction 15 minutes) for various network structures. As a comparison, the performance of the dummy model T(k) = T(k-1) (Reference Model) are given as well.

	Inside Air Temperature Inputs	*Solar Radiation Inputs*	*Standard Error [°C]*	*Average Error [°C]*
Reference	Ti(k-1)	-	0.86	-0.00008
Variant 1	Ti(k-1) ... Ti(k-5)	Gh(k) ... Gh(k-2)	0.07	-0.017
Variant 2	Ti(k-1) ... Ti(k-11)	Gh(k) ... Gh(k-2)	0.08	-0.007
Variant 3	Ti(k-1) ... Ti(k-5)	Gv(k) ... Gv(k-2)	0.05	0.001
Variant 4	Ti(k-1) ...Ti(k-11)	Gv(k) ... Gv(k-2)	0.03	0.003

Table 10: Prediction results for 4 variants of ANN models, compared to the reference model (T(k) = T(k-1)). Learning conditions: 8 iterations, Levenberg-Marquart Algorithm, data of January. Evaluation: data of February. Gh is the solar radiation on a horizontal plane, and Gv is the solar radiation on a vertical plane oriented like the window (i.e. South).

The following remarks can be given with reference to the previous table:

- The prediction errors for the 15 minutes prediction are very low, compared to the standard variation of the inside air temperature (0.07 for the variant 1, versus 0.86 for the reference case). The large value for the reference are essentially caused by the sudden variation of air temperature due to the convective heating.

- As a reference, the accuracy of an air temperature measurement can be evaluated as follow: reproducibility ± 0.5 °C (the air temperature and the surface temperatures are not uniform), systematic error ± 0.1 °C (depending on the calibration quality), random error ± 0.05 °C (this is the lower limit, under which any prediction model cannot get lower).
- An older "history" of inside air temperature does not make the prediction better (using T(k-1) ... T(k-11) instead of T(k) ... T(k-5)).
- Using the solar radiation in the same plane as the window (i.e. South vertical radiation) makes the prediction significantly better. It is not surprising, since the solar gains are proportional to the radiation in a vertical plane (if the blind is permanently open) and not directly to the horizontal radiation.

In order to evaluate the long term prediction quality of the ANN, the output has been fed back to the input for the next prediction time-step (see Figure 7). The graphics given below show the result for a 3-day prediction period (as a comparison, the prediction of a 1-node network is also given; for the characteristics of this model, see the equation given in chapter 6).

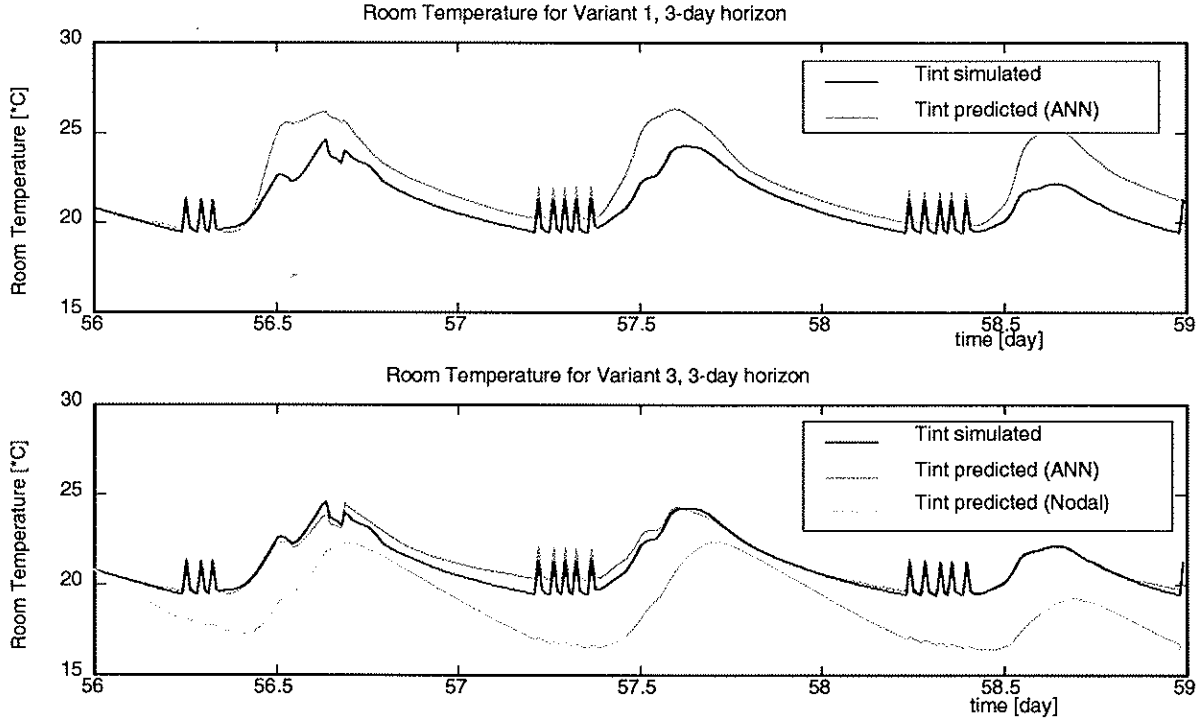

Figure 8: Temperature prediction on a 3-Day period, for variants 1 (above) and 3 (below) of Table 10. The graph below makes reference to the prediction of a one-node model as comparison.

The following remarks can be given with reference to Figure 8:

- The fast (convective heating) and medium-duration (night set-back) time constants are correctly modelled by the ANN. On the other hand, a significant discrepancy (1-2 °C after one day) on the long time constant can be observed. The input of the model for the inside air temperature is given from times k-1 to k-5, which corresponds to one hour behind (prediction timestep = 15 minutes). The model has therefore not much information on long term behaviour, and cannot give much at the output. Nevertheless,

such a limitation is not so critical, since the optimization is done on a 6 hour time horizon.

- The variant 1 overestimates the solar gains. The reason is that this model uses the horizontal solar radiation on the input. The learning process is done during January, where the ratio GVSouth / GH is lower than during the evaluation in February, thus the overestimation of solar gains in February.
- The one-node model does not allow a good estimation of the dynamic characteristics of the test room. The single time constant cannot take into account at the same time the fast, the medium-duration and the long time constants of the room.

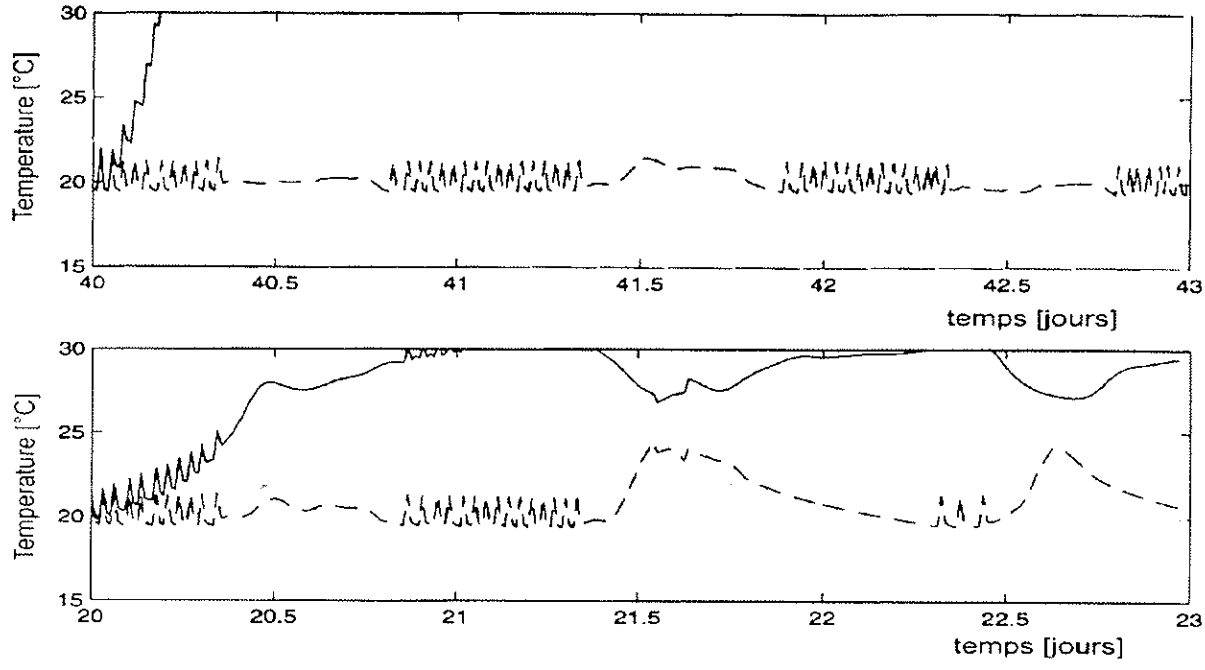

Figure 9: (a) Divergence of long term prediction caused by ANN divergence. (b) divergence of long term prediction caused by extrapolation out of learning example base, with network exhibiting no divergence.

These first tests have been done using random initialization of the ANN weights. In these conditions, the convergence is not always obtained. The Figure 9 shows the predictions for a ANN which did not converge properly. It has to be noted that even if the network has converged during the learning process, the iterative use of the ANN may also produce instability (Figure 9).

If the ANN model has learned correctly from the example base used for its training, the extrapolation to a situation situated far away from the example domain might function correctly. This is the case when using the network in an iterative way. In the example quoted in Figure 9, the training base corresponds to April, and the ANN is tested in January. Therefore, there are certainly some situations happening in January which were never trained during April.

As a first conclusion, the following results can be already summarized:

- The number of inputs and the size of the ANN should be reduced to the minimum possible (increasing the size does not make the prediction significantly better, but convergence and extrapolation problems arise).

- Considering the solar radiation in the plane of the window makes the prediction better. In order to keep the generality of using the horizontal radiation (more generally available), a transposition model can be used ([Duf 74]).
- A correct initialisation of the ANN weights is necessary to avoid divergence problems.
- The extrapolation issue must be considered carefully.

Nevertheless, further studies are needed to assess the prediction quality of the model: the data used for this first study are produced by simulation, and do not include any "noise" (for instance due to user's behaviour). Moreover, not all the requirements from the optimization method have been yet considered.

Model Structure: Study on Experimental Data

The goal of the second study is the determination of a ANN building model which can be included as good as possible in the global structure of the heating controller algorithm. This structure is explained in detail in sub-chapter 3.5, but a simplified description is given here in order to introduce the main concepts of the controller.

The controller is based on the principle of optimal calculation, where the heating system receives the command minimizing a cost function over a certain time horizon. The cost function includes two terms: one proportional to the energy used for heating over the whole time horizon and another term proportional to the discomfort felt by the user (estimated, using the Fanger's formulas). The minimisation process uses a discretization of state variables with the dynamic programming technique. The calculation time, which increases exponentially with the total number of states, is a strong limitation factor, and requires a limitation both of the variable number and of the discrete states number for each variable, in order to be able to perform the optimization calculation in a time shorter than the command interval (15 minutes). Also, the prediction time-step has been fixed to one hour in order to limit the calculation time.

Several ANN fulfilling these requirements have been compared. The prediction performances are compared with various auto-regressive linear models (ARX), and with the dummy prediction Ti(k) = Ti(k-1) (Reference Model). The data has been measured on the LESO building, room 03 (see chapter 5). The model training covers the period February14 to April 4, 1997, and the model has been tested using the period April 14 to May 1, 1997:

	P Heating Inputs	*Inside Air Temperature Inputs*	*Outside Air Temperature Inputs*	*Solar Radiation Inputs*
ANN 1	Ph(k)	Ti(k-1), Ti(k-2)	Te(k), Te(k), Te(k-1)	Gv(k), Gv(k-1)
ANN 2	Ph(k)	Ti(k-1), Ti(k-2)	Te(k)	Gv(k)
ANN 3	Ph(k)	Ti(k-1)		Gv(k)
ANN 4	Ph(k)	Ti(k-1), Ti(k-2)	Te(k)	Gv(k)
ANN 5	Ph(k)	Ti(k-1), Ti(k-2)	Te(k), Te(k-1)	Gv(k)
ANN 6	Ph(k)	Ti(k-1), Ti(k-2)	Te(k)	Gv(k), Gv(k-1)
ARX 1	Ph(k)	Ti(k-1)	Te(k)	Gv(k)
ARX 2	Ph(k), Ph(k-1)	Ti(k-1), Ti(k-2)	Te(k), Te(k-1)	Gv(k), Gv(k-1)

ARX 3	Ph(k), Ph(k-1), Ph(k-2)	Ti(k-1), Ti(k-2), Ti(k-3)	Te(k), Te(k-1), Te(k-2)	Gv(k), Gv(k-1), Gv(k-2)
Reference		Ti(k-1)		

Table 11: Inputs used for 6 ANN models, 3 ARX models, and reference model (Ti(k) = Ti(k-1)). Ph = Heating power, Ti = Room temperature, Te = Outside air temperature, Te = Average outside temperature during previous 24 hours, Gv = South vertical solar radiation. For all the variables, the value X(k) is the hourly average value on the interval [k-1, k], except for Ti(k) which is the instantaneous value at time k.

The initialisation of the ANN has been done randomly. Three trainings are done for 8, 12 or 16 iterations of the Levenberg-Marquart algorithm and only the best result over the test sample is considered. The training has been done on a one-hour prediction interval. The models have then been used iteratively in order to assess the performance on a 6-hour prediction interval (see table below).

	1 Hour	*2 Hours*	*3 Hours*	*4 Hours*	*5 Hours*	*6 Hours*	*Sum(Err)*
ANN 1	0.125	0.225	0.318	0.405	0.486	0.560	2.12
ANN 2	0.105	0.184	0.258	0.326	0.391	0.448	1.71
ANN 3	0.120	0.213	0.297	0.373	0.445	0.511	1.96
ANN 4	0.132	0.239	0.340	0.435	0.525	0.608	2.28
ANN 5	0.121	0.213	0.296	0.370	0.436	0.495	1.93
ANN 6	0.096	0.170	0.243	0.311	0.387	0.465	1.67
ARX 1	0.136	0.249	0.353	0.448	0.533	0.609	2.33
ARX 2	0.161	0.270	0.376	0.471	0.557	0.635	2.47
ARX 3	0.157	0.256	0.352	0.436	0.511	0.578	2.29
Reference	0.164	0.309	0.443	0.565	0.675	0.772	2.93

Table 12: Performance of prediction models (standard errors in [°C]).

It can be seen that the most performant models are the ANN 2 and ANN 6. These two models do not use current outside temperature. The information included in the average outside temperature during the previous 24 hours is enough to describe the building dynamics, even when the data includes several window openings (the air exchange heat flow from inside to outside depends directly from the instantaneous outside air temperature).

The ANN 1 has too many inputs and too many weights and interpolated parameters. Therefore it does not allow a good generalisation of the prediction as tested on the test example base. On the opposite, the model ANN 3 has not enough information (Ti(k-2) and Te(k) are missing) to produce a good prediction.

The ARX models are not so good. This can be explained by the rather noisy input data, which includes several non-linearities and makes a linear model not very adequate.

The Figure 10 shows the prediction at 6 hours for the best models of each category.

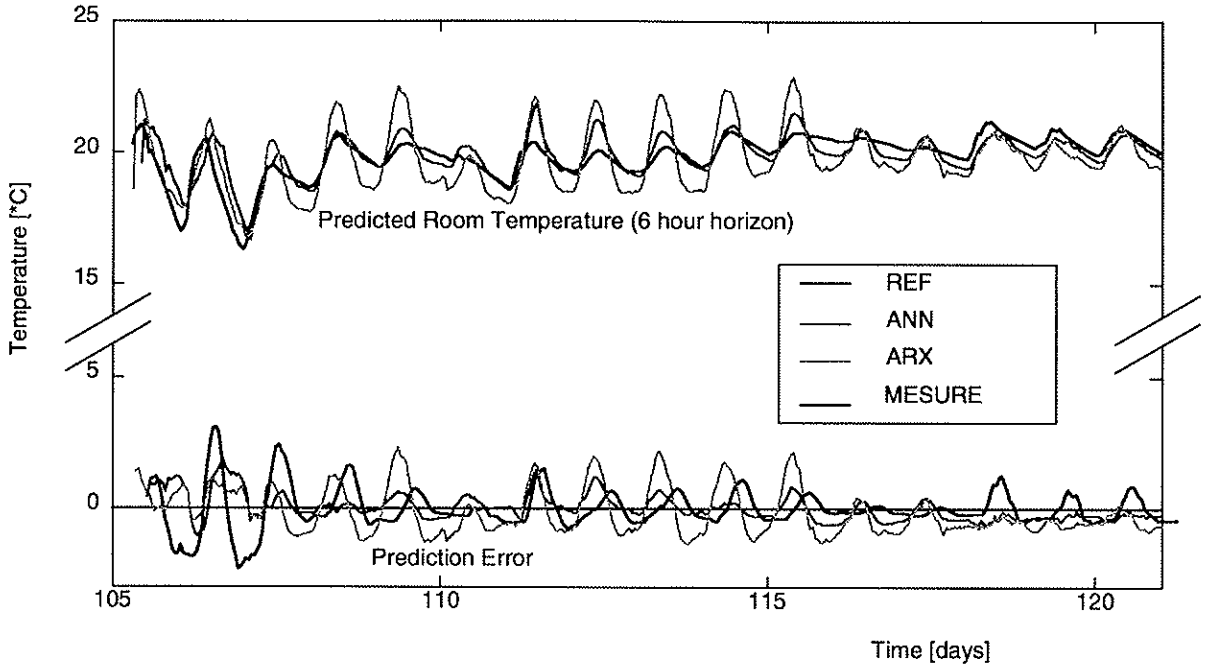

Figure 10: 6-hour prediction for ANN6, ARX3 and Reference Models. The results of the Reference Model, not shown in the figure above, correspond to a delay of six hours of the measurement.

The following remarks can be given with reference to Figure 10:

- The solar gain effect is frequently over-estimated by the ARX model (the predicted inside air temperature is higher than the real one), but not by the ANN model. This can be explained by the non-linearity of solar gains relative to the incident solar radiation, due to the user's behaviour (they pull down the blind when there is too much solar radiation) and the ability of the ANN to deal with such non-linearities.
- During the first two days, the window has been kept open, which explains the large variations of inside air temperature and the bad predictions of all the models, especially the ARX model. The inclusion of such data in the training example base emphasises the inefficiency of linear models: a large value of temperature gradient gives a high contribution to the total deviation for a linear model, while such a case can be taken into account much better by a non-linear model.

Additional conditions needed for using an adaptive building model

The ANN 2 model has been finally used for the prototype controller. Nevertheless, one has to be careful when using one of the building models in the controller. As an example, the inside air temperature and the hot water and return temperatures (which give an indication of the heating power) are represented for the day 61 of the year 1997on the Figure 11.

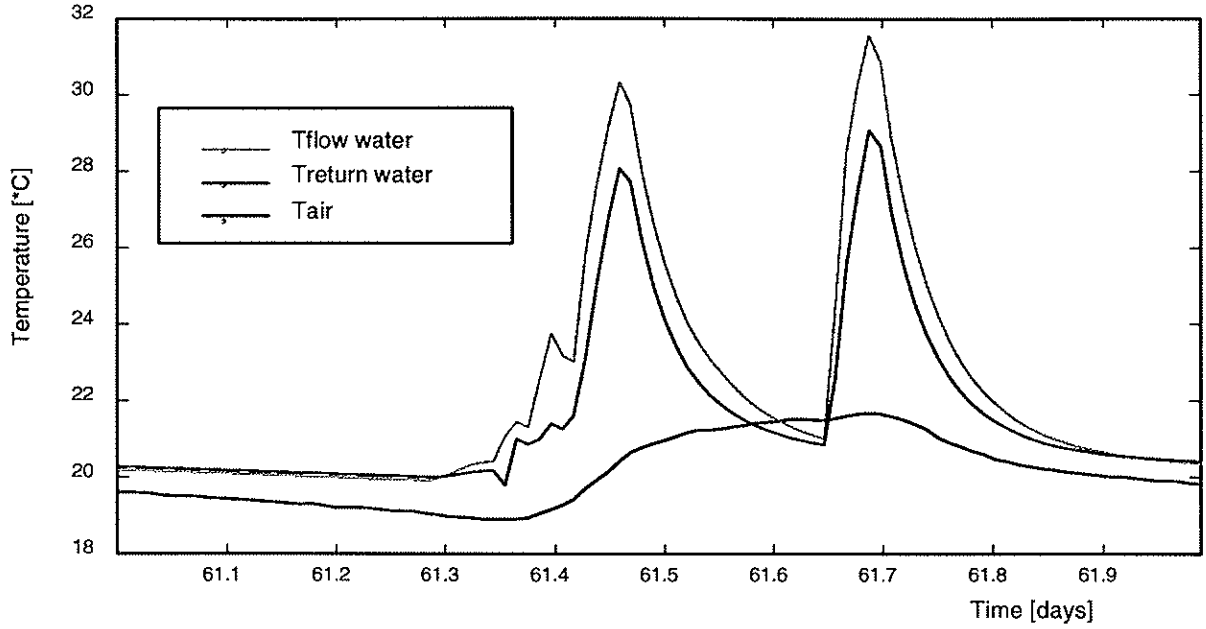

Figure 11: Example of inadequate building model included in the heating controller: a heating command is given even when the inside air temperature is around 22 °C (second heating peak).

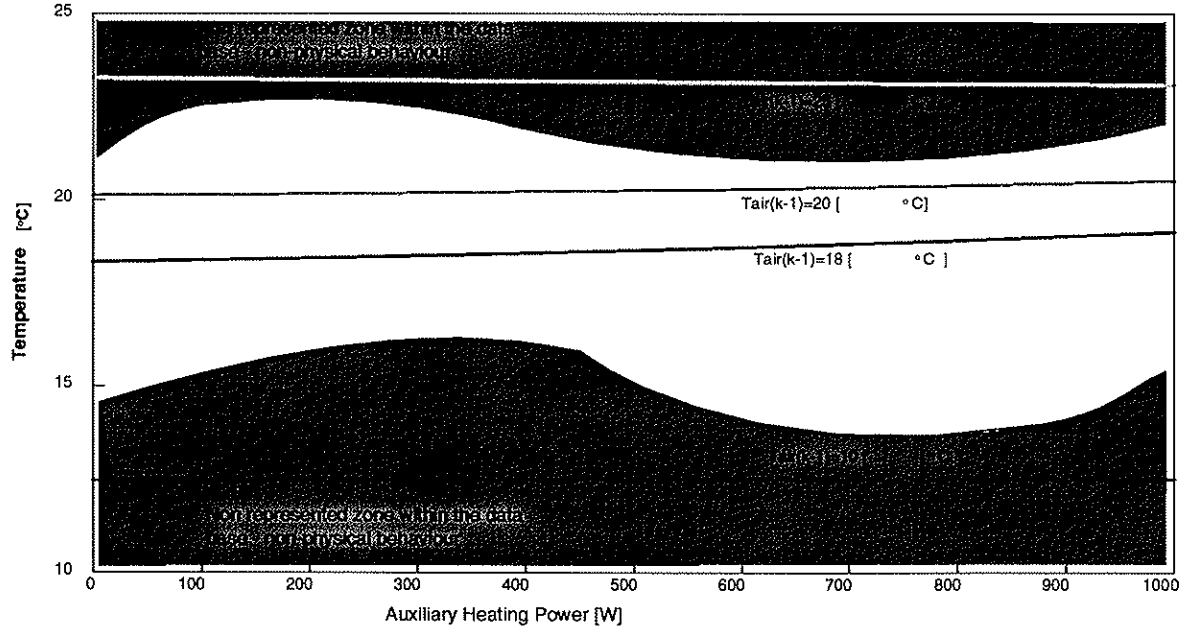

Figure 12: Inside air temperature predicted at time k, in function of heating power, with all other variables fixed.

It can be seen that, although the controller operates correctly during the morning (anticipating the free heat gains), there is an operation error during the afternoon with a peak of the heat delivery when the inside air temperature is around 22 °C. The figure above gives the behaviour of the corresponding building model, in function of the heating power, when all the other variables are fixed.

It can be seen that the inside air temperature predicted at time k is not always increasing with the heating power. For instance for Ti(k-1) = 25 °C, Ti(k) decreases when the heating power increases. This non-physical behaviour is the cause, as it can be seen in the Figure 11, of spurious heating commands by the controller.

Such a problem can appear when the ANN is used in a domain which was not trained enough. These situations can happen during the optimization process, because the dynamic programming explores all the possible ways towards the optimum command, even those which do not finally make sense.

In order to make the behaviour of the model better in the regions which are not supposed to be met normally, or which are met not very frequently, two complementary approaches have been used. Applying the following approaches a correct behaviour of the building model with reference to the Figure 11 and Figure 12 is the result.

A. Modify the structure of the ANN: imposing a constraint on the network weights allows a monotonous predicted inside air temperature in function of the heating power. The constraint to be applied on the synaptic weights is the following:

$$w^{[2]}j \bullet w^{[1]}jk \leq 0 \ \forall j$$

where $w^{[1]}$ is the matrix of synaptic weights for the hidden layer of neurons, $w^{[2]}$ is the matrix of synaptic weights for the output layer of neurons, and k is the index corresponding to the heating power input. Reference shall be made to the PhD thesis [MBa 98].

B. Spread the training example base over the whole input space: keeping in memory all the examples which do not happen frequently allows to fill nearly completely the whole input space. That approach is developed more in detail in chapter 6.

3.5 Dynamic Programming Optimal Control Algorithm

Cost Function

The algorithm aims at optimizing thermal comfort and energy consumption over a fixed time horizon. The chosen cost function depends therefore on these two aspects. Several authors ([Ger 84], [Ros 86], [Par 87], [Nyg 90], [Vis 93], [Lut 95]) have already applied optimal control theory to building heating. The mathematical expression of the cost function, which is used for the NEUROBAT controller is described hereafter:

$$J(U,T) = Cu \bullet U + Cp \bullet (\exp(PMV^2)-1)$$

where U = Heating Command [W]

PMV(T) = Predicted Mean Vote on the Fanger's Scale (-3 = very cold, 0 = neutral, +3 = very hot)

T = Comfort Temperature [°C]

Cu = Constant coefficient for the Heating Energy Consumption Term

Cp = Constant coefficient for the Thermal Discomfort Term

The function proposed here has the advantage of giving a significant weight to the very uncomfortable situations, thanks to the exponential function.

The PMV can be calculated using the Fanger's formula ([Fan 81]). In the model, both the mean radiant temperature and the air temperature are considered. In our case, we consider

that the mean radiant temperature is equal to the air temperature (that assumption is wrong only if the user is standing very near a cold surface like a badly insulated window, or a hot surface like a central heating radiator). All the other parameters are kept constant, except the clothing which is considered different in winter and in summer. They are given in the table below.

Parameter	*Summer*	*Winter*
Metabolism per unit area of body [W/m2]	75 (office work)	75 (office work)
Clothing [clo]	0.5	1.1
Air velocity [m/s]	0.1	0.1
Relative humidity	50 %	50 %
Optimal comfort temperature [°C]	24	20

Table 13: Fanger's model parameters.

The two terms of the cost function corresponding to the energy consumed and to the user's thermal discomfort. The two coefficients Cu and Cp allow a weighting of both terms. The following rule is proposed to determine these weighting coefficients (reference shall be made to [Nyg 90] concerning the derivation of the cost function): "A PMV increase of 0.2 corresponds to the cost of a full power heating". This proposition allows the determination of Cu and Cp (only the ratio between the coefficient has a significance, because the cost function itself has no physical meaning), but has the drawback of comparing two variables with inconsistent units, and on a undefined time interval.

Therefore, the weighting rule has been modified in the present research work the following way: "The cost of the energy consumption which is needed to compensate a 0.2 variation on the PMV is equal to the cost of the discomfort resulting from that same PMV variation". That rule takes into account the dynamic thermal capacity of the building (or of the considered room). If moreover we fix Cp = 1 during the room occupation, the following expression for Cu results after some calculation:

$$Cu = \Delta t \bullet k \bullet (\exp(\Delta PMV^2)-1) / (Cdyn \bullet \Delta PMV)$$

where Δt = Considered Time Interval during which the Heating Power is applied [s]

k = Linear Constant for the PMV linear Approximation: PMV = k • (T - Topt)

T = Room Air Temperature [°C]

Topt = Optimal Comfort Temperature [°C]

Cdyn = Dynamic Thermal Capacity [J/K]

The method allows a cost corresponding to a PMV difference independent from the building type (heavy or light construction) and from the heating system. Cu is calculated differently for each different building.

The coefficient Cp is fixed to 1 when the user is present, and 0 when the room is empty (ie no thermal comfort is needed).

Optimal Control

The optimal control receives the information from the building and climate models to elaborate an optimal heating command (the output of the user block model corresponds for

the herein presented work to the room temperature setpoint). At each timestep (15 min), the following information is available:

- The current state of the building (air temperatures Ti(k) and Ti(k-1).
- The predicted profile of the vertical solar radiation for the 6 next timesteps (Gv(k+1) ... Gv(k+6)).
- The predicted profile of the outside air temperature averaged on the last 24 hours (Te(k+1) ... Te(k+6)).

At each new timestep k, the optimal command Uk* is the command which minimizes the cost on the time horizon:

$$Uk^* \text{ such as } H = \min \left(\Sigma J(u_m, T_{m+1}) \right)$$

the sum being taken from m = k until the time horizon.

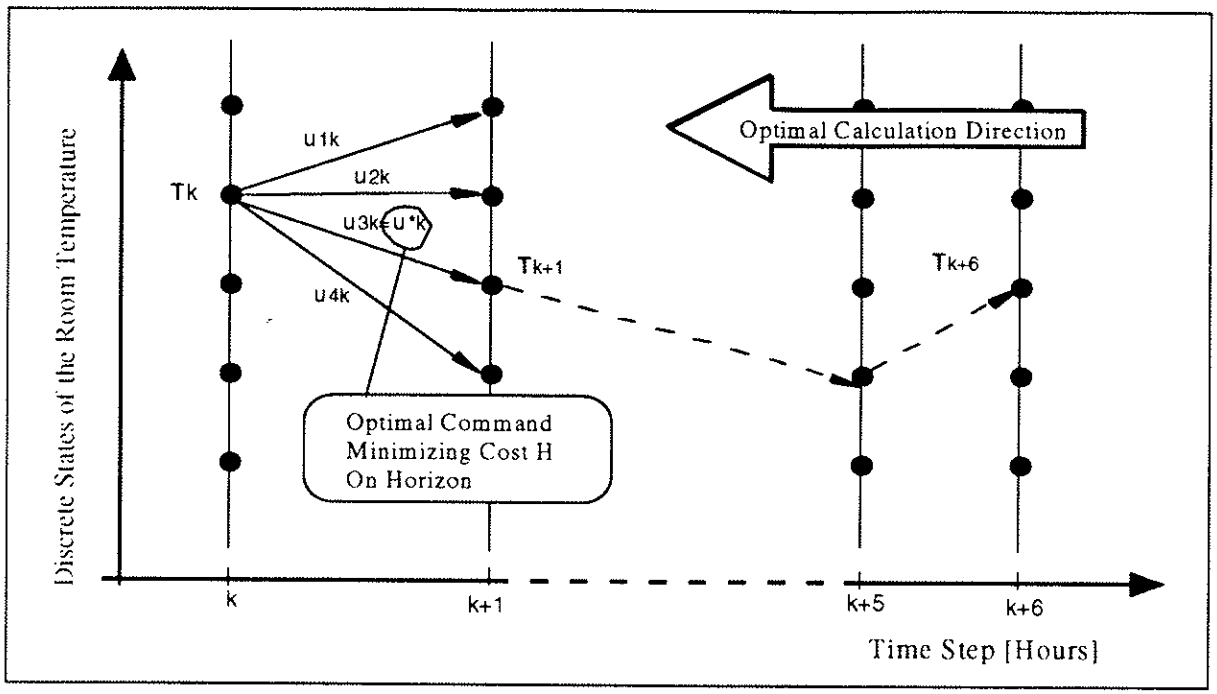

Figure 13: Calculation of the optimal command by minimizing the cost on a time horizon.

The calculation of Uk* uses the dynamic programming algorithm. A complete description of the algorithm can be found in the following literature: [Ber 76] or [Bau 94]. The method presents the following characteristics:

- Global minimum: the algorithm allows the determination of the global minimum of the cost function. If the prediction model are correct, then the method allows the optimization of heating and thermal comfort over the whole time horizon.
- Optimization time horizon: the time horizon has been chosen equal to 6 hours. The farthest the horizon the best the optimization of heating commands. Nevertheless, it is reasonable to say that the effect of a heating command is not longer than the building time constant. A second practical limit arises from the decreasing prediction quality of the models, especially the solar radiation prediction which degrades quickly after some

predicted hours. A third practical limit is the calculation CPU time, proportional to the time horizon. The chosen value of 6 hours represents a compromise between all these considerations.

- Floating horizon: the 6 hours time horizon is floating, i.e. it is always counted from the current time. The optimal command is repeated every 15 minutes, in order to take into account sudden variations of the perturbations (solar radiation, window opening, blind handling).
- Dynamic programming algorithm: this technique has been chosen because of the non-linearity of the models, which makes impossible the analytical resolution of the problem ([Ast 90]) and because it allows to find a global minimum instead of being trapped in a local minimum like it can happen with other techniques. The dynamic programming requires a discretization of the state variables and of the heating command. The following discretization has been used in our case:

	Ti(k) [°C] (current Air Temperature)	*Ti(k-1) [°C] (previous Air Temperature)*	*Heating Command [W]*
Number of discrete states	141	61	5
Interval	0.035	0.035	Pmax/4
Domain considered	[-2.45, +2.45]	[-1.05, +1.05]	[0, Pmax]

Table 14: Variable discretization.

The discretization used is very fine, since it allows to distinguish a temperature difference of 0.035 °C and a heating power difference of 250 W (with reference to a maximal heating power of 1000 W, as it was used for the NEUROBAT test phase) during one hour. Such a fine discretization is required for a good functioning of the controller, but is very demanding for calculation time ([Nyg 90]).

3.6 User Block

This sub-chapter summarizes the concept of the user block of the NEUROBAT heating controller. It should be mentioned, that the following analysis corresponds to a proposal for the NEUROBAT heating controller and that the concept has not been implemented within the framework of the NEUROBAT project, Phase I. Since the user block has an important impact on the user interface, such a proposal should be implemented in collaboration with an industrial partner and tested with several users either in a appropriate laboratory (reference should be made to the BEW study 'DIANE C3: Entwicklung einer BO-fördernden Benutzeroberfläche von Heizungsregelungsgeräten', ETHZ, Institut für Hygiene und Arbeitsphysiologie) or on a residential building.

The basic idea of the user block corresponds to a fuzzy logic processing module, enabling the processing of the user wishes such as 'Too Hot' and 'Too Cold' with reference to the thermal comfort of the user. Since the NEUROBAT controller concept optimizes the heating power and does not control a setpoint temperature, the concept fits well with such a fuzzy logic processing block. Figure 14 shows a possible user interface of the NEUROBAT heating controller summarizing the necessary functionalities and taking the conclusions of the mentioned BEW-study into account. The left-hand side of the front panel corresponds to

the user input functions, such as the user comfort expression ('Too Hot', 'Too Cold') and the user presence indicator. The right-hand side of the front panel represents the feed-back information to the user, such as the current room temperature and the degree of the heating power which is applied. With regard to the predictive characteristic of the NEUROBAT controller, the activation LED's inform the user about the future development of the applied heating power.

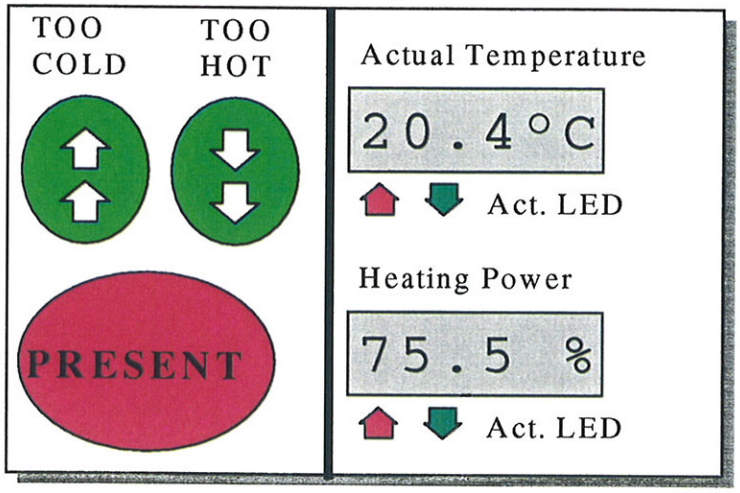

Figure 14: Possible front-panel design of the user interface of the NEUROBAT controller.

The possible concept of the user interface, shown in Figure 14, summarizes the required functionality of the user interface for a user processing block as it is proposed and shown in Figure 15. The user block of the NEUROBAT heating controller is set up by a processing block for calculating the future comfort periods (Schedule Block in Figure 15) and a module, processing the user input (Command Block in Figure 15). Whereas the schedule block will determine the C values of the cost function the command block will either modify the comfort temperature or generate an additional positive or negative heating power contribution. The features of these blocks should be detailed in the following.

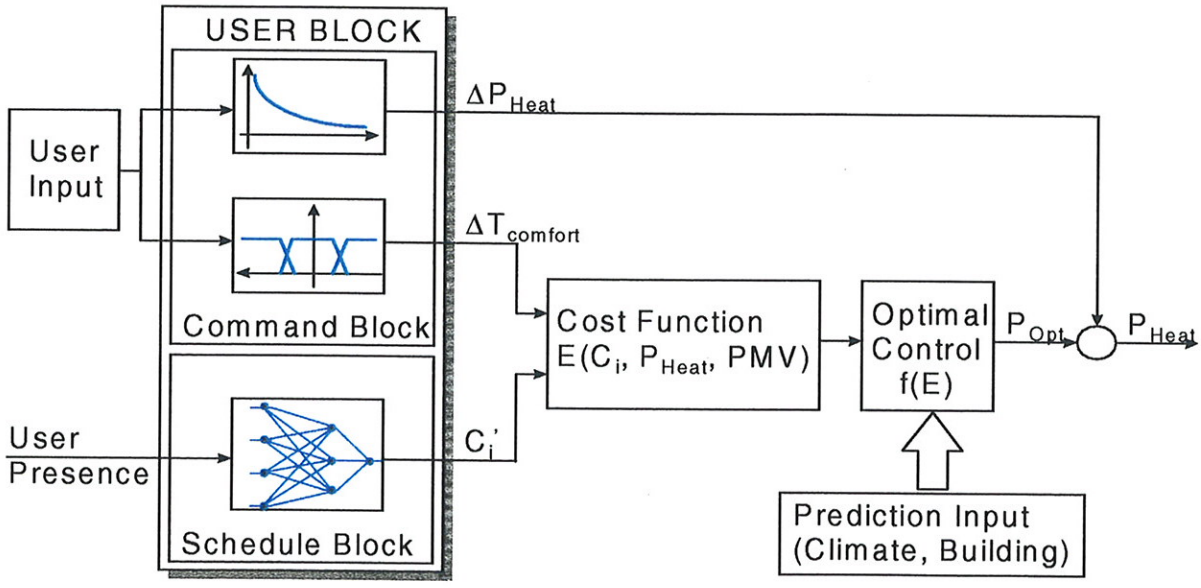

Figure 15: User processing block with comfort and presence processing modules.

Figure 16 summarizes the schedule processing block which has been tested with real data of the NEUROBAT test phase. The idea bases on the measurement of the presence of the user (infrared sensor, key sensor, user button etc.), which signal is processed with the help of a artificial neural network to determine a time schedule of the user occupation.

The graph on top of Figure 16 represents the measurement of the current user presence during the period of one week, as it occurred during the NEUROBAT test phase. The measurement of the user presence during the test phase of the NEUROBAT project, Phase I, has been completed with a light sensor. The ANN presence model, with the user presence signal of the previous time step, the hour signal and the day signal (day of week) as input calculates the future user presence on a fixed time horizon (6 hours for the NEUROBAT controller). As for the meteo ANN models, a simple feed-forward and fully connected neural network model with one hidden layer and 4 neurons in the hidden layer has been applied. As training algorithm the Levenberg-Marquart algorithm has been used due to its convergence capabilities. The graph on the lower right hand side of Figure 16 shows the six hour ahead user presence prediction for one week. Based on the user presence prediction, the C parameters are modified within the cost function, i.e. if no presence is foreseen by the ANN presence model respectively a non-comfort period is predicted and the C2 parameter of the cost function is set to zero, e.g. only the energy factor of the cost function is minimized during the dynamic programming algorithm to determine the optimal heating power.

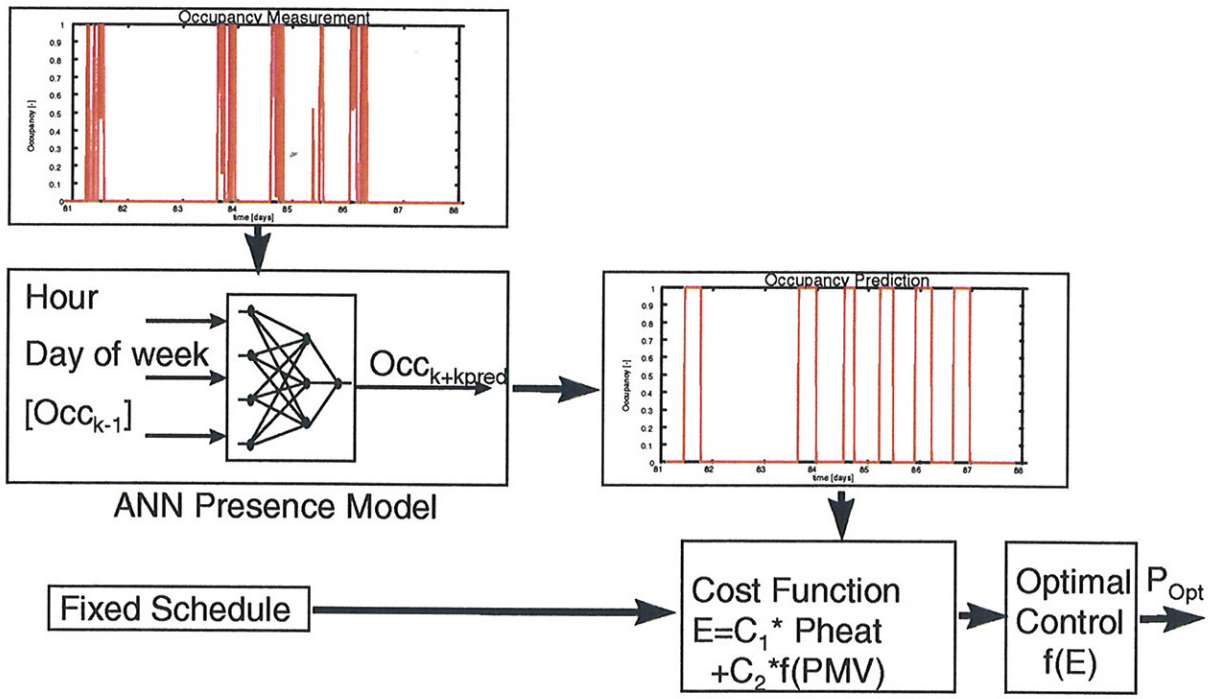

Figure 16: ANN schedule processing block of the NEUROBAT heating controller.

Figure 17 summarizes the command processing block of the user block of the NEUROBAT heating controller. The command processing block can be separated into a short term processing module and a long term processing module. The concept is based on the idea, that the heating controller should react immediately on a user expression, such as 'Too Cold' or 'Too Hot', independent of the optimal comfort temperature of the heating controller(the optimal comfort temperature is the temperature for which the PMV is equal to zero). Therefore the short term processing module will impact directly on the output of the

control algorithm with a requested heating power variation. This variation will be processed by a filter ensuring that the variation will converge to zero after a predefined time period.

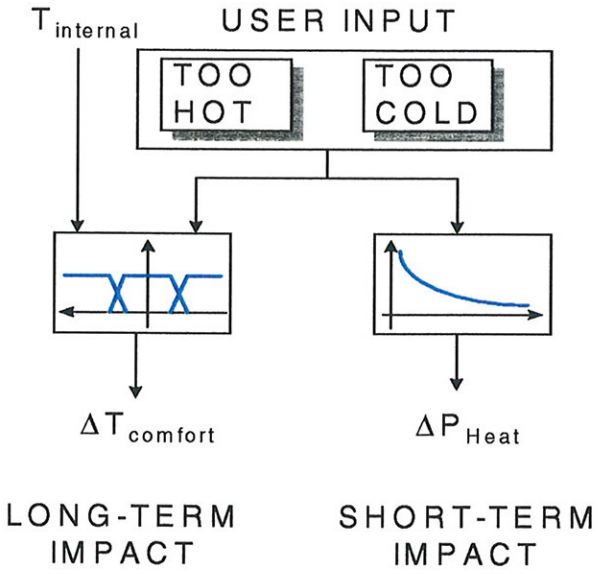

Figure 17: ANN command processing block of the NEUROBAT heating controller.

The long term processing module of Figure 17 will modify on base of a fuzzy logic block the nominal comfort temperature. According to the difference between the current measurement of the room temperature and the optimal comfort temperature ($T_{comfort}$: temperature setpoint by the user) and to the user input ('Too Hot', 'Too Cold'), the optimal comfort temperature is modified as shown in Figure 18, for instance, if the difference is negative (current room temperature higher than the optimal comfort temperature) and the user presses the button 'Too Cold', the fuzzy logic block of the long term processing module will increase the optimal comfort temperature.

ΔT \ U_I	TOO HOT	TOO COLD
NEG	0	$\Delta T_{comfort}$ ++
ZERO	$\Delta T_{comfort}$ -	$\Delta T_{comfort}$ +
POS	$\Delta T_{comfort}$ --	0

with: $\Delta T = T_{optimal\ comfort} - T_{internal}$

Figure 18: Fuzzy rules of the long term processing module of the user block of the NEUROBAT heating controller.

It should be mentioned once again at this point, that the user block of the NEUROBAT heating controller has not been implemented and tested and should be tested with an appropriate industrial partner.

3.7 Valve Control Block

To be able to interface the NEUROBAT heating controller with standard interfaces of HVAC controllers (motor command, mixing valve etc.) the valve control block has been added to the output of the NEUROBAT control algorithm. Whereas the optimal power of the NEUROBAT controller is updated every 15 minutes, the inner control loop of the valve control block is sampled with a sampling time of 5 seconds.

Figure 19 shows the SIMULINK model of the control loop of the valve control block. The input of this inner control loop corresponds to the nominal inlet temperature of the heating fluid, i.e. with the help of the current measurement of the return temperature of the heating fluid and the calculated optimal heating power the nominal value of the inlet temperature is determined.

The control concept of the valve control block is build up by a cascade control with a PID controller in the outer control loop and a three-point controller in the inner control loop. To overcome delay problems due to the big inertia of the heating system, a Smith Predictor has been introduced into the inner and outer control loop. The Zero-Order-Hold Blocks as well as the Plant Block of Figure 19 corresponds to the model of the heating system.

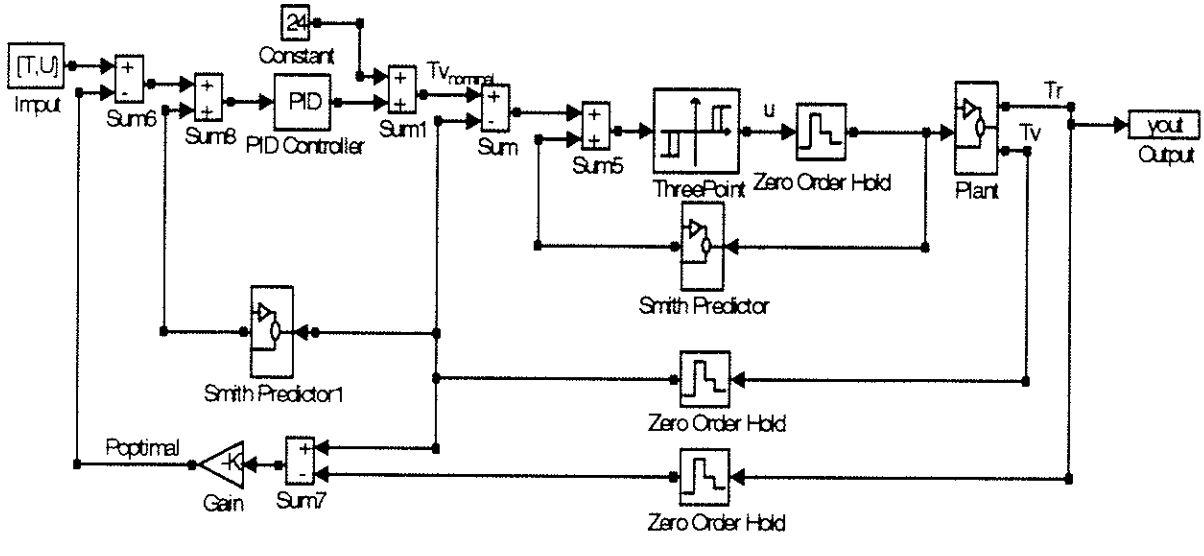

Figure 19: Valve control concept of the NEUROBAT heating controller with: Tv:inlet temperature; $Tv_{nominal}$: nominal inlet temperatur; Tr: return temperature; u: motor command; $P_{optimal}$: optimal heating power;

Since the control of a mixing valve is a common task within HVAC controllers, reference shall be made to the standard literature concerning the details of the valve control and the Smith Predictor [Unb 87]. The idea of the presented concept of the valve control block is, that the NEUROBAT heating controller can be interfaced with any standard interface of HVAC controllers.

4. SIMULATION

The following sub-chapter summaries the simulation work of the NEUROBAT project, with a description of the simulation setup in sub-chapter 4.1 and the simulation results in sub-chapter 4.2.

4.1 Simulation Setup

4.1.1 Simulation Program Description

A simulation program has been developed and used for completing the experimental results. The program allows to simulate the thermal behaviour of one room during a period of a whole year. The program includes a nodal network of the room itself (28 nodes), plus additional nodes for the heating subsystem (4 nodes), and fixed node temperatures to model the neighbouring rooms and the outside air.

The simulation program has been developed in the framework of the DELTA project, and is described in detail in the corresponding final report ([Bau 96]). It has been thoroughly validated on experimental data. Since the same rooms have been used in the NEUROBAT project, with the addition of a new heating system similar to a traditional central heating (see chapter 5), only the heating system model has been added to the simulation model.

The MATLAB software has been chosen for the programming due to its rich collection of library functions for fuzzy logic and artificial neural networks. The Figure 20 shows the graphical interface of the simulation program.

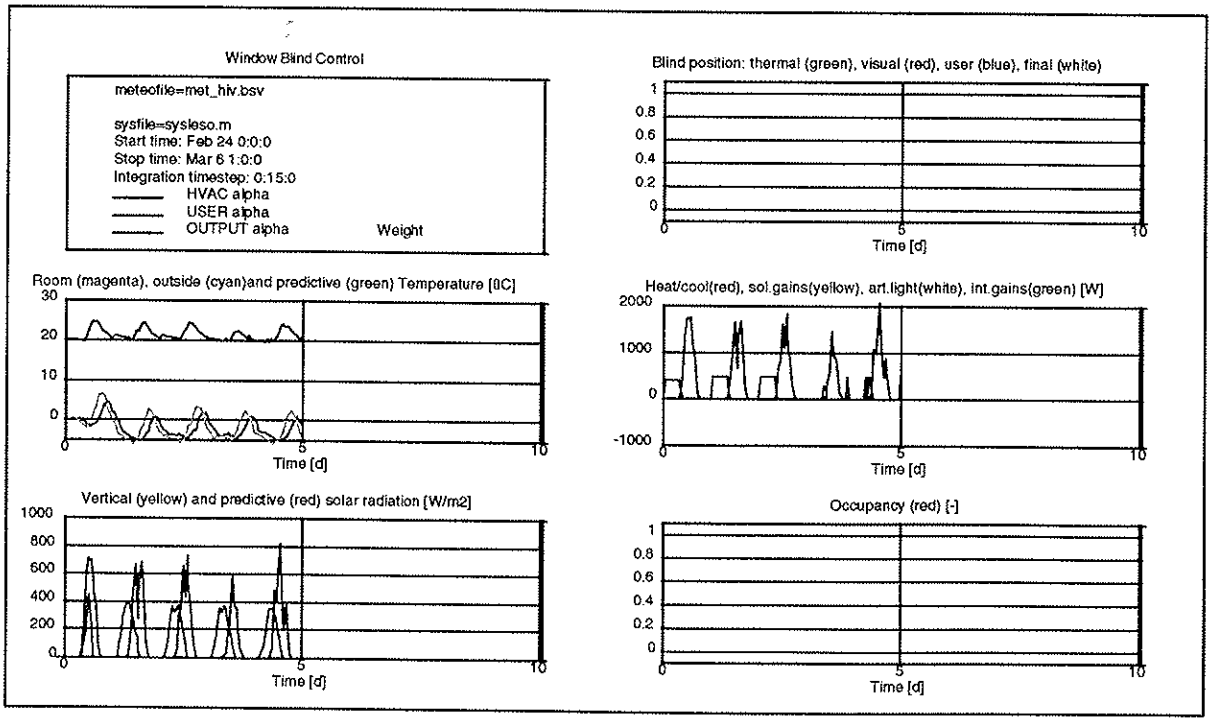

Figure 20: Simulation program graphical interface. From left to right and top to bottom: Simulation files and conditions, room and outside temperatures, solar radiation, blind position, heat gains and occupancy.

4.1.2 Simulation Conditions

Weather Data

For the NEUROBAT project real data was used for the simulations in order to avoid a possible miss of information within the synthetic data. Measurements of the Swiss Meteorological Institute for the station of Pully for the years 1981 and 1982 have been used. The measurement time-step is one hour, and an interpolation to 15 minutes has been done in the simulation program. The needed data include the time, the outside air temperature, and the solar radiation on an horizontal surface. Other data has been calculated in the simulation program:

- The global and diffuse components of the solar radiation on a South vertical surface (corresponding to the window orientation of the simulated rooms).
- The illuminance on a horizontal plane.

Blind Position

To keep the blind open permanently would not have been realistic. Indeed, the measurements taken during the heating season 1996-1997 show a good correlation between the average position of the blind (as chosen by the user) and the solar radiation in the window plane during the room occupancy (reference shall be made to Figure 70 concerning the measurements). Therefore, a simple model for the blind position has been used for the simulations as presented in Figure 21:

- During the occupancy period, the blind position is defined from the South vertical global solar radiation, according to the Figure 21:
- Out of the occupancy period, the blind position is kept at the last value chosen by the user.

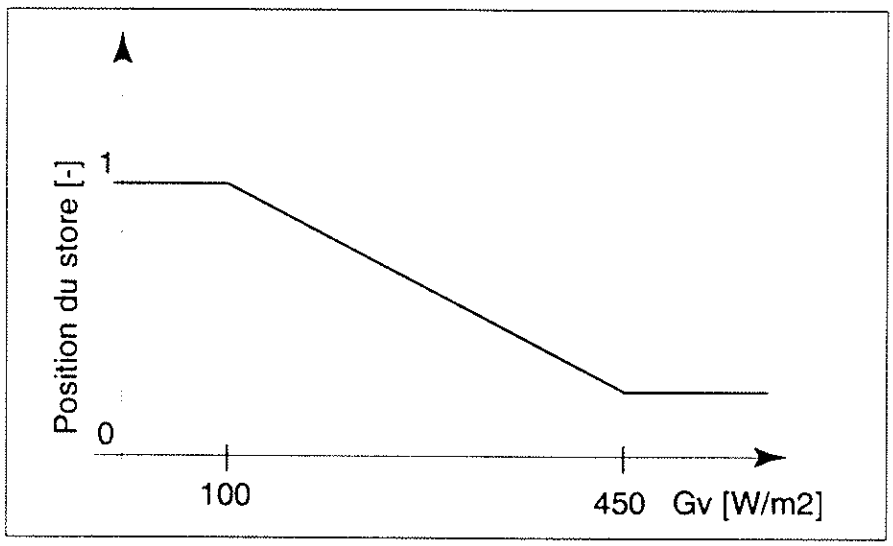

Figure 21: Relation between blind position (1 = completely open, 0 = closed) and south vertical global solar radiation, used for simulation.

Artificial Lighting

The artificial lighting requirements are evaluated from the illuminance on the user's desk, which was placed 2.5 meters away from the window. The daylighting is evaluated using the "daylight factor" method, with additional provision for the blind position. Depending on the outside illuminance on a horizontal surface, the blind position and two daylight factors (one with blind completely open, one with blind closed, both measured at the user's desk), the illuminance on the user's desk can be evaluated with the equation below:

$$Ei = Ee \bullet (DF1 \bullet a + DF0 \bullet (1-a))$$

where Ei = Inside Illuminance on the User's Desk [Lux]

Ee = Outside Illuminance on a horizontal Surface [Lux]

DF1 = Daylight Factor, Blind open

DF0 = Daylight Factor, Blind closed

α = Blind Position (1 = open, 0 = closed)

For the evaluation of artificial lighting requirements, the luminaire's characteristics were used ([Zum 95]). In the room, the luminaire has been calculated to get 500 Lux at the user's desk without daylighting and with full power (192 W). The luminaire can be dimmed until the daylighting reaches 500 Lux (to get a total illuminance daylighting + artificial lighting equal to 500 Lux). If the daylighting is equal or higher than 500 Lux, the luminaire uses only a base power of 25 W. And if there is no user in the room, the artificial lighting is switched of and the electric power is lowered to 3 W.

Strictly speaking, the daylight factor method can only be used for a diffuse sky. Nevertheless, it is used here for determining the artificial lighting requirements, which are needed only by low daylighting, therefore the hypothesis of a diffuse sky is rather often correct in these situations.

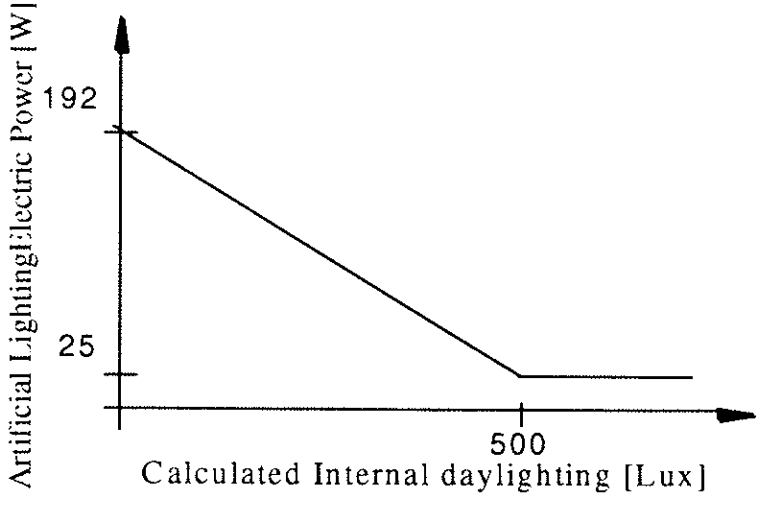

Figure 22: Artificial lighting power [W] versus daylighting [Lux], during occupancy period.

Blind and Window Characteristics

Light transmission: the parameters DF0 and DF1 of the equation of the preceding paragraph have been measured on the test room (see chapter 5) for various positions of the blind and for two different positions in the room. For the position at 2.5 meters from the window, used for the simulation, the measured values are respectively 0.006 ± 0.002 and 0.037 ± 0.005. The ratio DF0/DF1 is the blind transmission factor, independent on the position in the room, and equal to 0.13 ± 0.03.

Energy transmission: the energy transmission characteristics have been differentiated between the part of the window with only the glazing (fraction a of the total window area) and the part of the window covered by the blind (fraction 1-a). For the first one, a classical window energy transmission factor, depending on the incidence angle of the solar radiation, is used. For the second part, the measurements have shown that the diffusion was such, that the transmission was independent on the incidence angle ([Duf 74]). In that latter case, the most important part of incident solar radiation is absorbed in the blind itself, a fraction of 0.066 ± 0.010 being transmitted towards inside as diffuse radiation.

Other Characteristics

Air change rate: a constant value of 0.3 volume/hour between inside and outside has been used. No window opening and no air exchange between the considered room and the adjacent rooms are modelled.

Internal gains: during occupancy, the internal gains are fixed to 100 W, which corresponds coarsely to one person (and no other electric device, except the artificial lighting).

Occupancy schedule: the rooms are occupied from 8 am to 6 pm, during weekdays. During the weekends (Saturdays and Sundays), the rooms are not occupied.

4.2 Simulation Results

The following sub-chapter summarizes the simulation results of the NEUROBAT project, Phase I. For comparative reasons and to be able to assess the performance of the NEUROBAT heating controller, different heating controller simulation models have been implemented and simulated. Table 15 summarizes the commercial heating controller variants used during the NEUROBAT simulation phase for comparative reasons. These commercial heating controller variants base on the principle of the heating curve with extensions concerning the internal temperature adaptation, the start/stop algorithm, the control parameters adaptation and the application of a solar sensor. Due to its confidentiality the details concerning the algorithms of the commercial heating controller cannot be given hereafter. Nevertheless it shall be stated, that the applied commercial heating controller for the NEUROBAT simulation and test phase corresponds to any modern and advanced heating controller on the market.

Controller	*Sensors*			*Control Concept*	*Notes*
	temperature		*solar radiation*		
	external	*internal*			
(1) Standard	YES	NO	NO	open loop control referenced to the external temperature	common control system; bad adapted to buildings

(2) Advanced	YES	YES	NO	(1) + internal temperature adaptation	system with ext. tmp.sensor and thermo-valve
(3) Performant	YES	YES	NO	(2) + adaptation and start/stop algorithm	adapted to buildings with intermittent operation
(4) Very Perfomant	YES	YES	YES	(3) + solar radiation adaptation	solar gains are taken into account

Table 15: Description of different commercial heating controllers used for the NEUROBAT simulation.

As for the commercial heating controller different NEUROBAT versions have been tested during the simulation phase of the NEUROBAT project, which are summarized in Table 16:

Controller	*Sensors*			*Control Concept*	*Notes*
	temperature		*solar radiation*		
	external	*internal*			
(5) NEUROBAT	YES	YES	YES	optimal control + ANN models	
(6) NEUROBAT with ideal meteo prediction	YES	YES	YES	(5) + ideal meteo prediction	evaluation of a perfect meteo prediction
(7) NEUROBAT with 'pause at midday'	YES	YES	YES	(5) + occupation schedule: 8h to12h, 14h to 18h	evaluation of a more precise occupatin schedule
(8) NEUROBAT with 'night schedule'	YES	YES	YES	(5) + occupation schedule: 10h30 to 14h, 15h30 to 20h	evaluation of a more precise occupatin schedule

Table 16: Description of different NEUROBAT heating controllers used for the NEUROBAT simulation.

The different controllers are assessed with reference to the energy consumption, the thermal comfort, the intermittent management and the commissioning. In the following a qualitative assessment shall be given with reference to a winter and a mid-season period as summarized in Table 17:

Period	*Date*	*Characteristics of the Period*
Winter	1.1 to 8.1	period with low solar radiation low external temperature first and second day with no occupation (week-end) and occupation from 8h to 18h for day 3 to 7 (week-day)
Mid-Season	24.3 to 31.3	period with variant solar radiation medium external temperature day 84 and 85 with no occupation (week-end) and occupation from 8h to 18h for day 86 to 90 (week-day)

Table 17: Period description for qualitative heating controller assessment.

Winter Period

For the winter period Figure 23 and Figure 24 show the climate conditions, Figure 25 and Figure 26 the heating power distribution for the standard commercial controller, Figure 27 and Figure 28 the heating power distribution for the performant commercial controller and Figure 29 and Figure 30 the heating power distribution for the standard NEUROBAT heating controller.

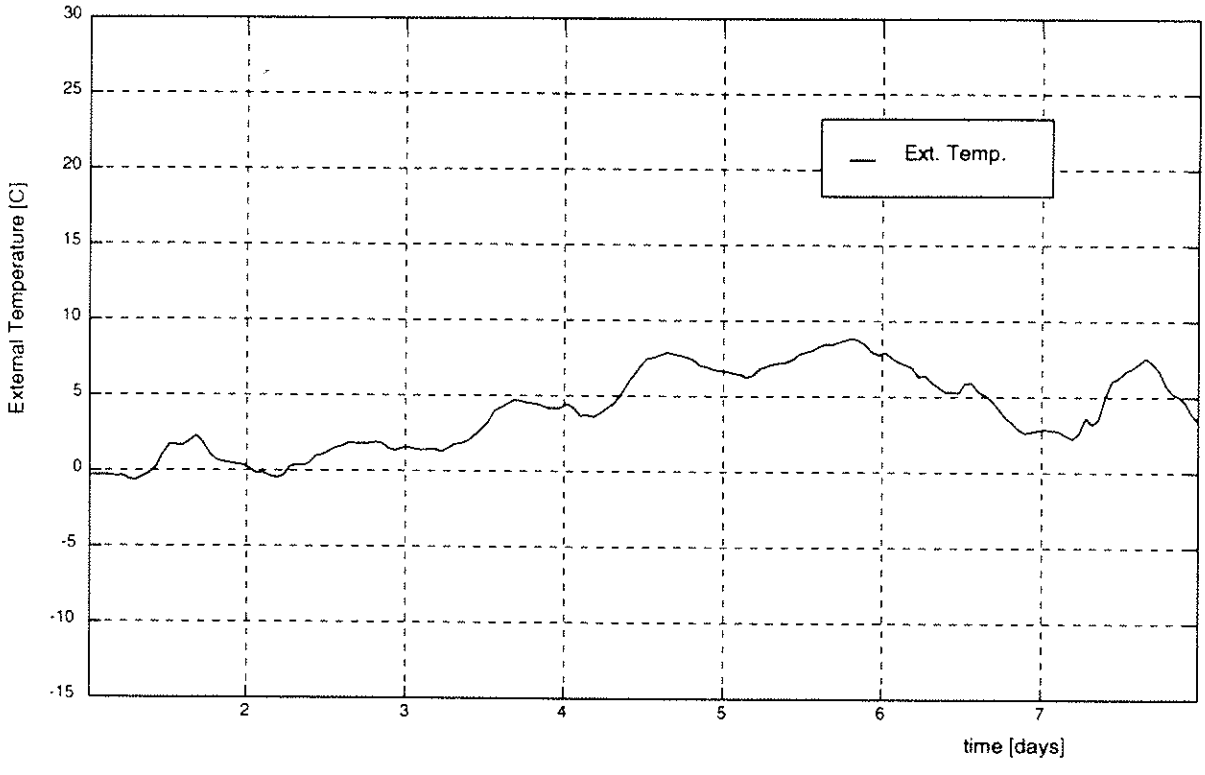

Figure 23: External temperature for the winter period.

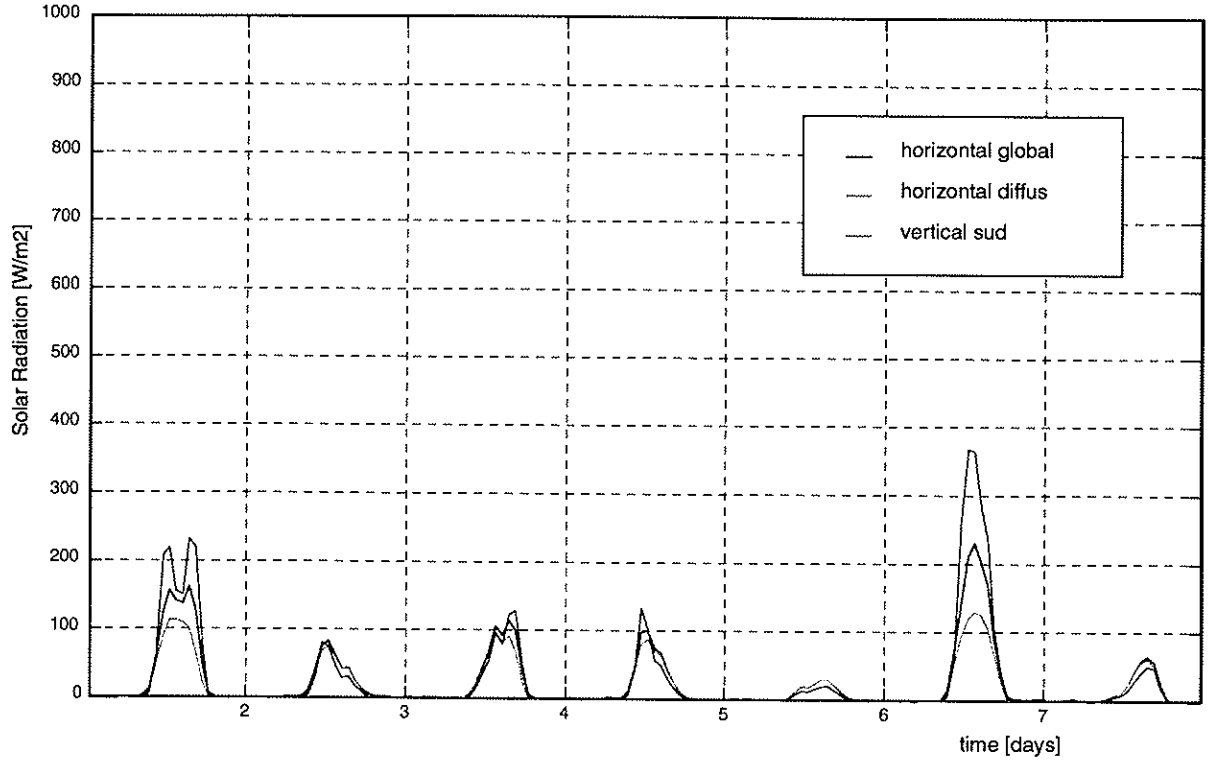

Figure 24: Horizontal solar radiation for the winter period (global, diffuse and global south).

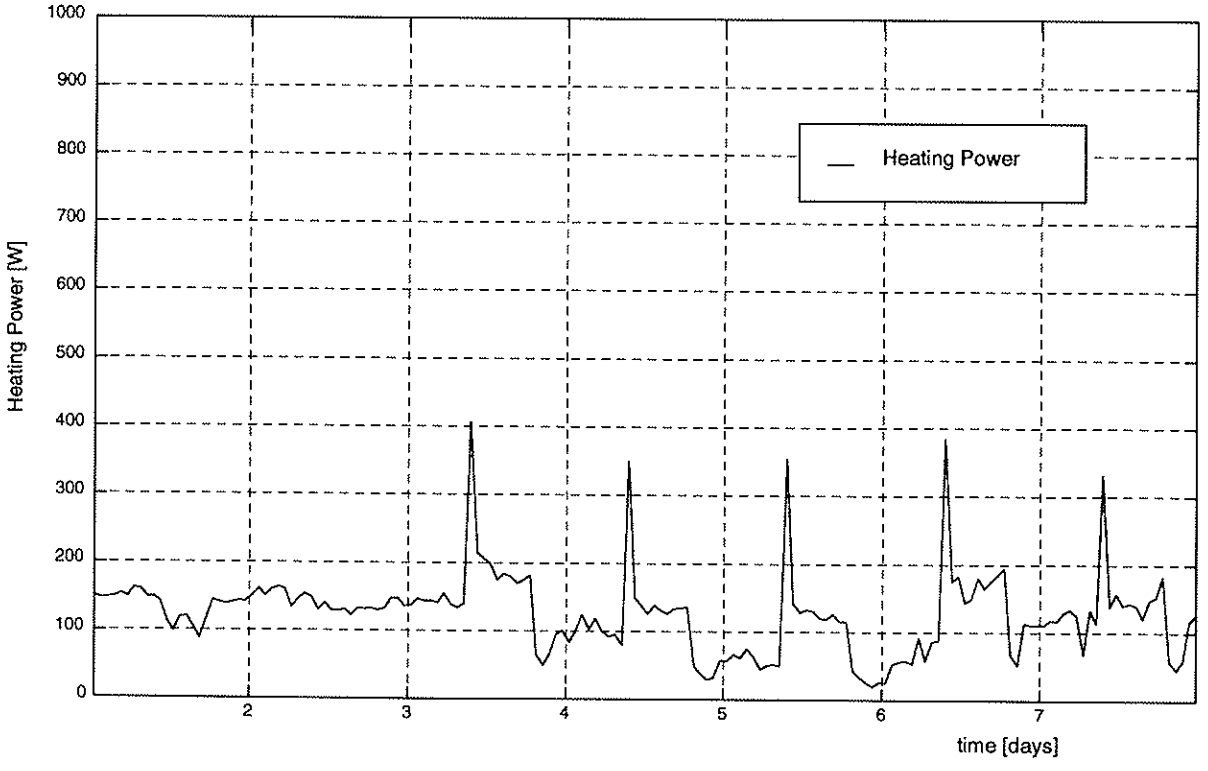

Figure 25: Heating power distribution for the standard commercial heating controller.

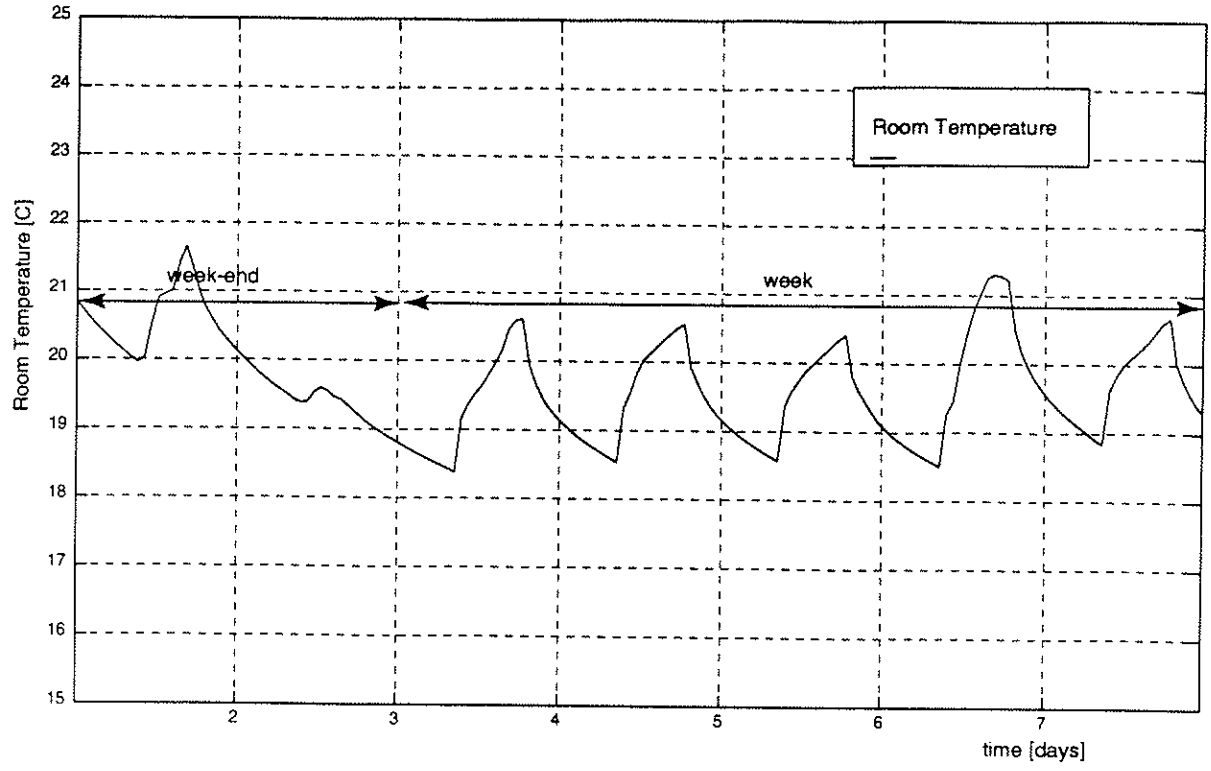

Figure 26: Room temperature for the standard commercial heating controller.

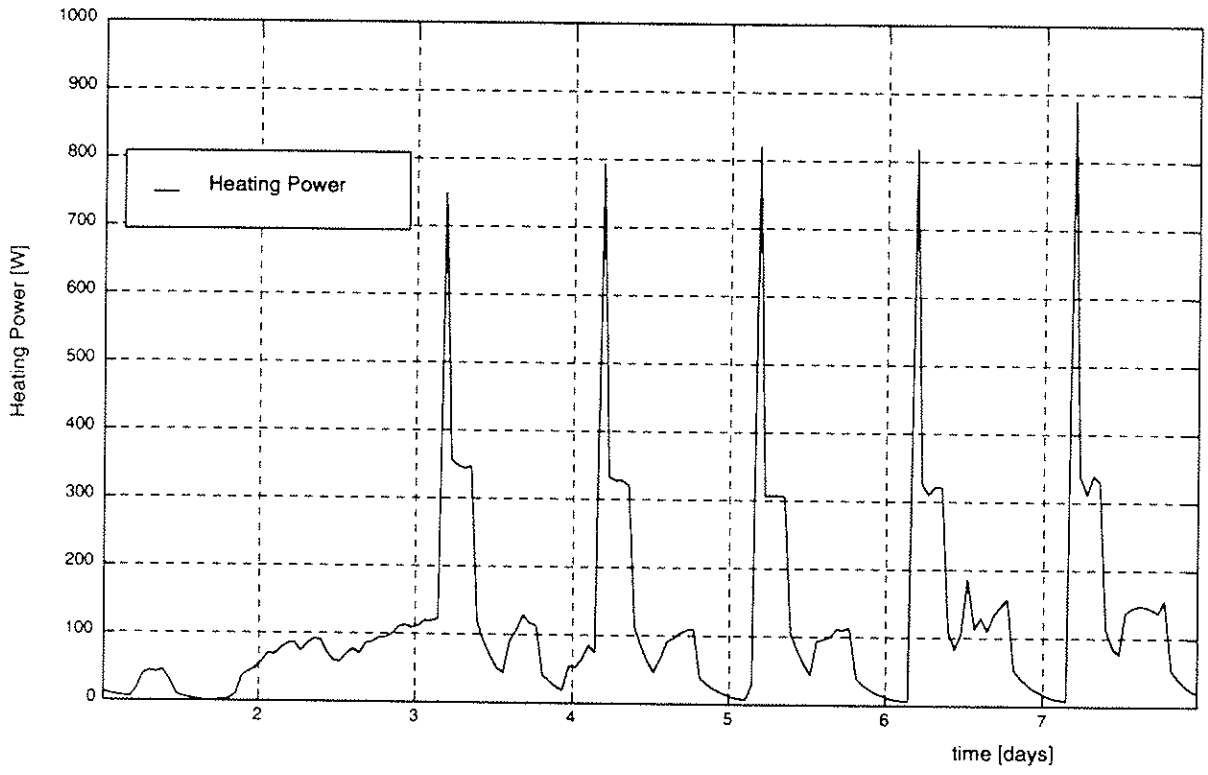

Figure 27: Heating power distribution for the performant commercial heating controller.

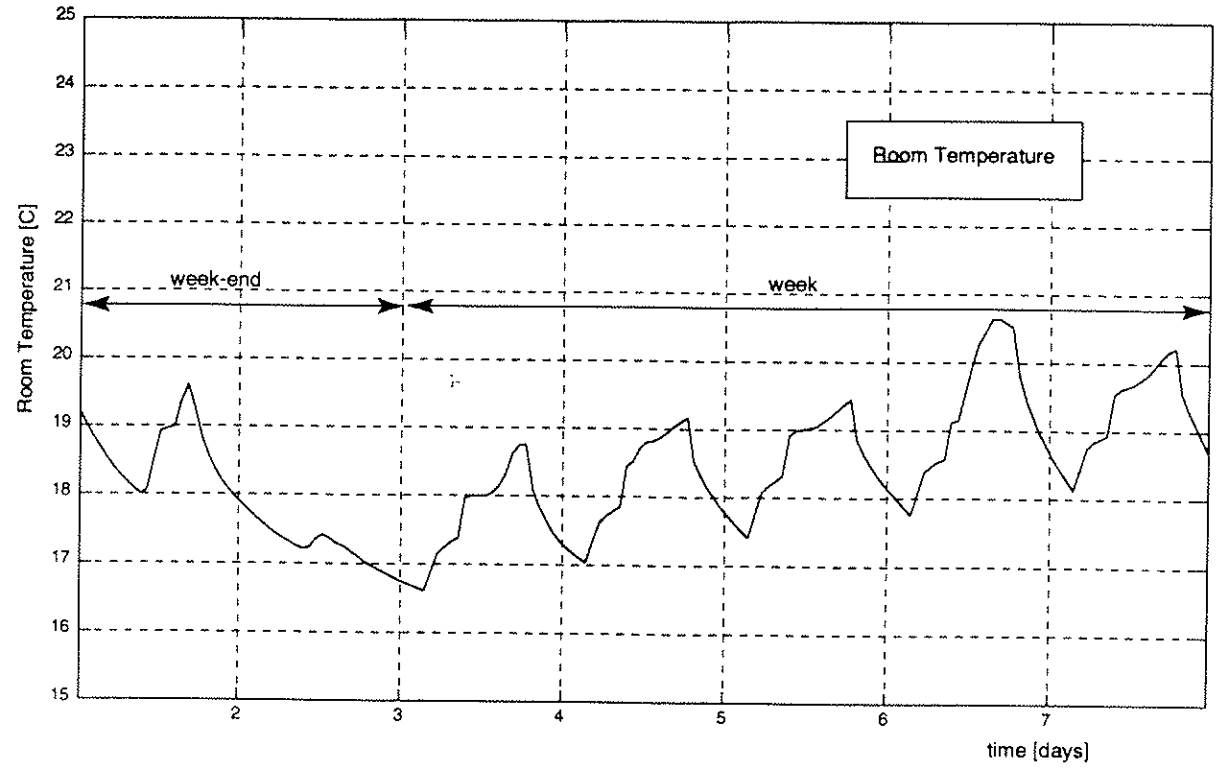

Figure 28: Room temperature for the performant commercial heating controller.

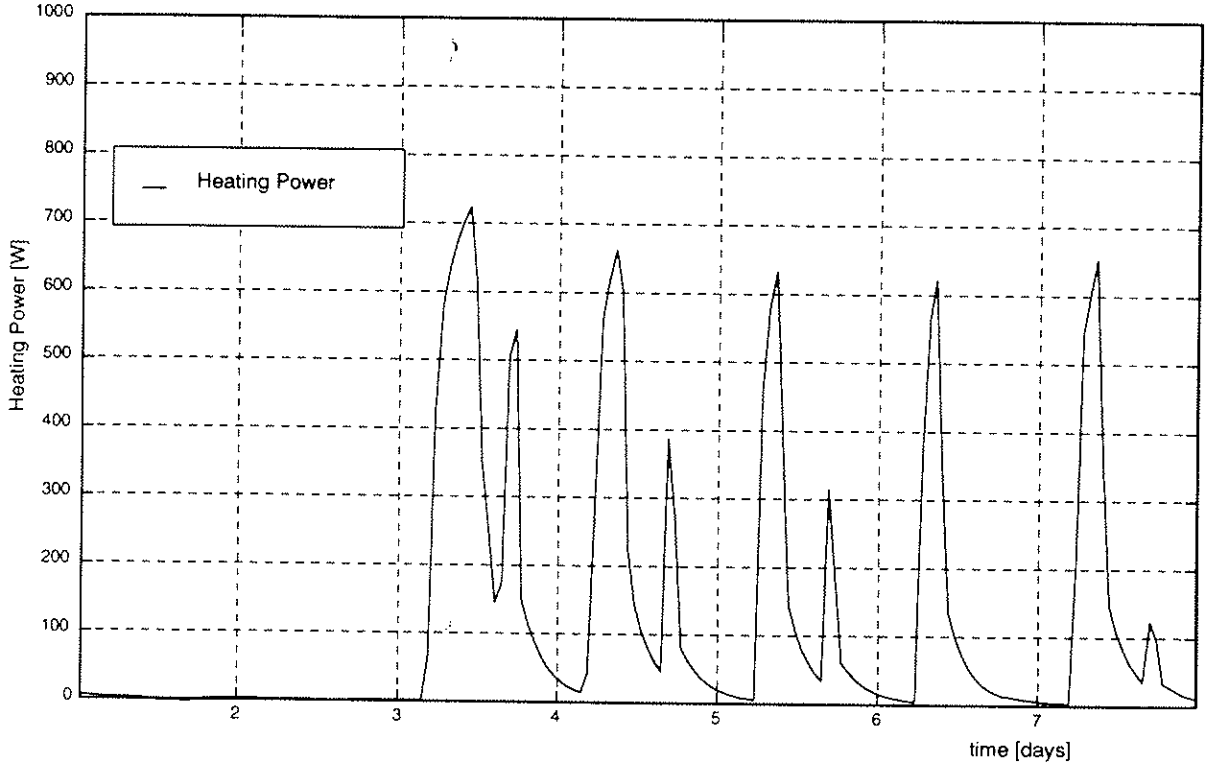

Figure 29: Heating power distribution for the NEUROBAT heating controller.

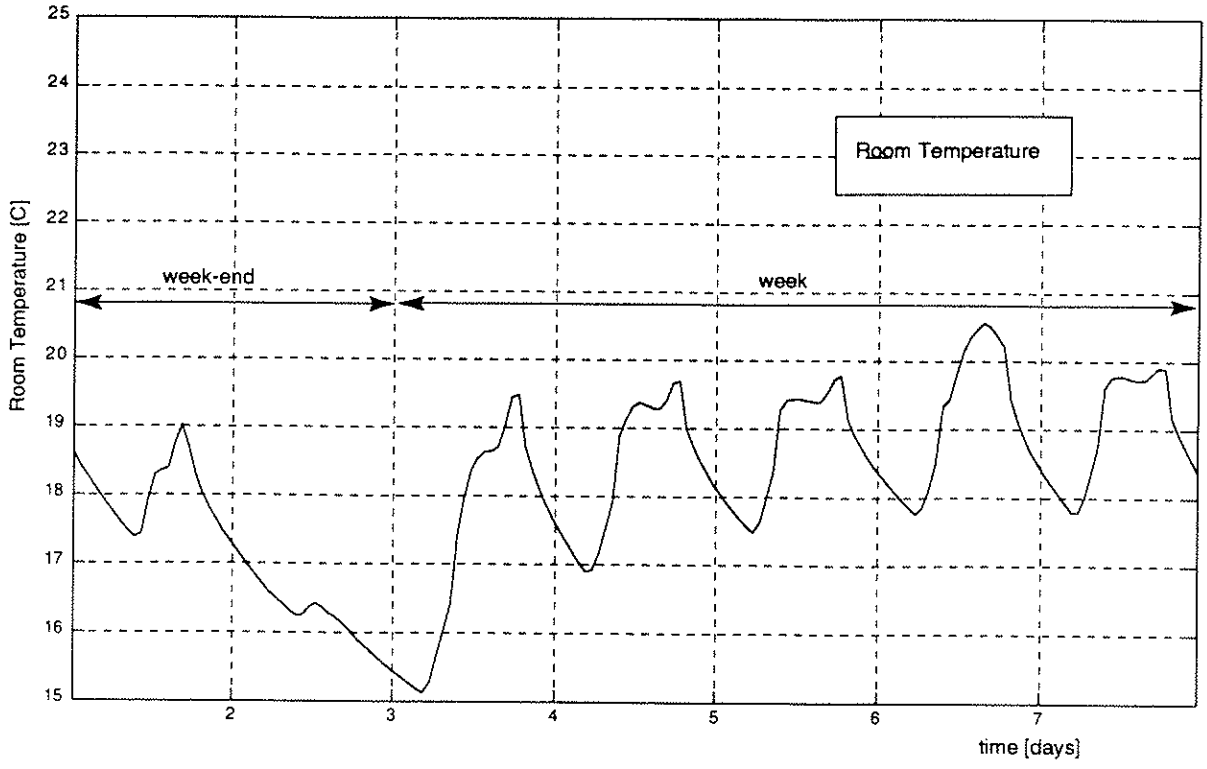

Figure 30: Room temperature for the NEUROBAT heating controller.

The following remarks can be made with reference to Figure 23-Figure 30:

- The standard commercial heating controller with no possibility to anticipate the occupation schedule, maintains a significant heating contribution outside the user presence schedule. This heating maintenance results into an important energy consumption during the week-end, but with a nearly optimal thermal comfort at the beginning of the week (no start-up problems).
- The performant commercial heating controller reduces the heating distribution during the week-ends and the nights, but the start-up period is not optimal: on Monday morning the room temperature is too low (18.5°C) and only on Thursday the room temperature stabilises on the comfort temperature setpoint.
- The NEUROBAT heating controller enables an intermittent operation. In comparison to the start-up period of the performant commercial heating controller, the start/stop algorithm functions nearly optimal. To improve the start/stop algorithm of the NEUROBAT controller, one can either increase the prediction horizon, or limit the fall of the room temperature outside the user schedule.

Mid-Season Period

The climate conditions are shown in Figure 31 and Figure 32, the heating power distribution and the room temperature can be seen in Figure 33 and Figure 34 for the standard commercial heating controller, in Figure 35 and Figure 36 for the performant commercial heating controller and in Figure 37 and Figure 38 for the NEUROBAT heating controller.

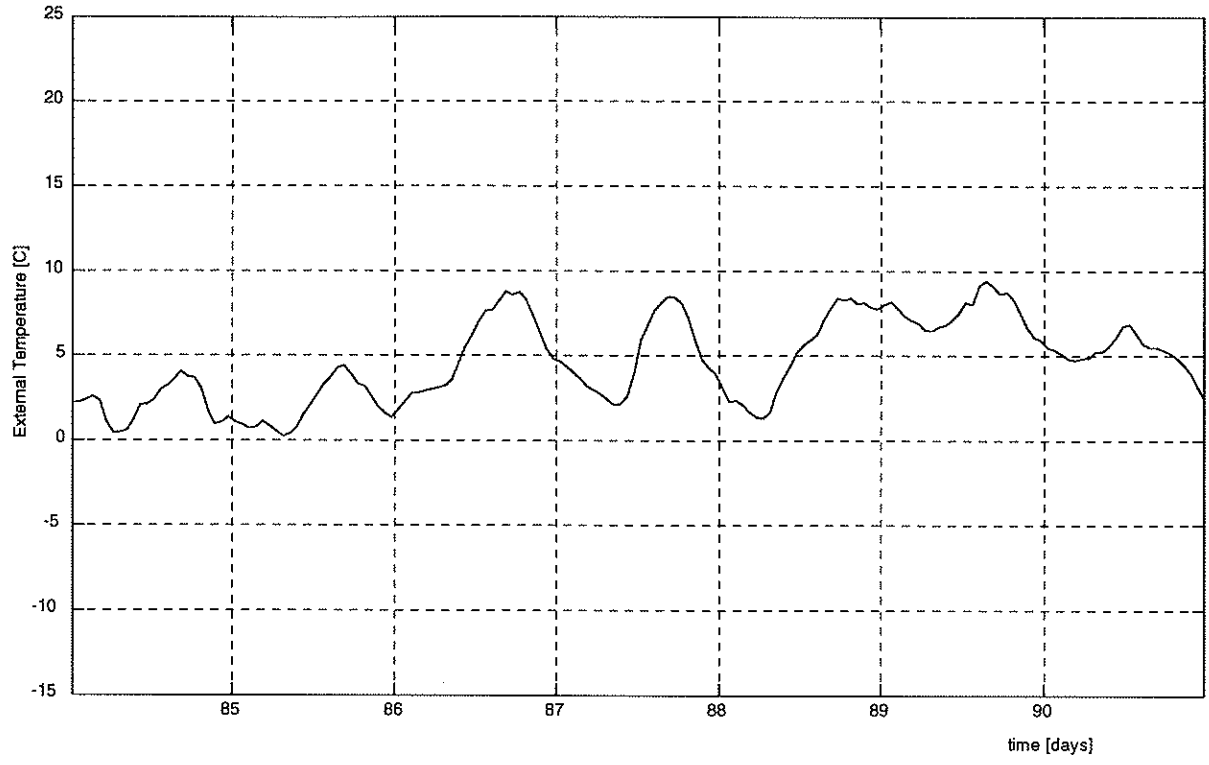

Figure 31: External temperature for the mid-season period.

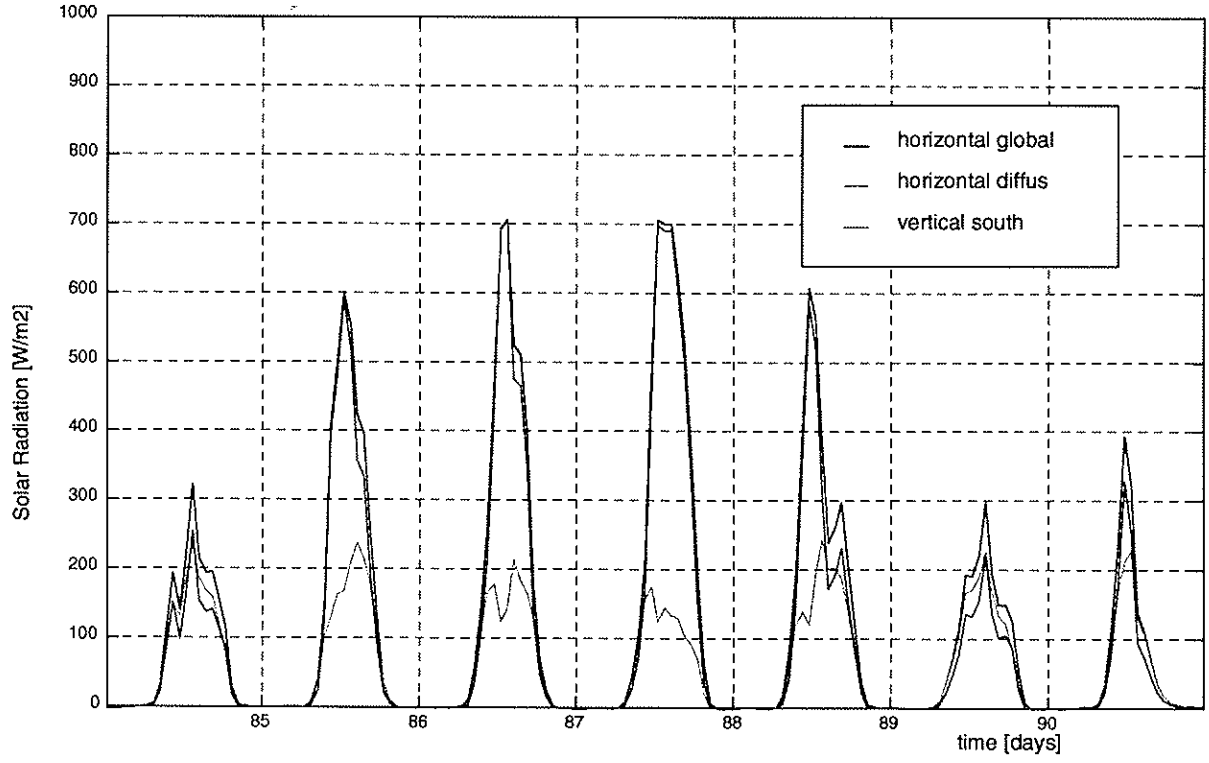

Figure 32: Horizontal solar radiation for the mid-season period (global, diffuse and global south).

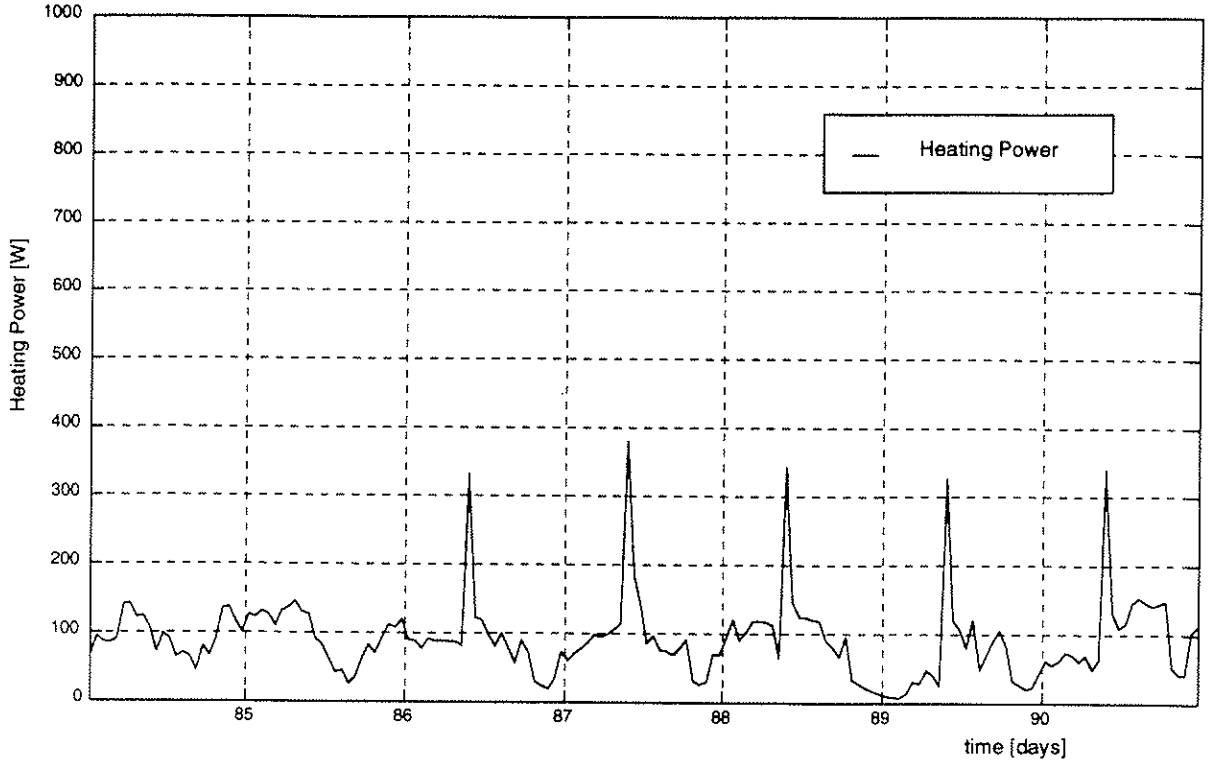

Figure 33: Heating power distribution for the standard commercial heating controller.

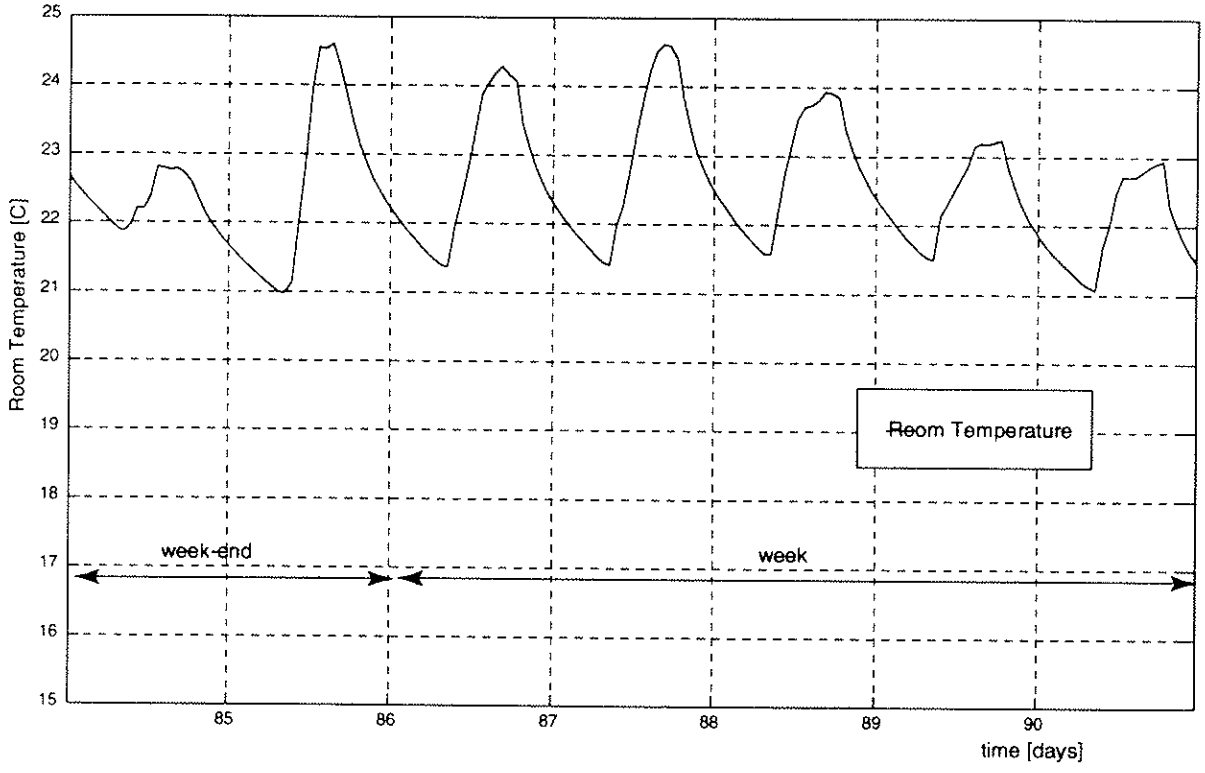

Figure 34: Room temperature for the standard commercial heating controller.

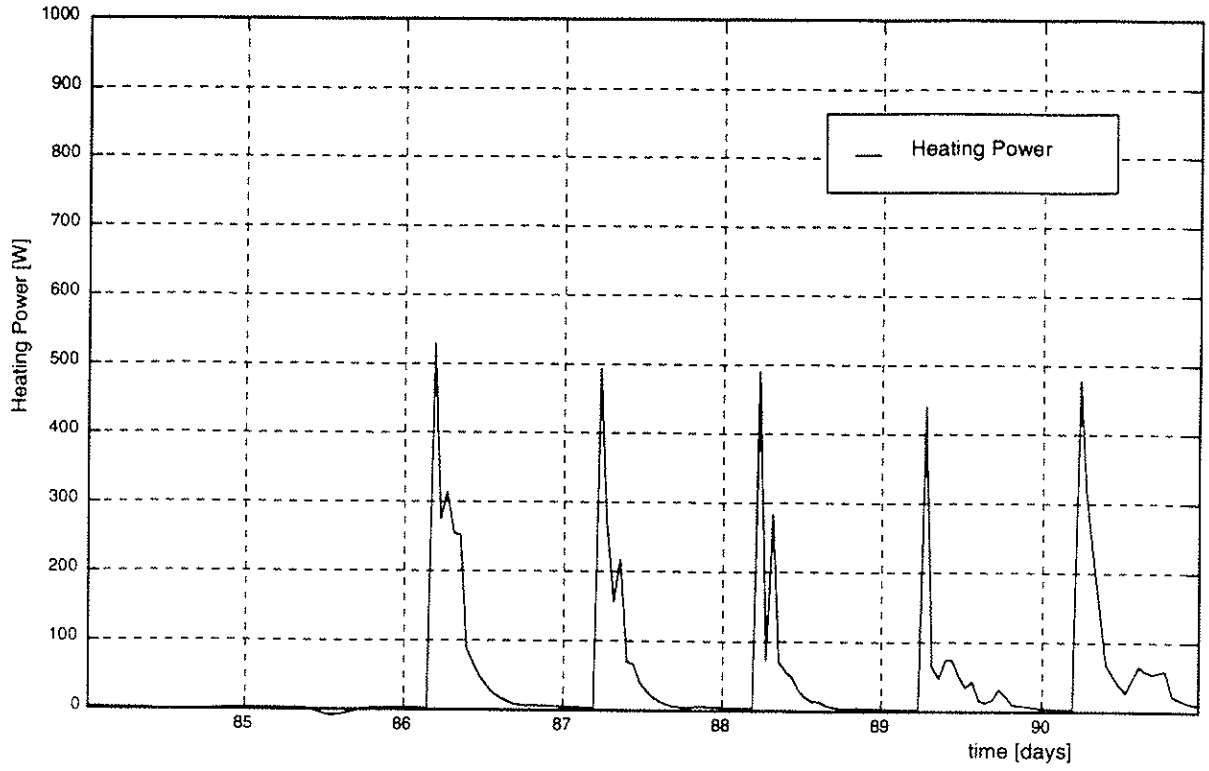

Figure 35: Heating power distribution for the performant commercial heating controller.

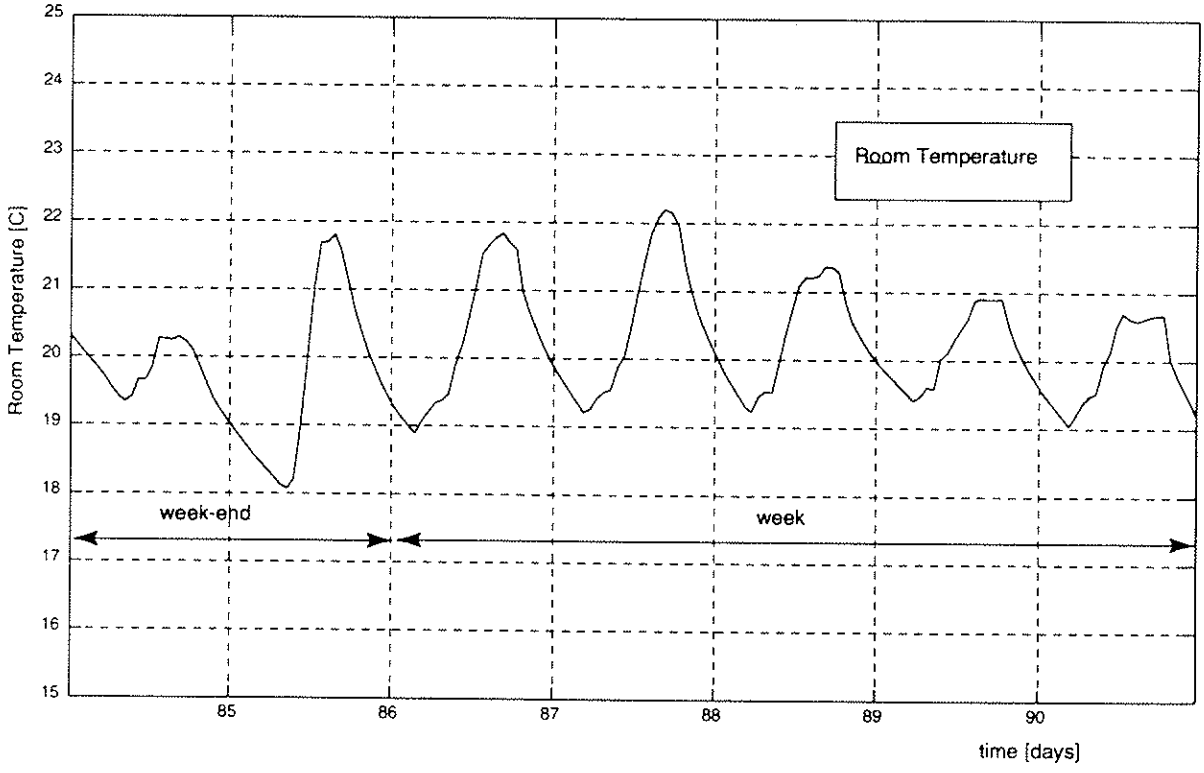

Figure 36: Room temperature for the performant commercial heating controller.

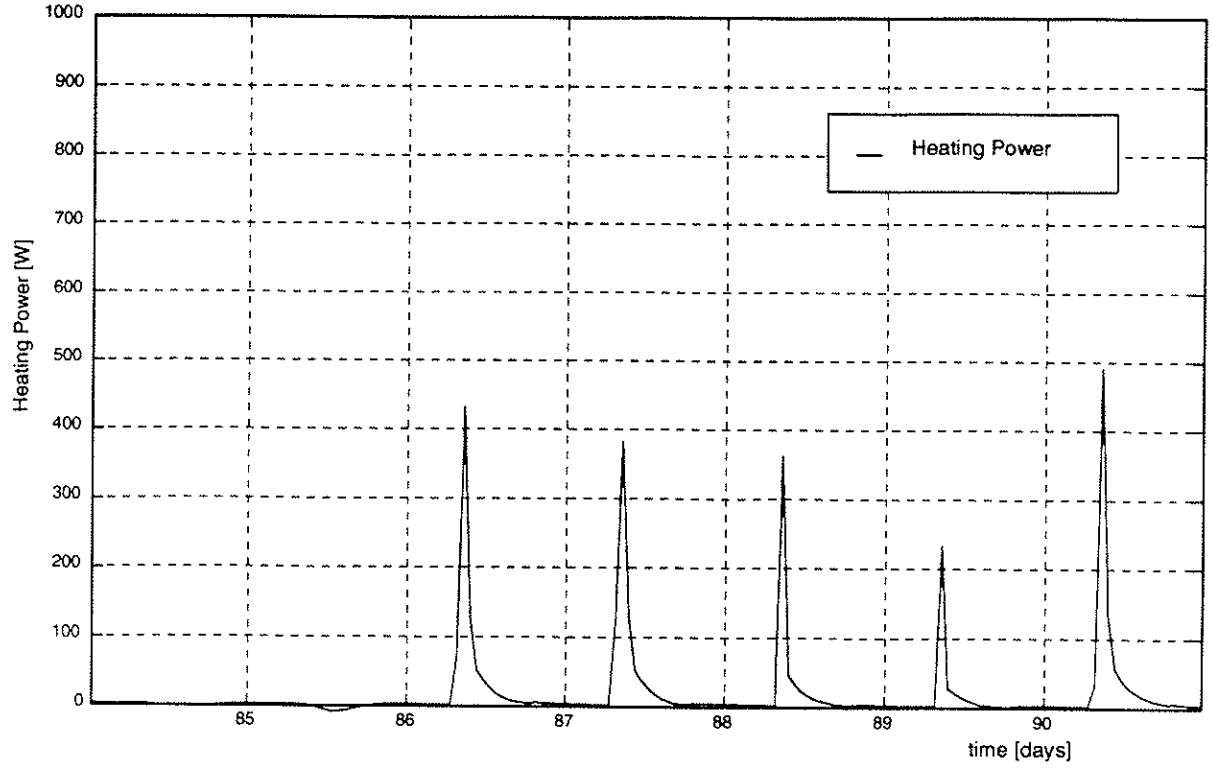

Figure 37: Heating power distribution for the NEUROBAT heating controller.

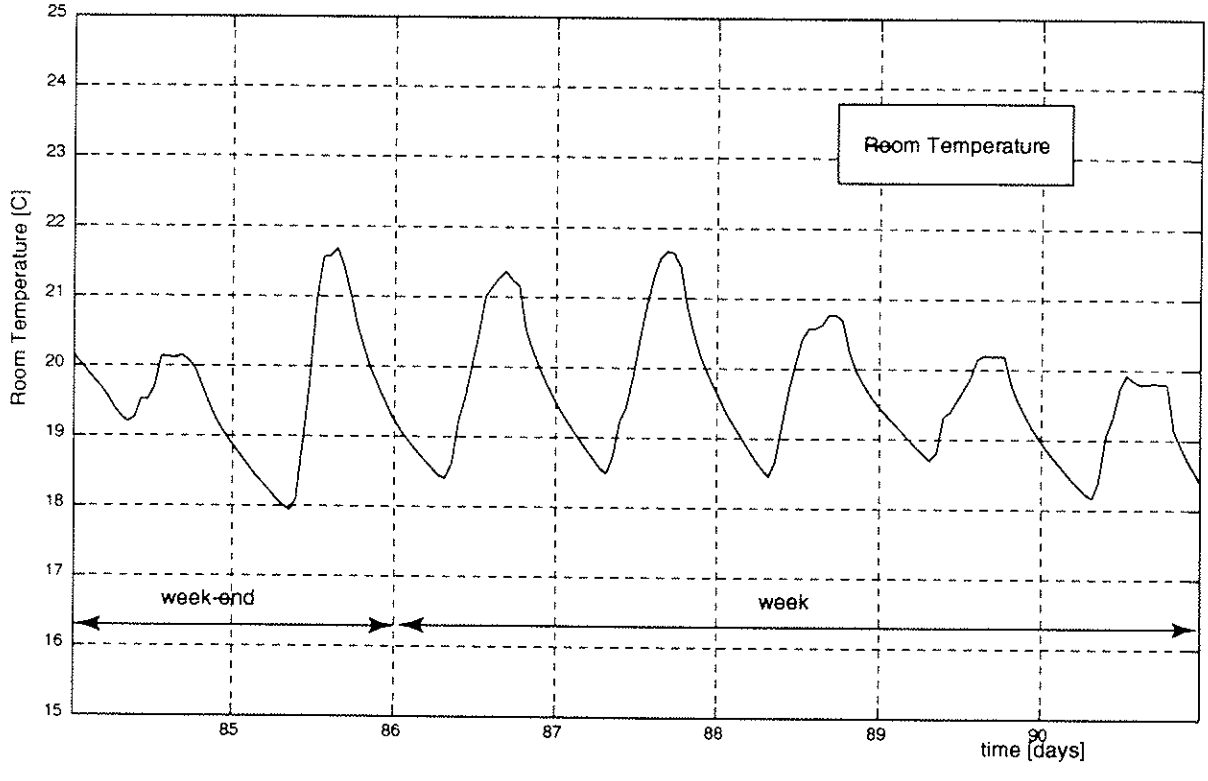

Figure 38: Room temperature for the NEUROBAT heating controller.

The following notes can be made with regard to Figure 31 to Figure 38:

- The standard commercial heating controller, having no reference to the room temperature and the solar gains, applies continuously too much heating power, which results into overheating periods (room temperature of 24.5°C during the afternoon).
- The performant commercial heating controller limits the heating power distribution, but the room temperature is still too high in comparison to the setpoint temperature.
- The NEUROBAT heating controller, taking into account the future solar gains, reduces strongly the heating power and the thermal comfort is nearly optimal.

Quantitative Results

The global results (energy consumption, comfort cost, solar gains etc.) of the different heating controllers for the heating season 82/83 is shown in Table 18. The adaptive heating controller variants have been trained on the season 81/83.

	Commercial Heating Controller			
	standard	*advanced*	*performant*	*very performant*
Simulated Days [days]	212	212	212	212
Hours of Occupation [h]	1510	1510	1510	1510
Heating Power (water) [MJ]	1626	1295	1183	1177
Heating Power (room) [MJ]	1477	1175	1073	1068
Direct Solar Gains [MJ]	2395	2395	2395	2395
Potential Solar Gains [MJ]	4105	4105	4105	4105
Artificial Light [MJ]	425	425	425	425
Internal Gains [MJ]	544	544	544	544
Energy Cost per Day [-]	0.03	0.03	0.02	0.02
Comfort Cost per Day [-] (during occupation)	3.68	1.77	1.49	1.47
Total Cost per Day [-]	3.71	1.80	1.52	1.49

Table 18: Global results of the NEUROBAT simulation phase with the commercial heating controllers.

The following remarks can be given with reference to Table 18:

- The standard commercial heating controller with its energy consumption (1626 [MJ]) and its comfort (cost of 3.68) is not optimal. It shall be mentioned at this point, that to have a mean value of 20°C during the winter period, the nominal temperature of the room temperature has been decreased to 16°C. If no such intervention has been applied, the energy consumption amounts to 2700 [MJ].
- The advanced commercial heating controller enables with its adaptation of the heating curve with reference to the internal temperature a strong reduction of the energy consumption (1295 [MJ]) and to optimize the comfort (cost of 1.77).

- The adaptation of the heating curve parameters and the optimal start/stop algorithm of the performant commercial heating controller enables a considerable reduction of the energy consumption (1183 [MJ]) and the optimization of the comfort (cost of 1.49).
- The introduction of a solar radiation sensor for the very performant commercial heating controller does not increase the performance: the energy consumption and the comfort cost is stable in comparison to the performant commercial heating controller.

The continuous adaptation of the heating curves enables to optimize the performance of the heating controller. On the other hand the principle of the heating curve limits the performance increase of the extension of the heating controller by a solar radiation sensor: the information of the additional heating gain is already covered by the room temperature sensor.

Table 19 summarizes the global simulation results of the NEUROBAT heating controllers for the heating season 82/83. With reference to the parameters of the adaptive commercial heating controllers, the modules of the NEUROBAT heating controllers have been trained during the season 81/82.

	NEUROBAT Heating Controller			
	standard	*ideal meteo prediction*	*pause at mid-day*	*night schedule*
Simulated Days [days]	212	212	212	212
Hours of Occupation [h]	1510	1510	1208	1208
Heating Power (water) [MJ]	1048	1082	1113	971
Heating Power (room) [MJ]	951	981	1010	881
Direct Solar Gains [MJ]	2395	2395	2433	2530
Potential Solar Gains [MJ]	4105	4105	4105	4105
Artificial Light [MJ]	425	425	395	461
Internal Gains [MJ]	544	544	435	435
Energy Cost per Day [-]	0.02	0.02	0.02	0.02
Comfort Cost per Day [-] (during occupation)	1.09	1.08	0.78	1.12
Total Cost per Day [-]	1.11	1.11	0.80	1.14

Table 19: Global results of the NEUROBAT simulation phase with the NEUROBAT heating controllers.

The following remarks can be given with reference to Table 19:

- The NEUROBAT heating controller enables a reduction of the energy consumption to 1048 [MJ] and an optimization of the comfort (cost of 1.09). With reference to the most performant commercial heating controller this corresponds to an energy gain of 11% and a comfort optimization of 27%.
- The NEUROBAT heating controller variant with an ideal meteo prediction consumes slightly more energy (+38 [MJ]). This surprising result derives from the fact, that the ANN meteo prediction of the NEUROBAT controller averages the ANN prediction to an

intermediary value to minimise the square error of the ANN meteo prediction. The energy consumption of the NEUROBAT heating controller with an ideal meteo prediction consumes more energy during the morning period, since the solar gains are not overestimated, as for the standard NEUROBAT heating controller. Moreover, the thermal comfort is near to the optimum for the NEUROBAT heating controller with an ideal meteo prediction as it can be seen in Figure 39. In fact, the energy consumption gain of the basic NEUROBAT controller goes in hand with a loss of thermal comfort.

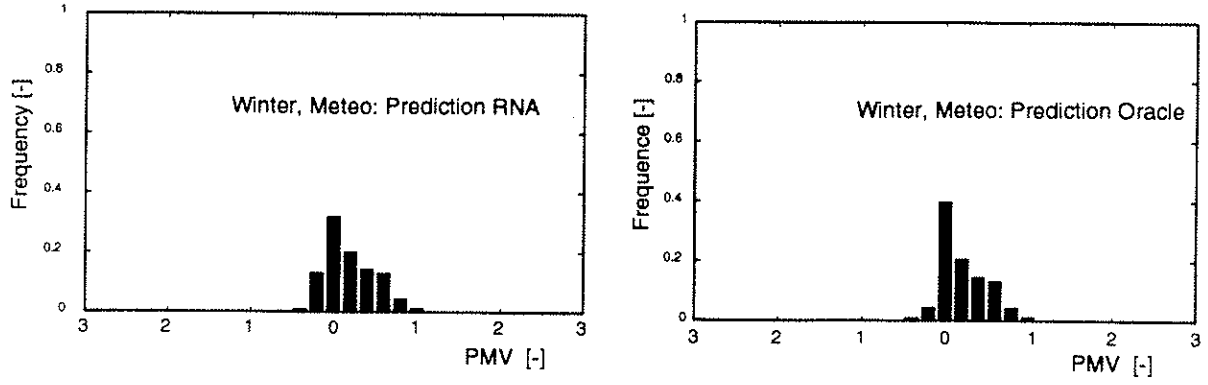

Figure 39: Comparison of the thermal comfort with the NEUROBAT prediction on the left hand side and the ideal meteo prediction data at the right hand side.

- The NEUROBAT heating controller with a pause at mid-day consumes unexpectedly more energy than the NEUROBAT standard heating controller. The following remarks must be made:

  - The internal gains are, due to the occupation and the artificial lighting inferior in comparison to the NEUROBAT standard heating controller (-30 [MJ] respectively -109 [MJ]).

  - The solar gains are superior, due to the fact, that the blind position is not modified during the user absence.

  - The optimal algorithm does not optimise the comfort during the period from 12h to 14h and the comfort period at mid-day corresponds to a period, where the room temperature is superior to the setpoint of the room temperature. Therefore the optimal algorithm reduces its heating distribution during the morning since the overheated period at mid-day is no more penalised. The thermal comfort is therefore better than for the standard NEUROBAT heating controller but with an additional energy consumption.

- The energy consumption of the NEUROBAT heating controller with a night schedule for the occupation (user presence from 10h30 to 14h and 15h30 to 20h) is inferior in comparison to the NEUROBAT standard heating controller (-77 [MJ]). The following remarks can be made:

  - The internal gains are inferior in comparison the standard NEUROBAT heating controller due to the occupation (-109 [MJ]), but the gains du to the artificial lighting are superior (+36 [MJ]).

  - The solar gains are superior due to the fact, that the blind position is not modified during the user absence before 10h30 and between 14h and 15h30.

The NEUROBAT heating controller enables to reduce the energy consumption and to optimize the user comfort during the room occupation in comparison to the commercial heating controllers. Moreover the NEUROBAT heating controller provides the possibility to fix a non-nominal user schedule with an optimal comfort for the user with regard to an optimization of the energy consumption.

Figure 40 summarizes the global energy consumption results with regard to different seasons of a full heating season. The figure stresses the fact, that the NEUROBAT heating controller works especially efficient during the in-between seasons with a variant meteo data, such as autumn and spring.

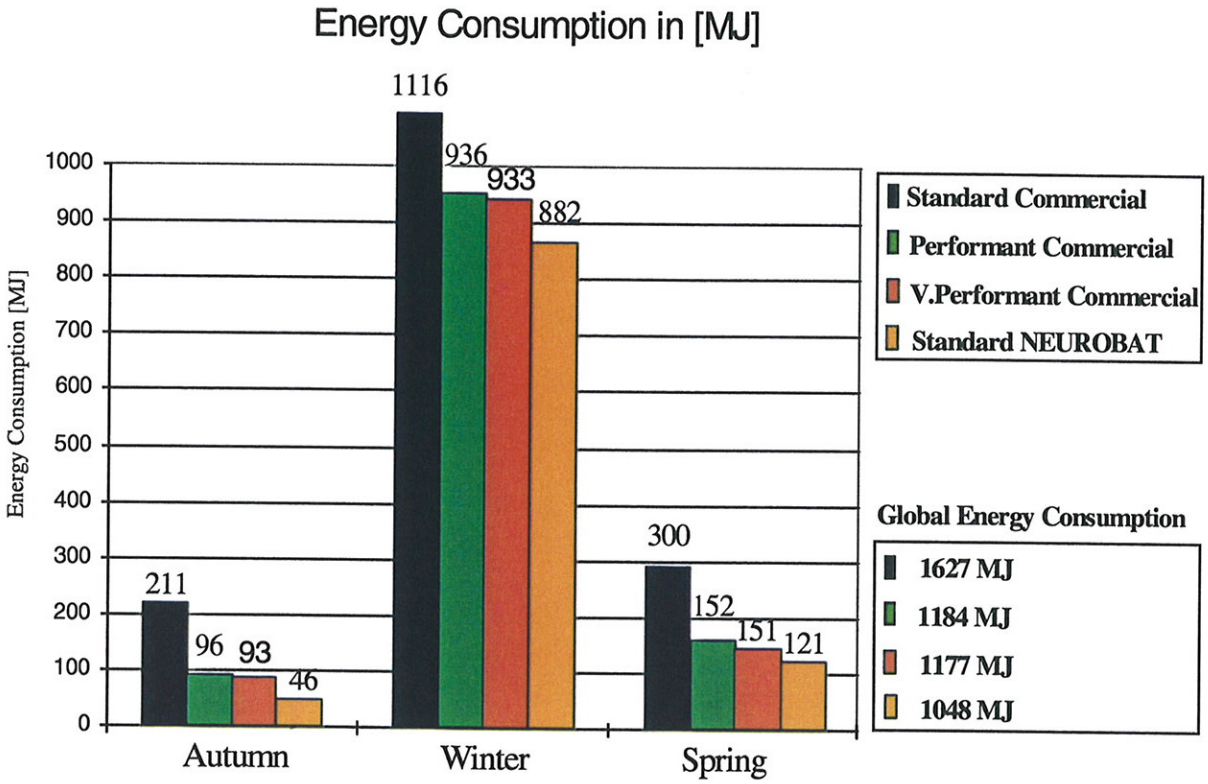

Figure 40: Simulation results on the energy consumption of the NEUROBAT simulation phase.

Heating Distribution

In the following the behaviour of the different heating controller versions are examined. Figure 41 to Figure 43 show the average heating power distribution per daily hour for each of the heating controller versions for different heating periods. This method enables to assess the heating controller behaviour:

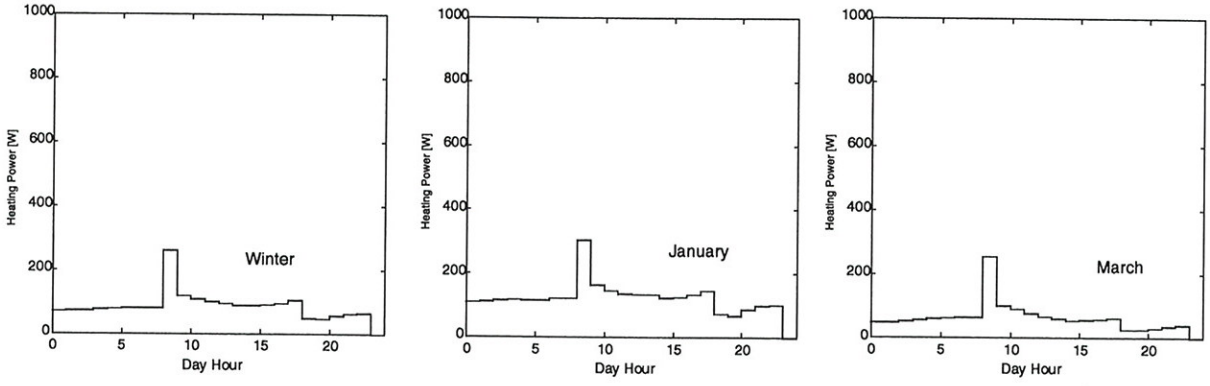

Figure 41: Mean value of the heating power distribution of the standard commercial heating controller in function of the daily hour.

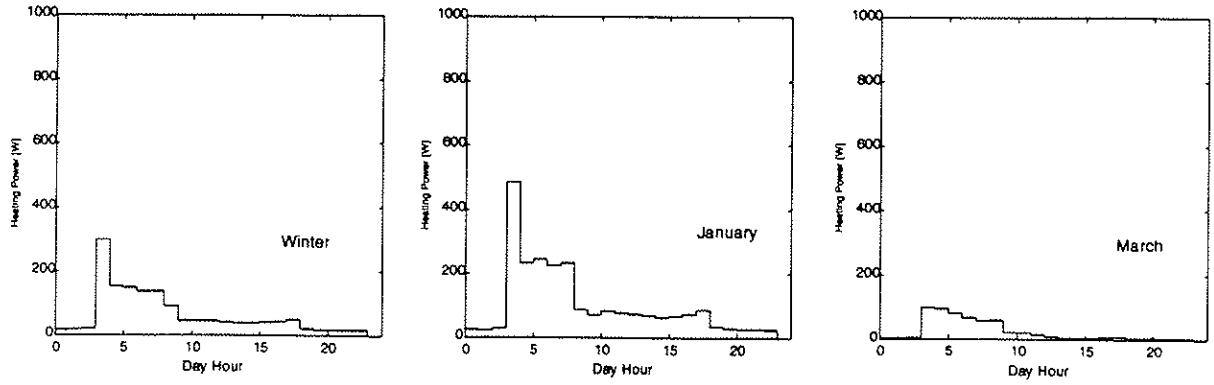

Figure 42: Mean value of the heating power distribution of the performant commercial heating controller in function of the daily hour.

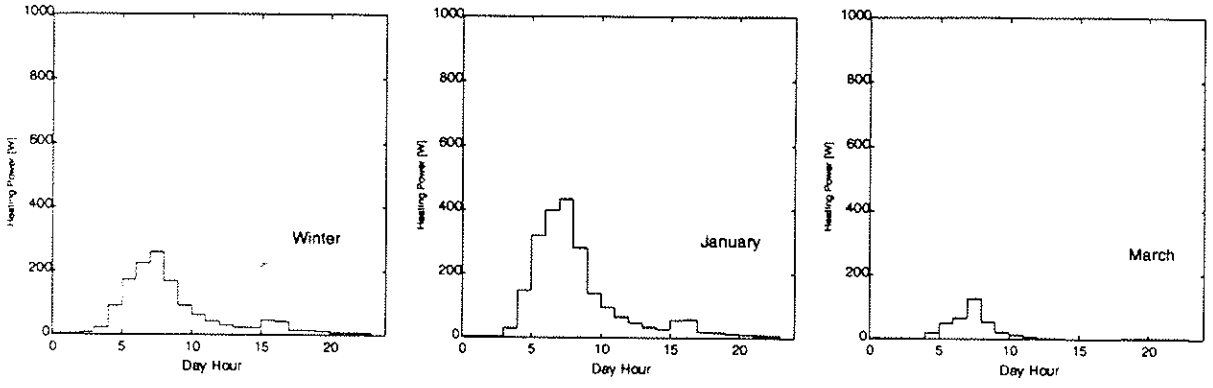

Figure 43: Mean value of the heating power distribution of the standard NEUROBAT heating controller in function of the daily hour.

The following remarks can be given with regard to Figure 41 - Figure 43:

- The standard commercial heating controller provides the maximum heating power at the beginning of the comfort period. The rest of the day the heating power distribution is nearly constant with no hourly distinction. No optimisation exists with regard to the user schedule.
- The performant commercial heating controller distributes the maximum of the heating power during the morning period of 3h-4h in order to anticipate the comfort period. The heating distribution is strongly reduced during the afternoons.
- The behaviour of the NEUROBAT heating controller shows its predictive features. During the winter period, the heating power distribution anticipates the comfort period but with a certain delay in comparison to the performant commercial heating controller. During the period of 10h and 15h the heating distribution is reduced with a certain heating contribution afterwards to prevent a drop-out of the room temperature.

Thermal Comfort Evaluation

The thermal comfort is evaluated with the help of PMV histograms. The following figures summarize this thermal comfort evaluation with regard to different heating periods.

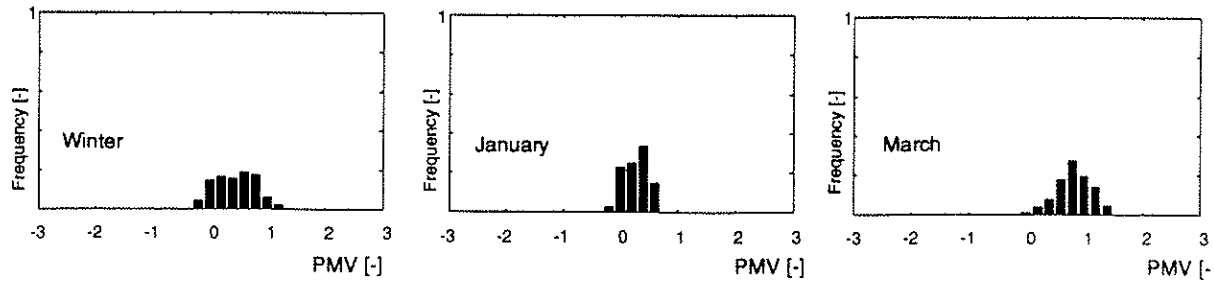

Figure 44: PMV histogram for the standard commercial heating controller during a full winter period, the month of January and the month of March.

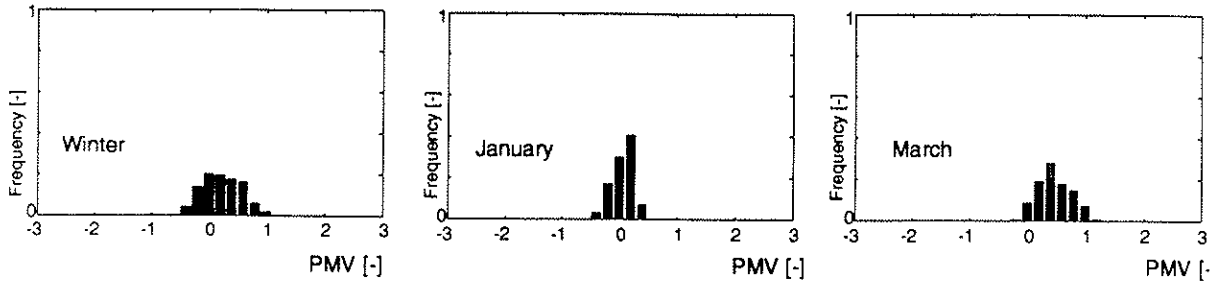

Figure 45: PMV histogram for the performant commercial heating controller during a full winter period, the month of January and the month of March.

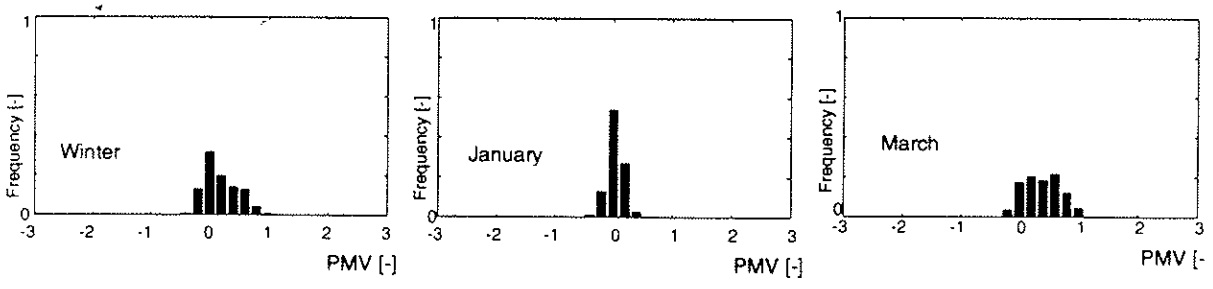

Figure 46: PMV histogram for the standard NEUROBAT heating controller during a full winter period, the month of January and the month of March.

The following remarks can be given with regard to the previous figures:

- For all heating controller versions the comfort can be regarded as sufficient except for the standard commercial heating controller, for which the PMV factor for the month of March is often bigger than 1.
- With regard to the standard commercial heating controller, the performant commercial controller optimizes the comfort considerably, since the PMV factor centres around zero, which corresponds to an optimal comfort.
- In comparison to the performant commercial heating controller, the NEUROBAT heating controller proves a better user comfort, reducing the dispersion around the optimal zero PMV factor.

5. EXPERIMENTAL TESTS

The performances of the NEUROBAT controller has been checked experimentally during the heating season 1996-1997 on an experimental site, the LESO building of the Federal Institute of Technology, Lausanne (EPFL). The building is made of 9 "thermal units" insulated one from the others and each unit has a particular facade. The South facade of the whole building is shown in the Figure 47.

Figure 47: South facade of LESO building. Room03 and Room04 used in the NEUROBAT experiment are outlined with a white frame.

The thermal unit situated in the centre ground floor includes two office rooms which have been used for the NEUROBAT experimental tests, separated by an insulated wall. The two rooms are numbered 03 (towards East, on the right in Figure 47) and 04 (towards West, on the left in Figure 47).

The characteristics of one room is given in the table below.

	Component	*Area [m2]*	*Layers (from inside to outside)*
South facade	glazing	3.77	triple glazing 4/12/4/12/4, U-value = 2 W/m2K
	window frames	2.85	U-value = 3 W/m2K
	outside wall (heavy)	3.55	concrete (14 cm) / glass-wool (10 cm) / ventilated air layer / aluminium
East Wall	wall (heavy)	14.6	concrete brick (10 cm) / glass-wool (10 cm)
West Wall	wall (light)	14.6	plaster panel / glass-wool (8 cm) / plaster

			panel
North Wall	wall (heavy)	7.5	concrete brick (10 cm) / glass-wool (8 cm)
	door	2	wood (5 cm)
Horizontal Partitions	ceiling	15.6	concrete (25 cm) / insulation (6 cm) / chape (6 cm) / plastic coating (0.5 cm)
	floor	15.6	plastic coating (0.5 cm) / chape (6 cm) / insulation (6 cm) / concrete (25 cm)

Table 20: Thermal characteristics of Room03.

The rather low heat exchange with adjacent rooms, compared to the exchange with the outside (< 5 %) allows to consider each room as a room thermally insulated from the rest of the building.

The outside facade is oriented towards South, and the ratio window area / floor area is important (24 %, see [Nyg 90]). The passive solar gains are therefore significant. The solar protections are outside textile blinds of mediocre quality, motorized.

The air change rate towards outside, when the window is closed, is around 0.1 vol/hour ([Com 91]). The window opening is up to the users.

Figure 48: Inside view of Room04.

5.1 Experimental Test Setup

The experimental setup, besides the building itself, includes two basic building blocks:

- the data acquisition system, which monitors the whole building through sensors placed at various locations in the building,
- the controller system, which implements the control algorithm using its own sensors.

5.1.1 Data Monitoring

Around 50 sensors located in the two experimental rooms and on the building roof allow a continuous monitoring of the experiment. The sensors are listed in the table below.

Location	*Sensor*	*Type*	*Accuracy*
ROOF	outside temperature [°C]	Pt 100	0.2 °C
	global horizontal solar radiation [W/m2]	Pyranometer, Eppley PSP	5 %
	diffuse horizontal solar radiation [W/m2]	Pyranometer, Eppley PSP	5 %
	global South vertical solar radiation [W/m2]	Pyranometer, Eppley PSP	5 %
	global horizontal illuminance [Lux]	Luxmeter, Licor Li-50	5 %
ROOM 03	air temperature, middle level [°C]	Pt 100, ventilated	0.2 °C
	air temperature, ceiling level [°C]	Pt 100	0.2 °C
	air temperature, floor level [°C]	Pt 100	0.2 °C
	comfort temperature [°C]	Pt 100 in black sphere	0.2 °C
	floor temperature [°C]	Pt 100, inside concrete	0.2 °C
	ceiling temperature [°C]	Pt 100, inside concrete	0.2 °C
	North wall temperature (inside) [°C]	Pt 100, surface	0.2 °C
	South wall temperature (outside) [°C]	Pt 100, surface	0.2 °C
	person counter	photoelectric cell	0.2 [p/day]
	door opening	potentiometer	5 %
	window opening	potentiometer	5 %
	door opening	switch	-
	window opening	switch	-
	inside illuminance, near window [Lux]	Luxmeter, BBC MX4	10 %
	inside illuminance, near door [Lux]	Luxmeter, BBC MX4	10 %
	blind position	ad-hoc magnet sensor	3 %
	electric power 1 [W]	electricity meter L&G MK4	2.5 %
	electric power 2 [W]	electricity meter L&G MK4	2.5 %
	water temperature, heating radiator inlet [°C]	Pt 100, immerged	0.2 °C
	water temperature, heating radiator	Pt 100, immerged	0.2 °C

	outlet [°C]		
	water temperature, boiler outlet [°C]	Pt 100, immerged	0.2 °C
	water temperature, after mixing valve [°C]	Pt 100, immerged	0.2 °C
	water flow [m3/s]	Flowmeter Aquametro, 2.5 m3/h	5 %
ROOM 04	same sensors as room 03		
ADJACENT SPACES	air temperature, main LESO hall [°C]	Pt 100, ventilated	0.2 °C
	air temperature, room 02 (East of room 03) [°C]	Pt 100	0.2 °C
	wall temperature, room 05 (West of room 04) [°C]	Pt 100, surface	0.2 °C
	floor temperature, room 103 (above room 03) [°C]	Pt 100, surface	0.2 °C
	floor temperature, room 104 (above foom 04) [°C]	Pt 100, surface	0.2 °C

Table 21: Sensors used for monitoring of experiment. Pt100 temperature sensors were calibrated. Electric power 1 corresponds to the electricity except artificial lighting; Electric power 2 corresponds to the electricity used for artificial lighting.

A data acquisition system is dedicated to the whole building. A measurement is taken every minute, and a data recording takes place every 15 minutes. The data acquisition system is connected to the LESO data network (Ethernet), which allows the computer used for the NEUROBAT experiment to read the monitored data ([VNR 96]).

5.1.2 Artificial Lighting

The artificial lighting system corresponds to a standard lighting system allowing the user to fix the artificial lighting at any lighting level.

5.1.3 Heating Controller

The algorithm which was developed in chapter 3 has been implemented on a computer, along with the other control needed by the experiment. Basically, it is made of two main blocks:

The real time control module handles the acquisition of control sensors (every minute), the control of mixing valves (every 5 seconds), the user interface to the experiment and the recording of data on disk files (every 15 minutes). This module also reads the monitored data from the VNR data acquisition system (sub-chapter 5.1.1) and rewrites the data on the same disk file as the heating controller data in such a way as to have both data available on the same file for convenience. The module has been elaborated with the measurement and automation LabView software ([Nat 97]).

The NEUROBAT algorithm module calculates, every 15 minutes, a new optimal command for the heating power, which optimizes the cost function integrated over the time horizon of

6 hours (see the description in chapter 3). The module is written in MATLAB language and is identical to the corresponding module of the simulation software ([Mat 97]).

The table below shows the sensors needed for the NEUROBAT controller, which are not identical with the monitoring sensors of Table 21:

Location	*Sensor*	*Type*	*Accuracy*
ROOF	outside temperature [°C]	Pt 100	0.2 °C
	global horizontal solar radiation [W/m2]	Pyranometer, Eppley PSP	5 %
ROOM 03 / 04	air temperature [°C]	Pt 100	0.2 °C
	radiator water inlet temperature [°C]	Pt 100, immerged	
	radiator water return temperature [°C]	Pt 100, immerged	
	presence sensor [-]	infrared L&G QPA 82.2, switch on delay 30 s, switch off delay 15 min	-

Table 22: Sensors used by NEUROBAT heating controller.

The Figure 22 shows the user interface which has been implemented with the LabView software. It displays and allows the change of file names, measuring intervals, manual operation and offers also a display of predicted quantities over the 6 hours time horizon.

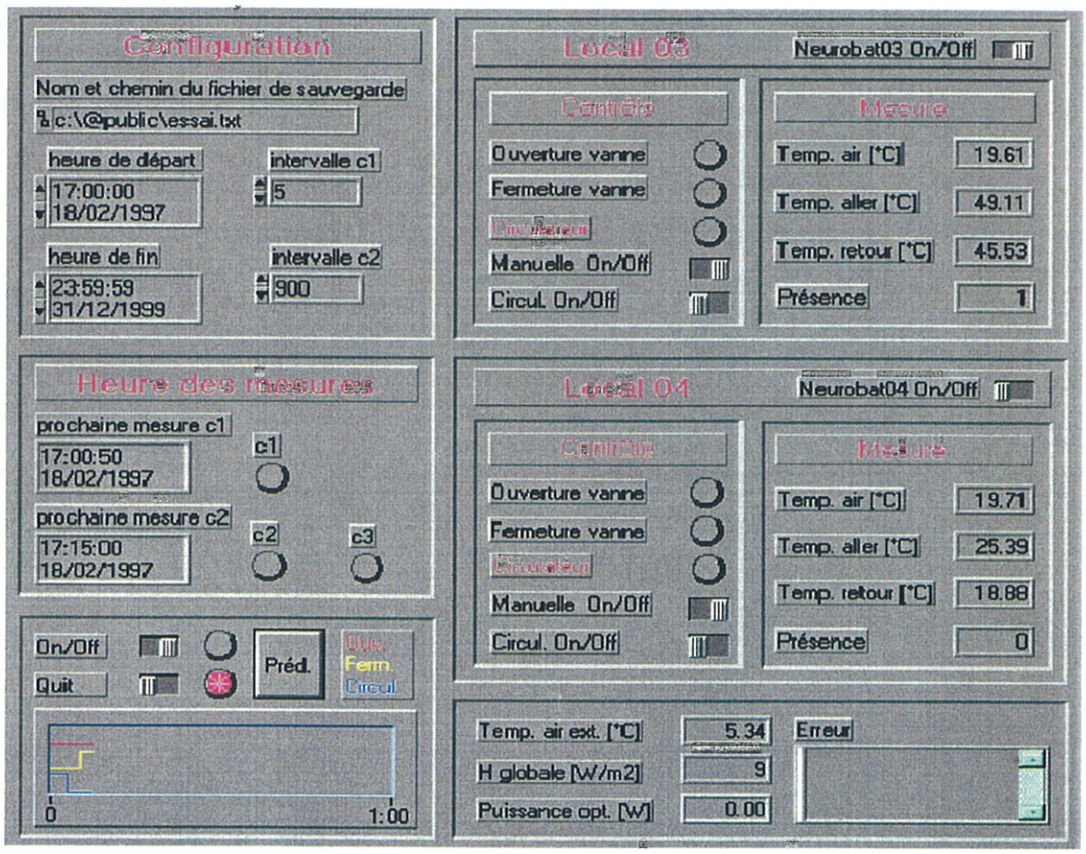

Figure 49: User Interface of NEUROBAT experiment.

Reference Controller

In order to perform a comparison, an advanced conventional controller has been implemented in one of the test rooms. To avoid experimental bias due to the difference between thermal characteristics of both rooms and between their respective users, the two controllers were exchanged at regular interval: during some weeks, the heater of Room03 was connected to the NEUROBAT controller and the one of Room04 connected to the reference controller; then during a similar time interval, the NEUROBAT controller was used for Room04 and the reference controller for Room03.

The reference controller may be described by the following characteristics and for more details concerning the control philosophy reference shall be made to the product manual [Sau 96]:

- open loop control depending on the outside air temperature,
- correction of the heating curve depending on the inside air temperature,
- automatic self-adapting of the heating curve and
- adaptive start-stop algorithm.

The complete block diagram of the whole equipment, including the data monitoring, is represented in the Figure 50.

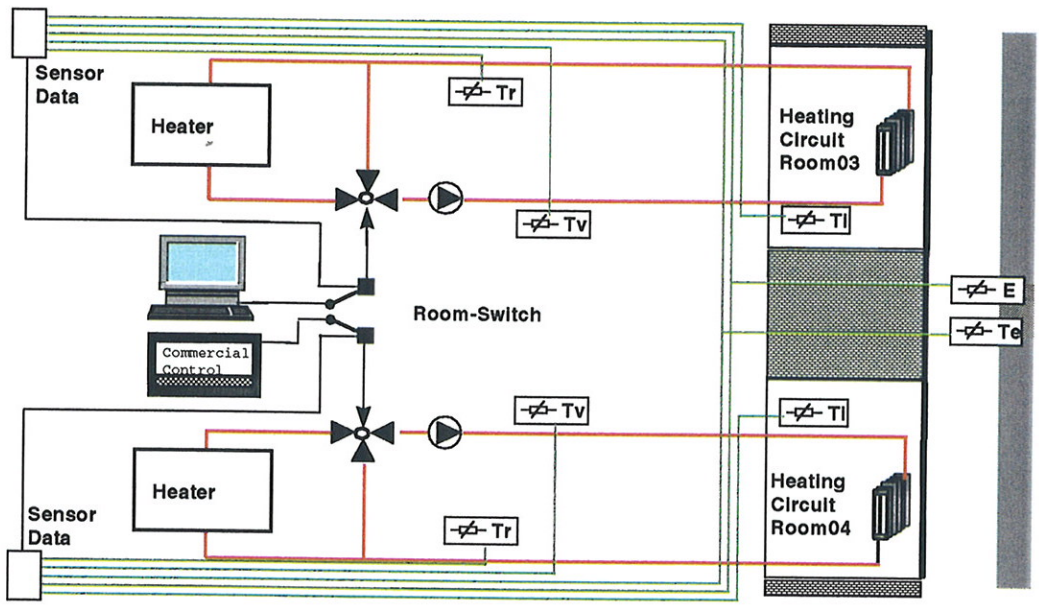

Figure 50: Block diagram of experimental setup. A switch allows to exchange the NEUROBAT and reference controller between the Room03 and Room04. Tv: Inlet temperature; Tr: Return temperature; Ti: Room temperature; Te: External temperature; E: Horizontal global solar radiation.

5.1.4 Heating Equipment

The two rooms have been equipped with conventional water radiators, with small individual boilers which simulate the traditional central heating equipment most commonly found in Switzerland. The two figures below show how the equipment has been installed. The two boilers and the reference controller are located in the cellar, just under the two rooms 03 and 04, in order to minimize the heat losses.

Figure 51: Heat production circuits located under Rooms03 and Room04. The picture shows: (1) Boilers (Electric domestic hot water boilers have been used, in order to make heat measurement easier), (2) Sensors for measurement of inlet and return temperatures, (3) Mixing valves, (4) Flow-meters, (5) Water pumps, (6) Reference heating controller.

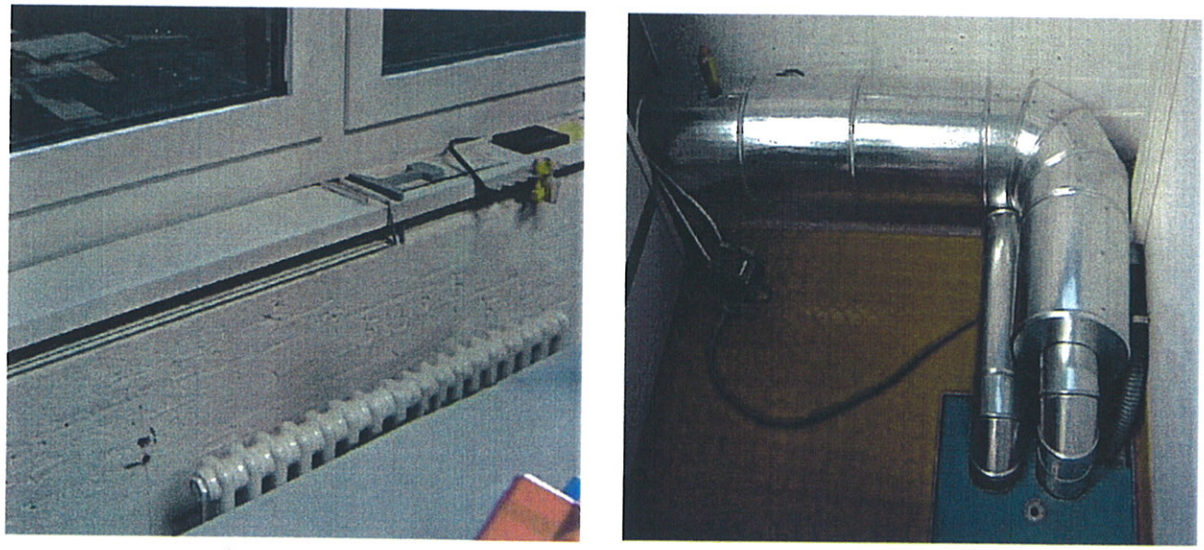

Figure 52: Left, water radiator; Right, 10 litre water stock, allowing the simulation of the distribution inertia.

5.2 Experimental Test Results

5.2.1 Qualitative Analysis

A first qualitative comparison between the NEUROBAT controller and the reference controller is done on two periods of time, respectively in winter and in mid-season. The two periods are described in the following table.

Season	Dates	Characteristics
winter	29.1.1997 - 31.1.1997	overcast sky (Gh = 300 W/m2 maximum) low outside air temperature (-1 < Te < +5 °C)
mid-season	20.3.1997 - 24.3.1997	variable solar radiation (Gh = 700 W/m2 maximum) mild outside air temperature (+4 < Te < +16 °C)

Table 23: Periods used for qualitative comparison between heating controllers.

Winter Period

During that period, the reference controller is connected to the Room03 and the NEUROBAT controller to the Room04. The weather conditions are illustrated by Figure 53. The inside temperatures are given by Figure 54, the heating powers by Figure 55, the water heating circuit temperatures by Figure 56, and the blind positions and solar gains by Figure 57 and Figure 58 below.

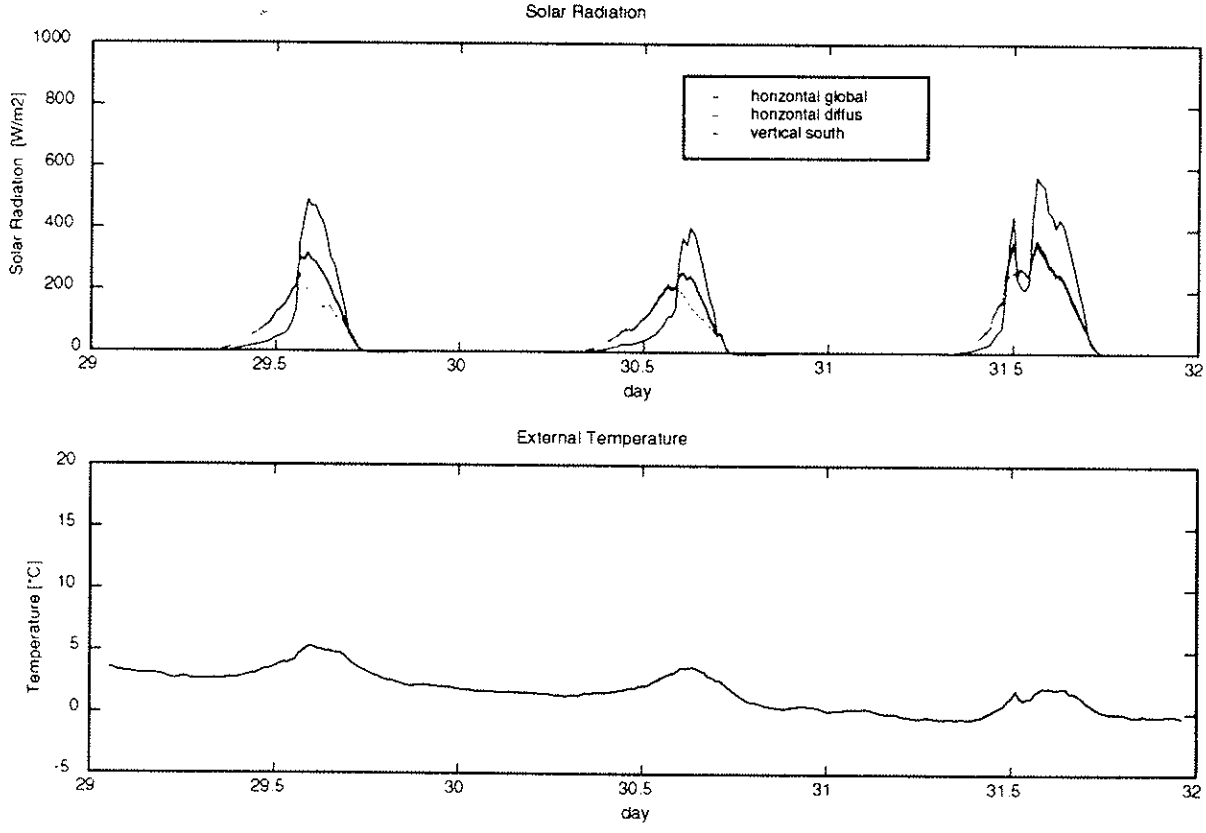

Figure 53: Weather conditions during winter period (solar radiation in [W/m2] on top, and outside air temperature in [°C] on bottom).

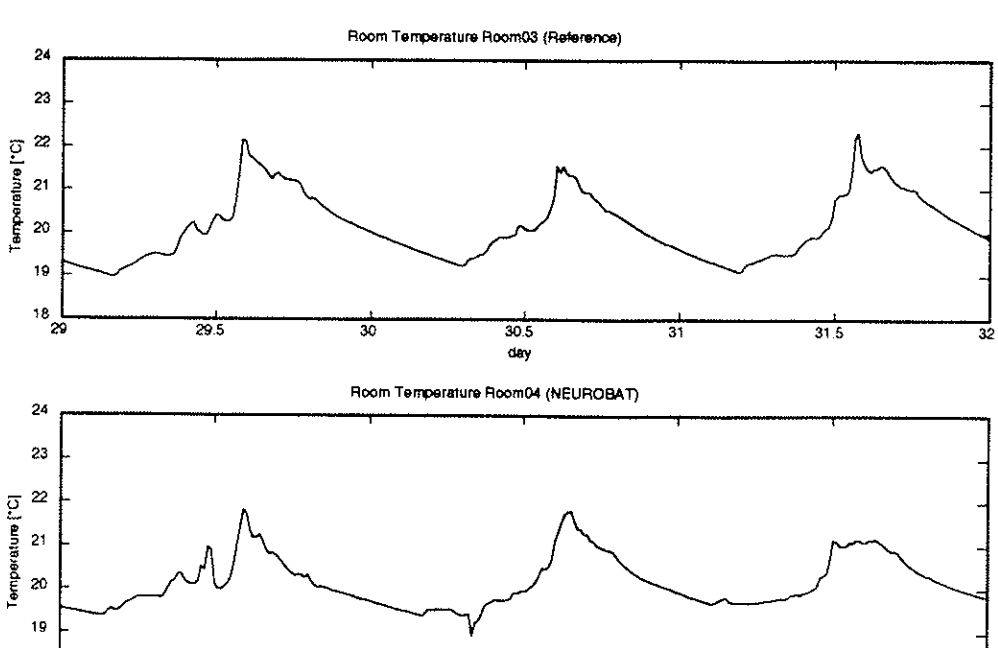

Figure 54: Inside air temperature in Room03 (reference controller) and Room04 (NEUROBAT controller).

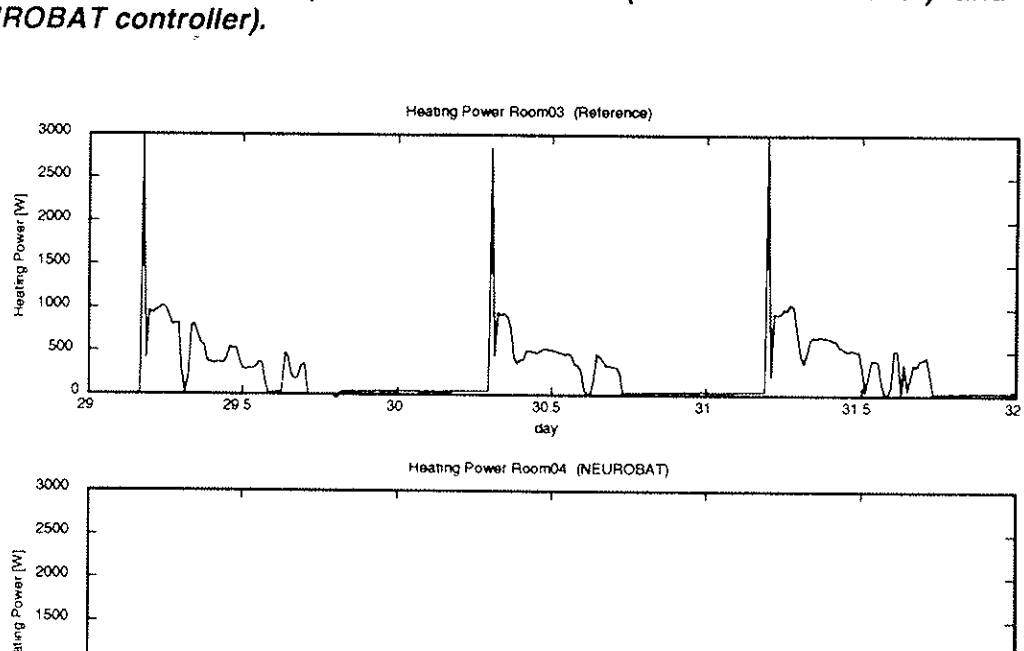

Figure 55: Heating power in Room03 (reference controller) and Room04 (NEUROBAT controller).

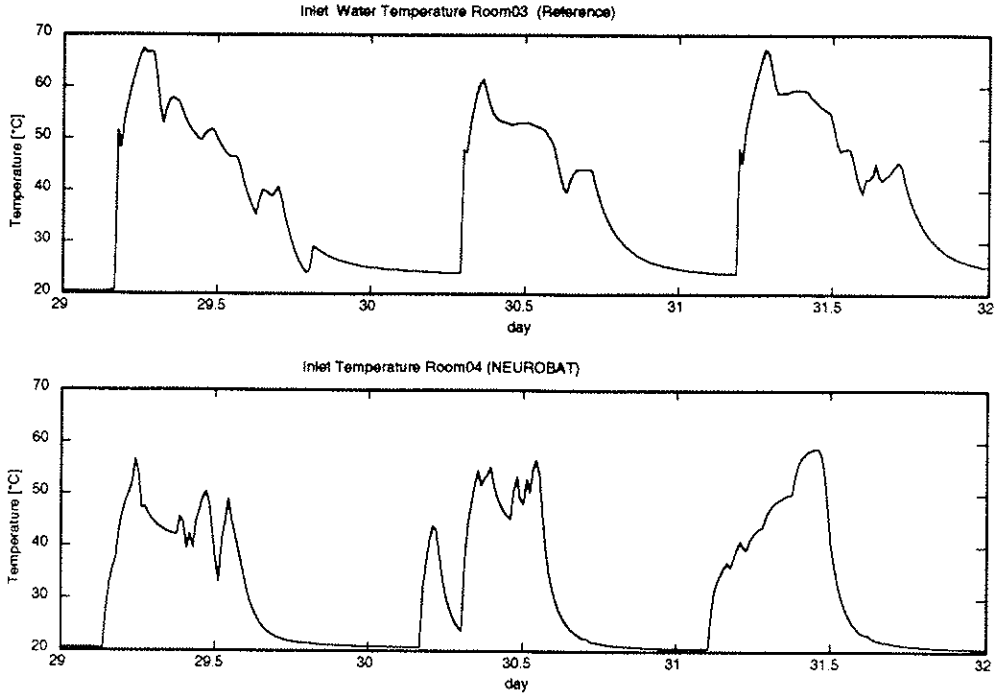

Figure 56: Hot water radiator inlet temperature in Room03 (reference controller) and Room04 (NEUROBAT controller).

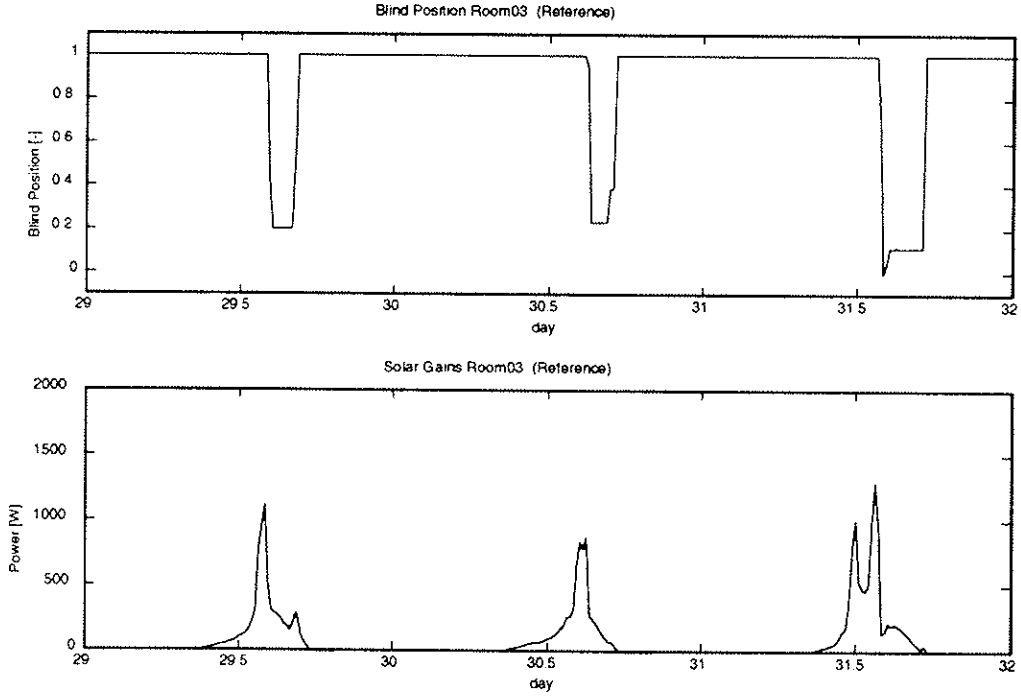

Figure 57: Blind position (chosen by the user) and solar gains in Room03 (reference controller).

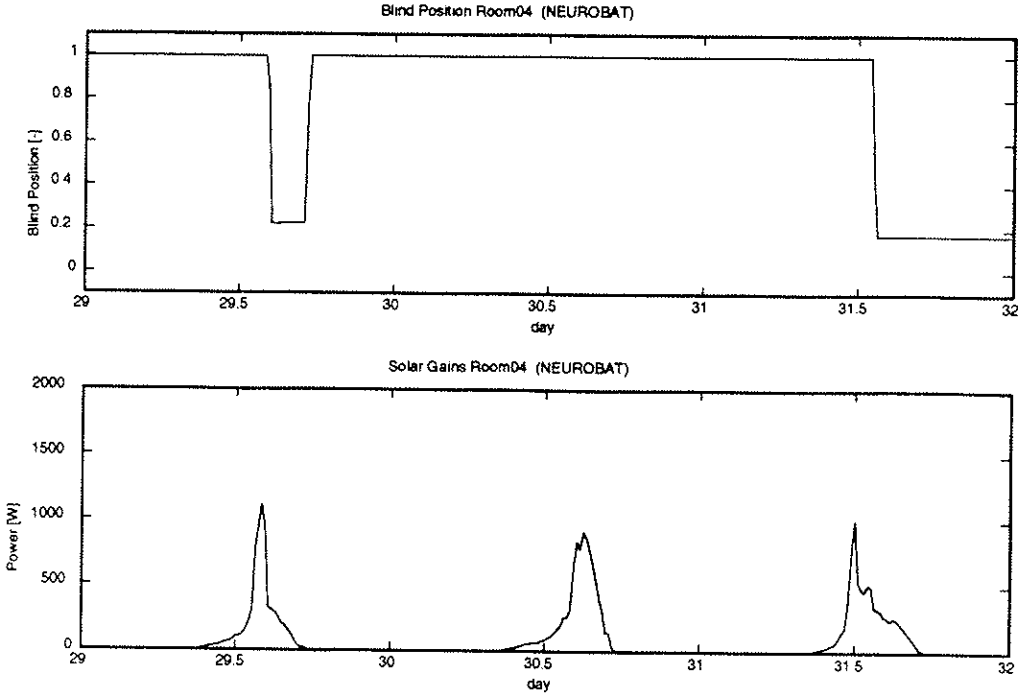

Figure 58: Blind position (chosen by the user) and solar gains in Room04 (NEUROBAT controller).

The following remarks can be made:

- During the winter period, the reference heating controller anticipates the comfort time schedule by starting the heating near at 4 am (days 29 and 31). During the afternoon, the water inlet temperature (thus the heating power) is reduced when the inside air temperature becomes higher than the setpoint temperature (i.e. when there are significant passive solar gains).
- The NEUROBAT controller has a rather similar behaviour during the winter period: the heating starts near at 3 am, then the predicted passive solar gains allow to stop the heating near 12 am. Concerning the inside air temperature, both controllers behave similarly: the measured differences are essentially due to perturbations such as variable solar gains (see Figure 57 and Figure 58), more than to a different heating control.

Mid-Season Period

During that period, the reference controller is connected to the Room03 and the NEUROBAT controller to the Room04, like during the winter period. The weather conditions are illustrated by Figure 59. The inside temperatures are given by Figure 60, the heating powers by Figure 61, the water heating circuit temperatures by Figure 62, and the blind positions and solar gains by Figure 63 and Figure 64 below.

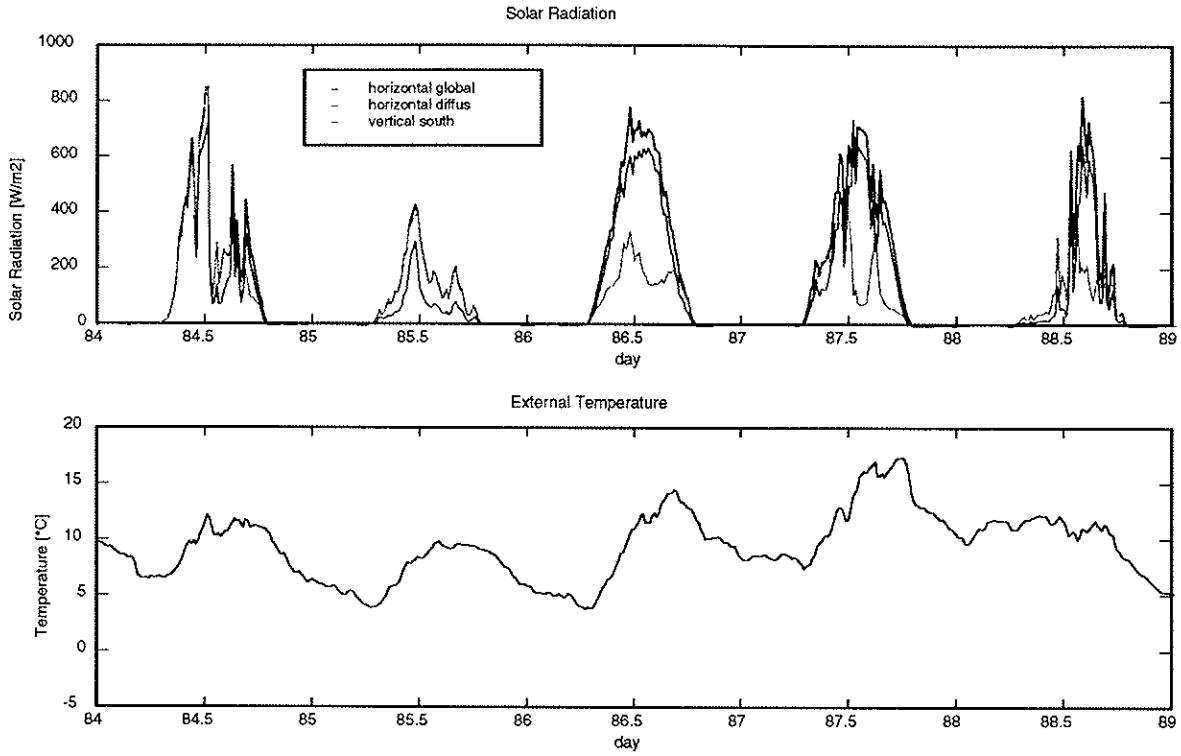

Figure 59: Weather conditions during mid-season-period (solar radiation in [W/m2] on top, outside air temperature in [°C] on bottom).

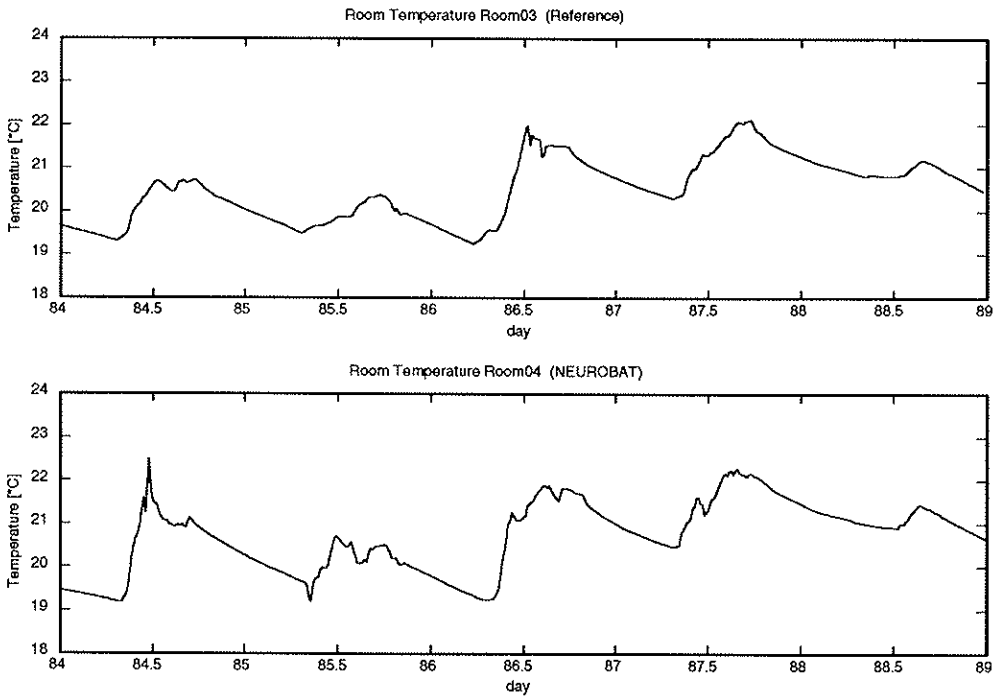

Figure 60: Inside air temperature in Room03 (reference controller) and Room04 (NEUROBAT controller).

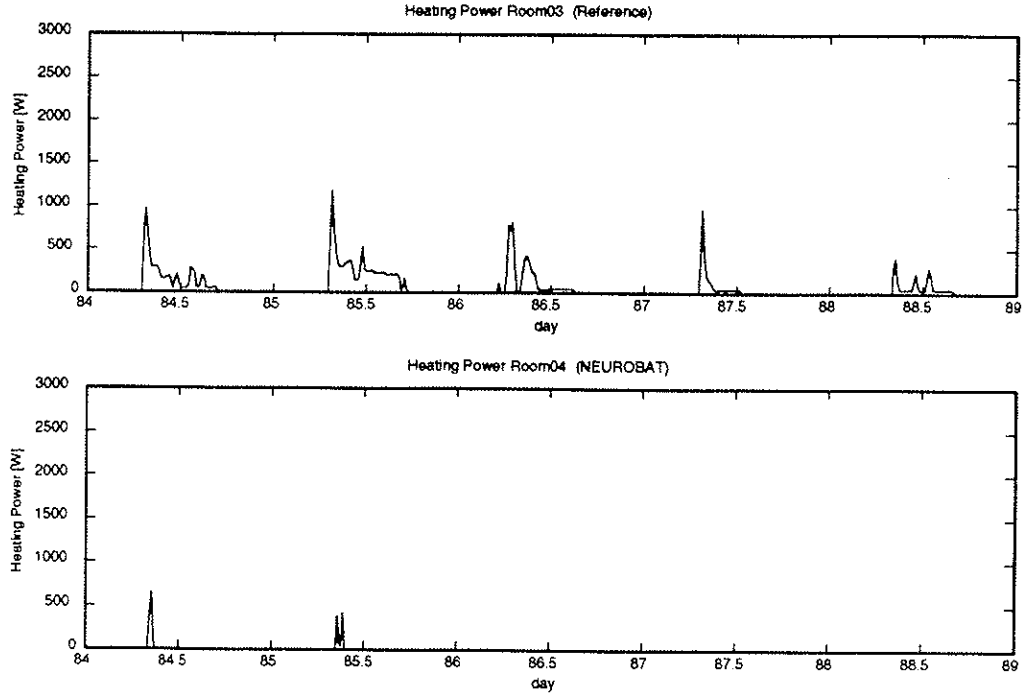

Figure 61: Heating power in Room03 (reference controller) and Room 04 (NEUROBAT controller).

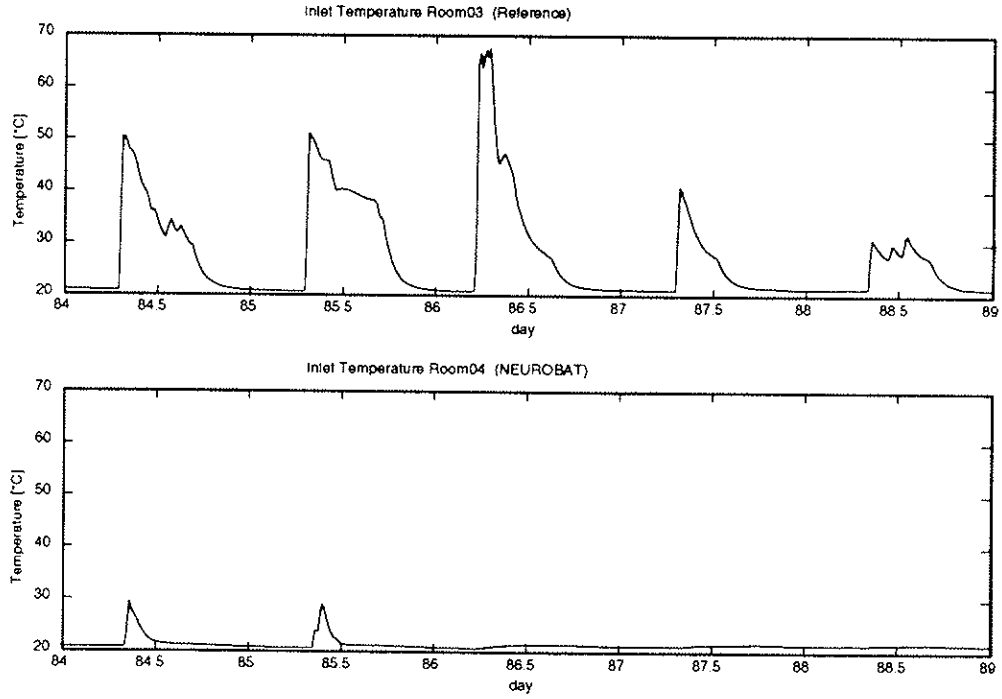

Figure 62: Hot water radiator inlet temperature in Room03 (reference controller) and Room04 (NEUROBAT controller).

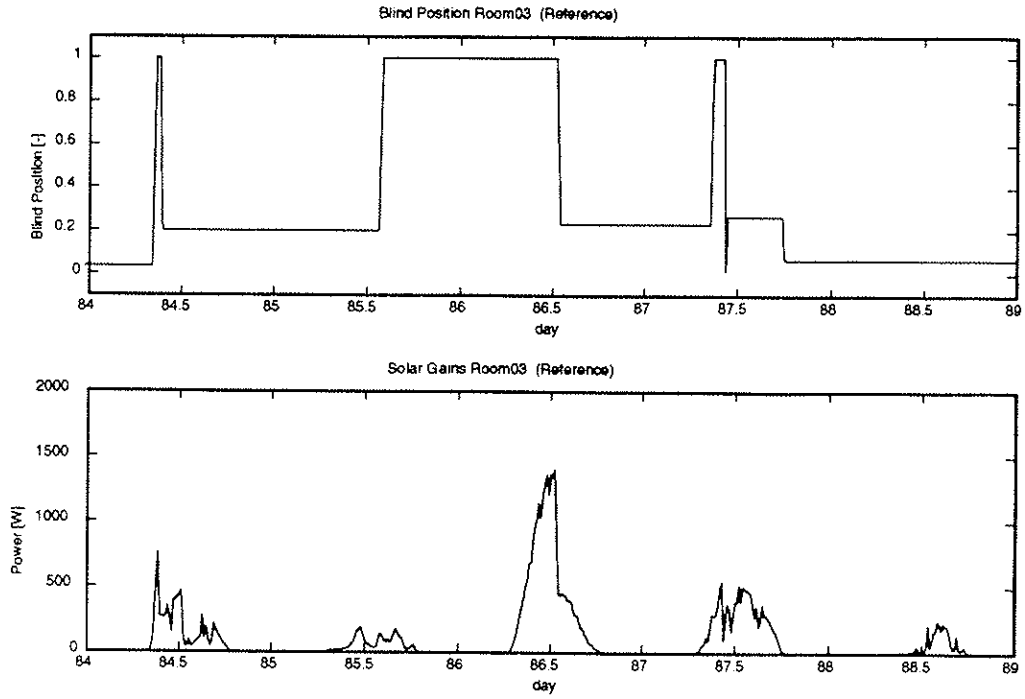

Figure 63: Blind position (chosen by the user) and solar gains in Room03 (reference controller).

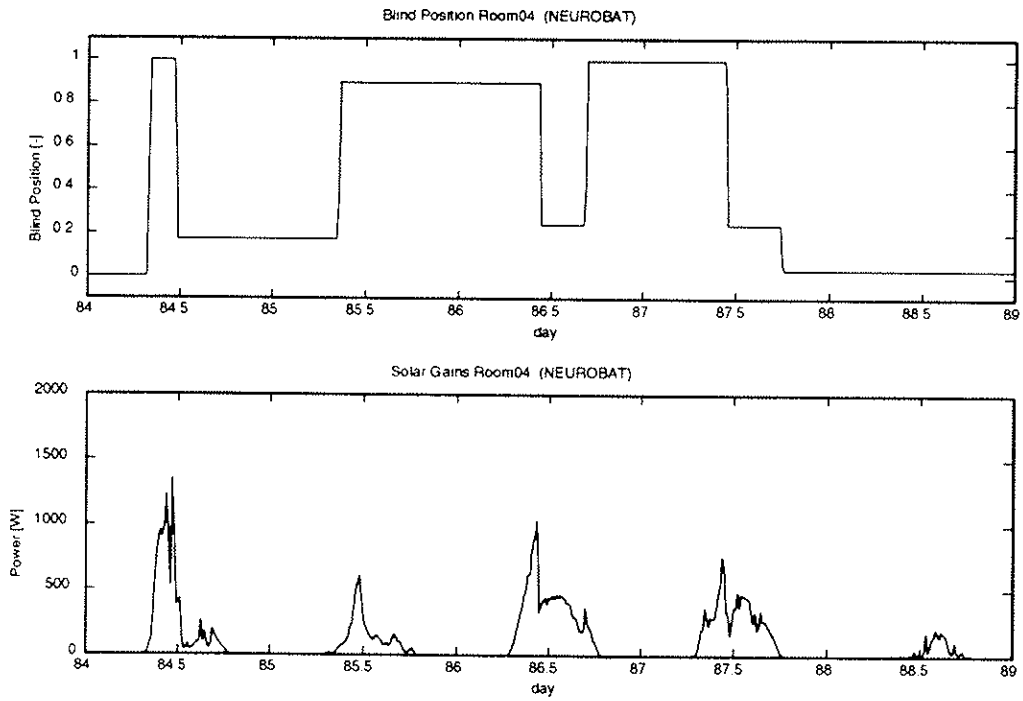

Figure 64: Blind position (chosen by the user) and solar gains in Room04 (NEUROBAT controller)

Remarks with reference to these figures:

- During the second part of the mid-season period, the reference controller gives only small heating contributions, because of the relatively high outside air temperature. During the afternoon, the heating power is strongly reduced because the inside air temperature becomes higher than the setpoint temperature.
- The NEUROBAT controller reduces the heating power to a value near to zero, even in the morning. The anticipation of free heat gains (passive solar gains) allows to avoid unneeded heating in the morning, which would be the cause of overheating during the afternoon.

5.2.2 Heating Energy Consumption Comparison

Every two or three weeks, the controllers (NEUROBAT and reference) are exchanged between the two rooms, in order to avoid a systematic bias because of thermal characteristics of rooms and users' behaviour. Therefore, we have four possible configurations:

- NEUROBAT Room03
- Reference Room03
- NEUROBAT Room04
- Reference Room04

The Table 24 below gives a summary of all the results on the heating season 1996-1997, after elimination of the days used for special experiments (heating during night, passive cooling during the week-end, etc.) and the days where the heating controller and/or the data acquisition system did not run properly. It displays the following data:

- The internal gains include electric appliances and artificial lighting.
- The solar gains are calculated from the solar radiation on a South vertical surface and the measured blind position, using the blind and window characteristics.
- The potential solar gains are the solar gains when the blind is kept completely open.
- The heating circuit losses include the losses from the boiler and additional water circuit situated in the cellar (these losses are not transmitted to the heated room but to the cellar).
- The boiler electricity is the total electric energy used by the boiler. By subtracting from that quantity the heating circuit losses, the result is the heat actually delivered to the heated room (heat, measure 1). Another possible measurement results from the temperature difference between inlet and return hot water temperatures, multiplied by the water mass flow rate [kg/s] and the water thermal capacity [J/kgK] (heat, measure 2).
- The cost function optimised by the NEUROBAT controller and integrated over one day, is tabulated independently for the thermal discomfort term (during and outside the occupation period) and for the energy term.

	NEUROBAT, Room03	*Reference, Room03*	*NEUROBAT, Room04*	*Reference, Room04*
Measured Days [days]	80.6	65.6	65.6	80.6
Occupation Hours [hours]	263.4	229.2	244.0	271.5

Boiler Electricity [MJ]	1147	1074	632	927
Heating Circuit Losses [MJ]	195	159	174	214
Heat, Measure 1 [MJ]	952	895	458	713
Heat, Measure 2 [MJ]	918	873	403	696
Actual Solar Gains [MJ]	712	522	486	753
Potential Solar Gains [MJ]	1383	975	975	1383
Energy Cost [1/day]	0.20	0.24	0.11	0.15
Discomfort Cost during Occupancy Schedule [1/day]	6.50	2.57	2.63	8.15
Discomfort Cost during actual Occupancy [1/day]	0.48	0.53	0.74	1.69
Total Cost [1/day]	0.68	0.77	0.85	185

Table 24: Global results for heating seasons 1996-1997. The difference between the two measurements of heat delivered to the room by the heater is lower than 8 % in every case.

The Figure 65 gives the most significant heat contributions, for the four configurations of the heating control system.

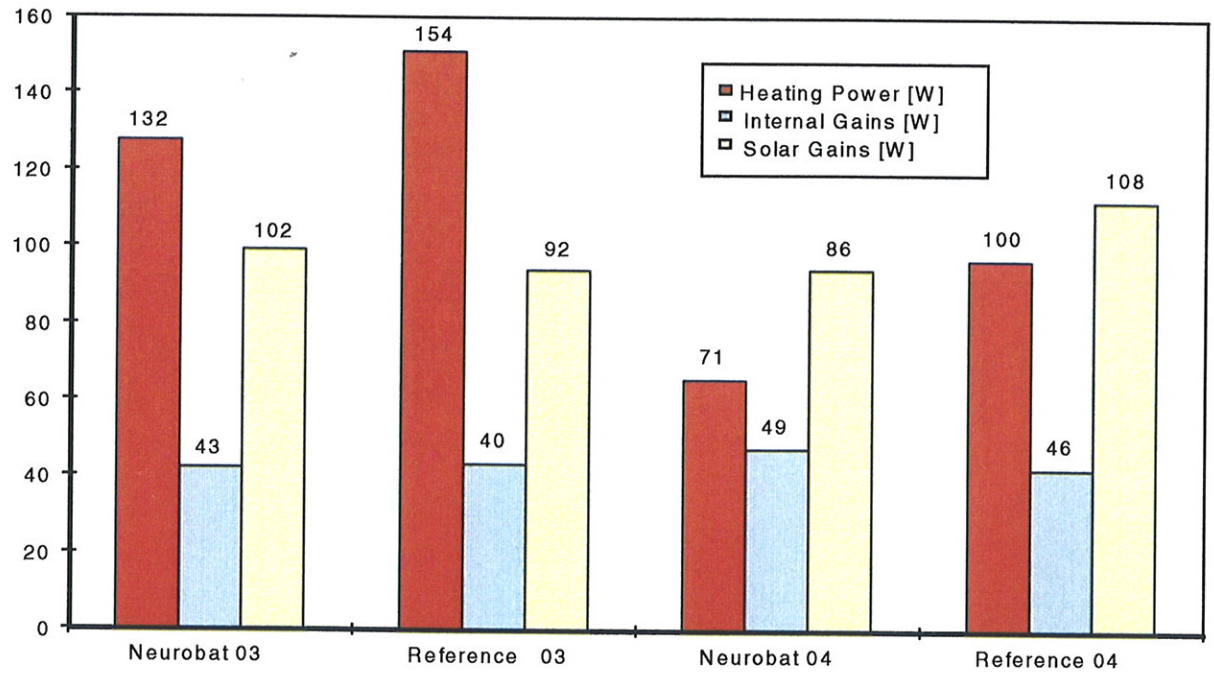

Figure 65: Most significant heat contributions for four possible configurations of the heating control system (numbers are given as average power in [W]).

From that figure, the following statements can be given:

- The heat used by the room using the NEUROBAT controller is significantly lower than the heat used by the other room, independently of the room considered.

- The Room03 has a higher heat demand than the Room04. A test with smoke has shown that the outside facade of Room03 has a leak (which has been obstructed during the heating season 1997-1998), moreover that room presents a small thermal bridge revealed by infrared thermography. Thanks to the systematic exchange between the two rooms, that disymetry has no severe consequences on the experimental results.

In order to be able to compare both systems and avoid any bias due to the different thermal characteristics or users' behaviour, the energy consumption has been summed over the whole measurement period, then again averaged:

$$Pneu = (Eneu\_03 + Eneu\_04) / (t1 + t2)$$

$$Pref = (Eref\_03 + Eref\_04) / (t1 + t2)$$

where Pneu = Average Heating Power for the NEUROBAT Heating Controller [W]

Pref = Average Heating Power for the Reference Heating Controller [W]

Exxx_03 = Energy used by the Heating Controller xxx in the Room03 [J]

Exxx_04 = Energy used by the Heating Controller xxx in the Room04 [J]

t1 = Time Period of using NEUROBAT in Room03 and Reference in Room04 [s]

t2 = Time Period of using NEUROBAT in Room04 and Reference in Room03 [s]

In order to compare the evolution of performances in function of the season, Pneu and Pref have been evaluated over the whole heating season, which results are shown in Table 25 and in Figure 66:

	NEUROBAT	Commercial Controller
Energy consumption (room03 and room04) [MJ]	1410	1627
Number of measured days [days]	146.2	146.2
Mean Heating Power Pxxx [W]	112	129

Table 25: Global results for the heating season 96/97

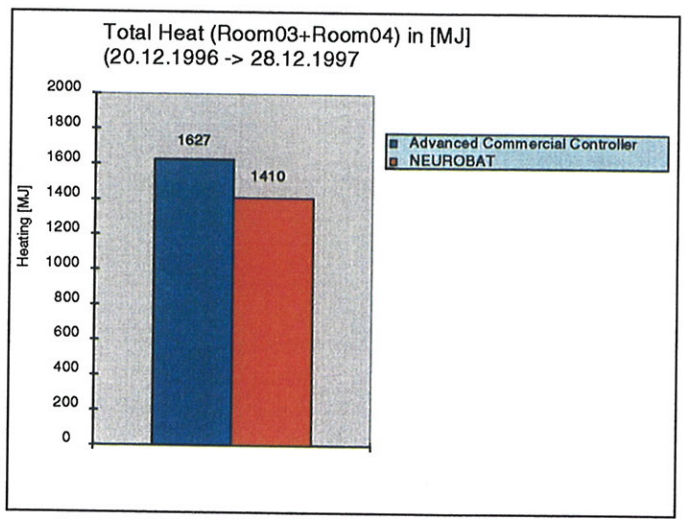

Figure 66: Average heating power over the whole heating season (period 1) and over two smaller time periods: from 10.2.1997 (period 2) and from 14.3.1997 (period 3).

It can be stated that the NEUROBAT energy consumption is 1410 [MJ], while the reference energy consumption is 1627 [MJ] for the whole heating season. This amounts to an energy saving of 13 %. An evaluation by seasons (autumn, winter, spring) shows, that for the autumn and spring season, the relative energy saving increases even further (50 to 60 %), due to the following factors:

- The solar gains at the end of the heating season are more important, and the NEUROBAT controller handles these gains more smartly.
- The prediction models of the NEUROBAT controller (weather and building) have been made better during the whole heating season.

A similar treatment has been done on the cost function. For the comparison, the discomfort cost outside the real actual occupancy has not been considered: indeed, the frequent over-heating due to the uncontrolled blind when there is no user present in the room would hide the cost variations due to the controller themselves.

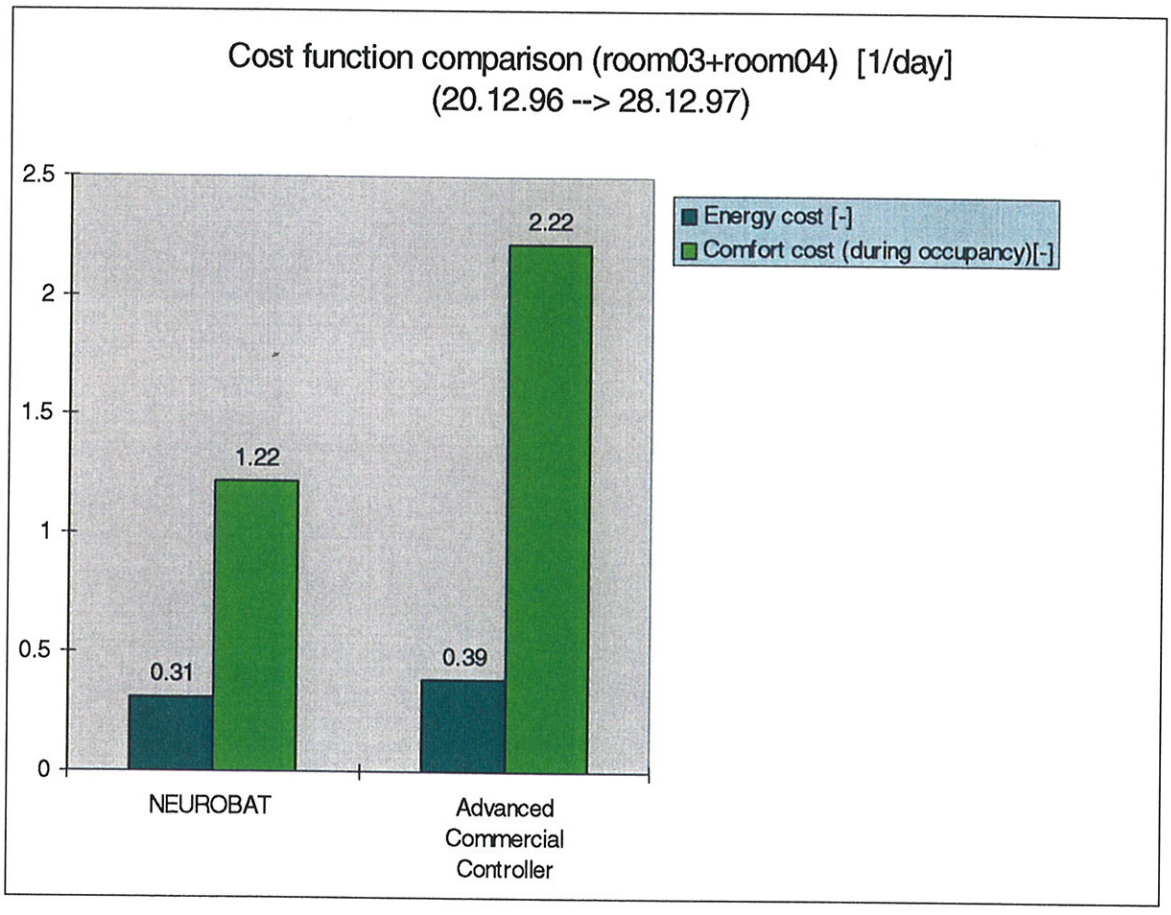

Figure 67: Cost function [1/day] for energy and discomfort (during actual occupation).

The cost function (energy and discomfort) is lower for the NEUROBAT controller than for the reference controller. It is not surprising, taking into account that the NEUROBAT controller minimises the cost function. The cost relative to the discomfort is much higher than the one relative to the energy, essentially because the discomfort cost due to overheating cannot be cancelled (there is no cooling in the rooms).

5.2.3 Thermal Comfort Comparison

The thermal comfort has been evaluated using the Fanger's model. The PMV (Predicted Mean Vote) and the PPD (Predicted Percentage of Dissatisfied people) histograms have been evaluated over the whole heating season during the actual occupation. The PMV histograms are given in the two figures below.

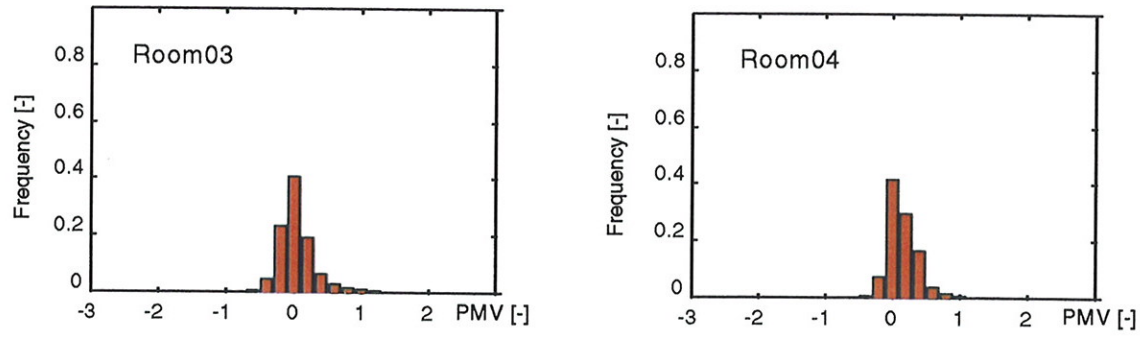

Figure 68: PMV histogram during actual occupation of room, during the whole heating season, with NEUROBAT controller.

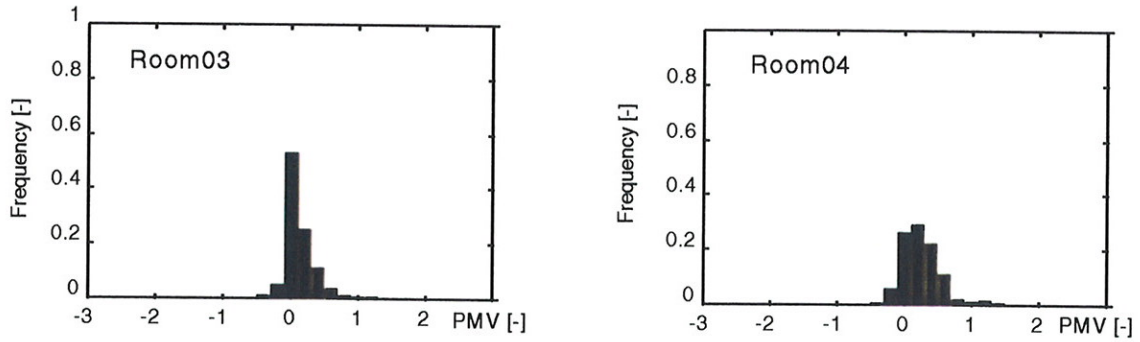

Figure 69: PMV histogram during actual occupation of room, during the whole heating season, with reference controller.

The thermal comfort is satisfactory in all the cases (the PMV is included in the interval [-0.5, +1]). Both controllers are therefore efficient and provide a good thermal comfort. Nevertheless, the NEUROBAT controller is a bit better, because the PMV histogram is more centred on the optimal value 0. It has to be noted that the over-heating is limited by the users, through window opening or blind lowering.

5.2.4 Other Aspects

The blind position during actual occupancy, in function of the solar radiation incident on the window surface, is shown in Figure 70. The blind position has clearly a stochastic nature, but it is also clear, on Figure 71, that the average position of the blind is regularly decreasing with the solar radiation. Therefore, the solar gains are not directly proportional to the South vertical radiation (Figure 72): it emphasises the interest of using a non-linear model for the building model of the controller.

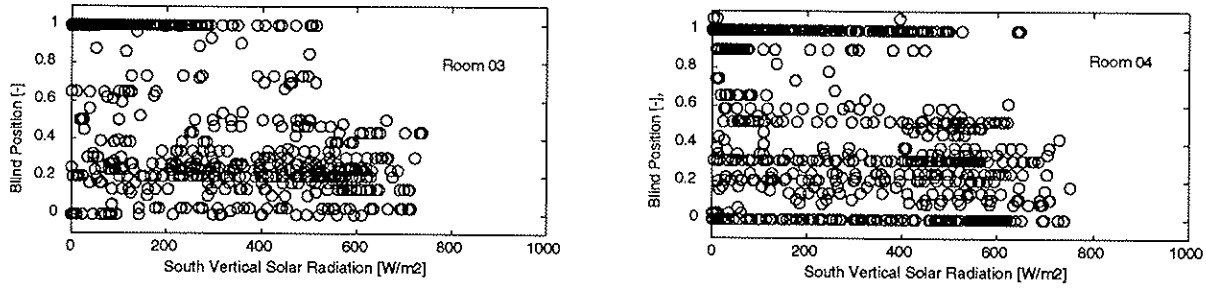

Figure 70: Blind position during actual occupation, versus solar radiation incident on the window surface.

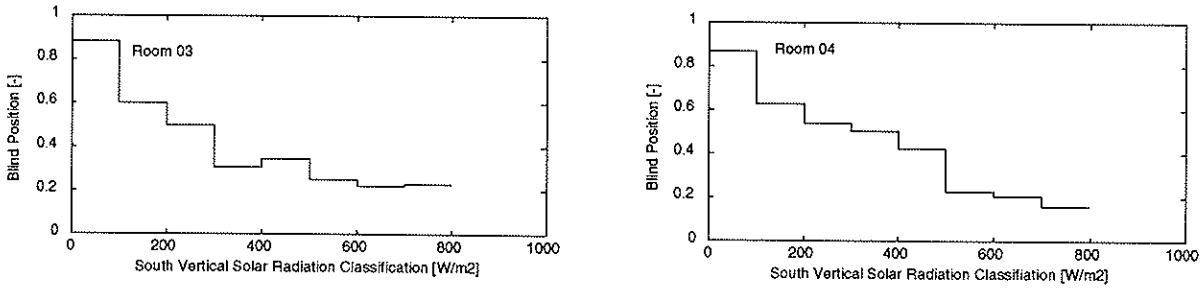

Figure 71: Average blind position histogram during actual occupation, versus average solar radiation incident on the window surface

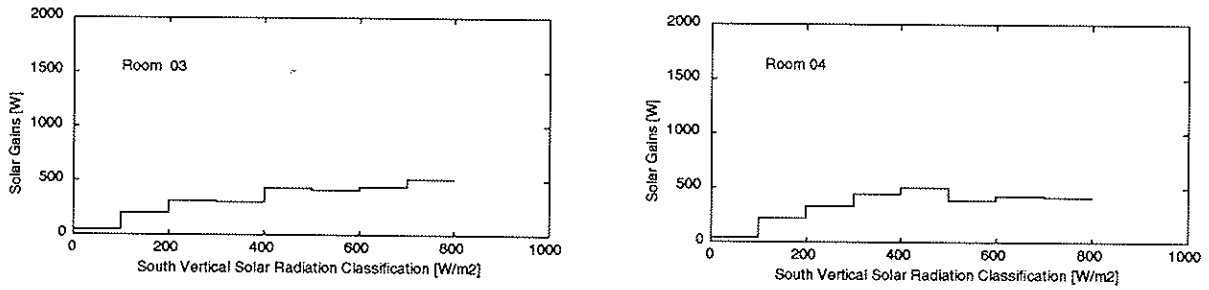

Figure 72: Average solar gains histogram during actual occupation, versus average solar radiation incident on the window surface

5.2.5 ETA Analysis

The ETA analysis allows to derive thermal characteristics of both, the building and the control system. Concerning the details of this method reference shall be made to [Bau97].

ETA diagrams for the Room03 and Room04 have been plotted, using a 4 day integration time-step (such a value is a little too low, relative to the time constant of the building, but has been used to get enough points despite the few available data; it explains the significant scattering of the points on the diagrams). The values derived in Table 26 should therefore be considered with caution.

Nevertheless, a clear trend can be shown:

- The thermal transfer coefficient H0 is higher in Room03 than in Room04 (18.2 W/K instead of 15 W/K). The leak and the thermal bridge already mentioned are probably at the origin of that discrepancy.

- In the Room03, the utilization factor of the free heat gains is higher for the NEUROBAT controller than for the reference controller (0.9 instead of 0.54). In the Room04, no derivation of ηc has been possible because of the too low number of available data points.

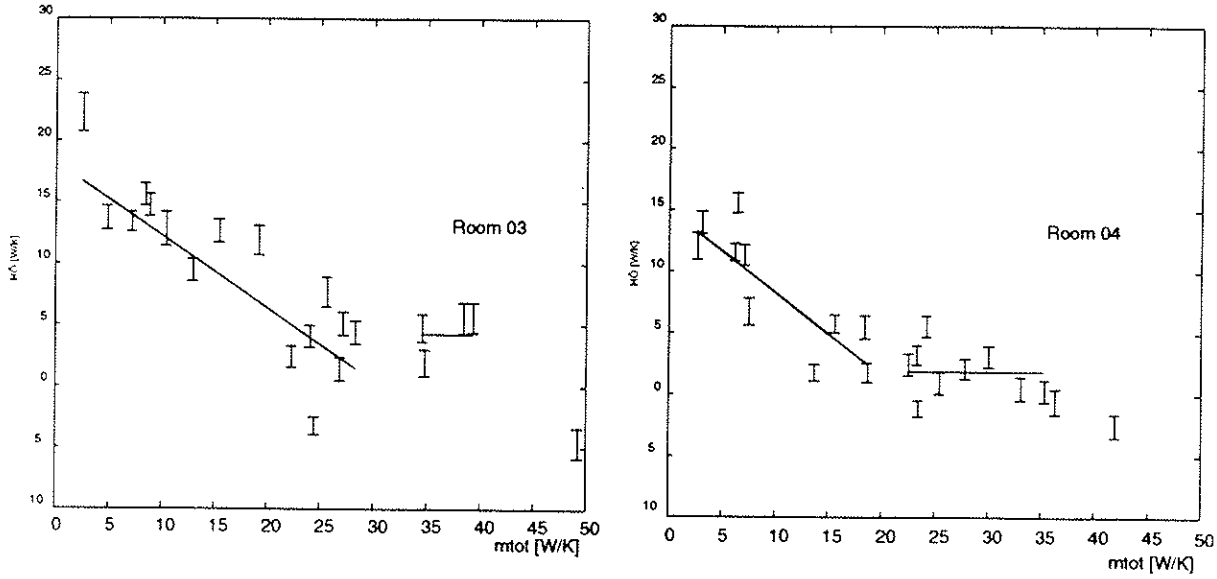

Figure 73: ETA diagram for Room03 and Room04, both control systems together: difference of thermal characteristics between both rooms is clearly visible.

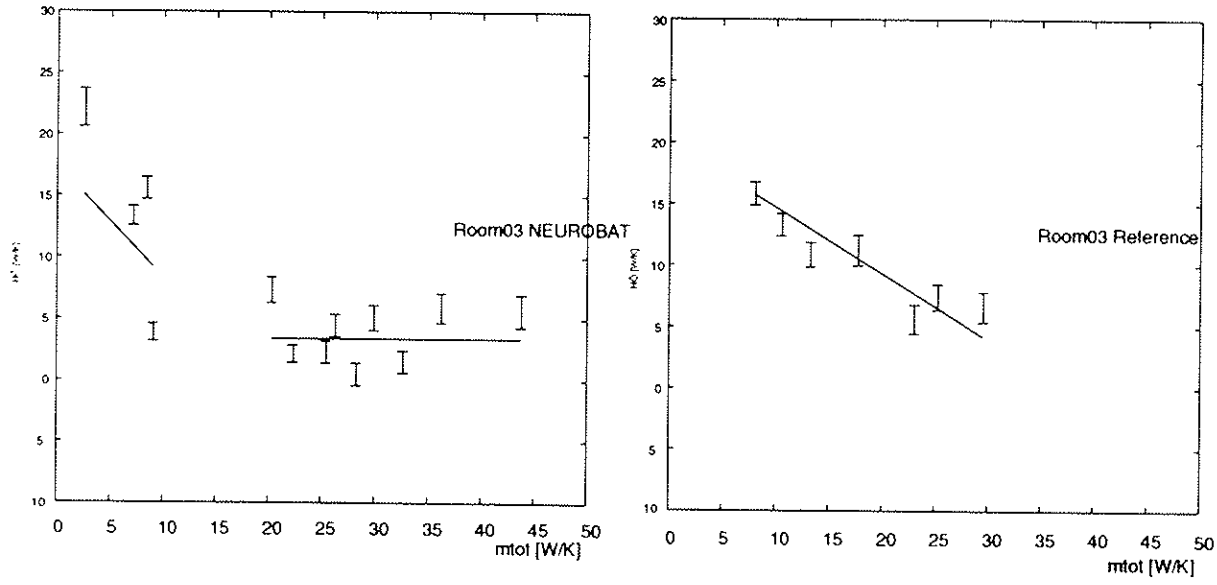

Figure 74: ETA diagram for Room03: the utilization factor of the free heat gains is higher for the NEUROBAT controller.

Heating controller and room	*H0 [W/K]*	*ηc [-]*	*H1 [W/K]*	*m1 [W/K]*
Room03, both variants	18.2 ± 0.2	0.59 ± 0.02	4.3 ± 0.6	23.6
Room03, NEUROBAT	17.4 ± 0.2	0.90 ± 0.06	3.4 ± 0.3	15.6
Room03, reference	20.1 ± 0.4	0.54 ± 0.03	undefined	37.3
Room04, both variants	15.0 ± 0.1	0.67 ± 0.02	1.7 ± 0.3	19.9
Room04, NEUROBAT	12.1 ± 0.2	0.51 ± 0.03	undefined	24
Room04, reference	16.4 ± 0.2	0.63 ± 0.02	1.8 ± 0.5	23.2

Table 26: Thermal parameters derived by the ETA analysis, for Room03 and Room04, and for the two heating controllers (NEUROBAT and Reference). The parameters ηf and m2 cannot be determined because there is no cooling

5.2.6 Experimental Results Conclusion

The measurements carried on with the NEUROBAT controller and the reference (advanced but traditional) controller confirm the simulation results. The experiment shows an energy saving of 20 % when comparing the NEUROBAT controller with the reference controller. This value is higher than the simulated results (an energy saving of 11 %). That discrepancy may be explained by several reasons:

- Both office rooms have been considered for the experimental results, with an exchange between the rooms to avoid a systematic bias due to different thermal characteristics of the rooms and different users' behaviours. But only one room is equipped with the start/stop optimization for the traditional controller, which makes the traditional controller appear not so good as if both rooms would have this optimization.
- The users have a direct influence on the energy use through window opening and blind handling. The performance of a controller which does not take the free heat gains into account will be even worse, if these free heat gains are more rejected by the user, a fact which is confirmed by the ETA diagrams.

6. 'SELF-COMMISSIONING'

6.1 General Considerations

The commissioning of the technical equipment is very important. A good commissioning can save a lot of energy and at the same time make the installation much more comfortable for the users (for instance, avoiding overheating or too high ventilation rates, which lead to a high discomfort).

Very often, the commissioning is not well done, sometimes simply "forgotten". The default values for the controllers are used, instead of better values which need a careful tuning by experts.

Thus the interest of elaborating controllers which can adapt themselves to their environment. The neural networks of the NEUROBAT heating controller represent such a capability: they can progressively "learn" the building model and the weather model, using the values measured by the controller through its normal function.

Nevertheless, when starting a heating equipment, the function must be correct from the beginning, even when it is not yet optimal. Therefore, it is necessary to initialize the models realistically, i.e. at least as well as in the case of a conventional heating controller based on a heating curve. In the following, the self-commissioning of the building model is detailed.

6.2 Initialization Model

The initialization model must fulfil the two requirements:

A. To give a fair approximation of the building thermal behaviour. For instance, the influence of the main perturbations (solar radiation, outside temperature) must be taken into account correctly.

B. To be defined without a significant calculation effort. The model should not need the introduction of a detailed physical description of the building by the user. Therefore, the choice to use a simple one-node model (see Figure 75). The model does not describe in detail the thermal behaviour of a building, but it is sufficient for the initialization step. The model includes three physical parameters:

- the thermal transfer coefficient of the building H0 [W/K],
- the equivalent area for solar gain collection Ae [m2] and
- the "effective" thermal capacity of the building C [J/K].

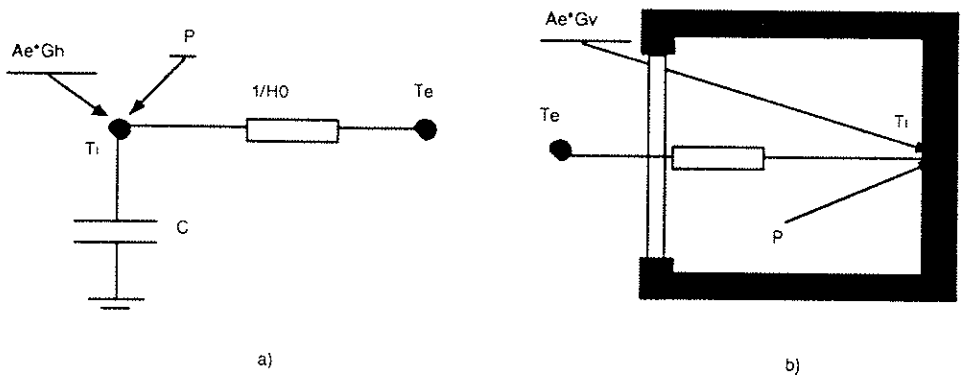

Figure 75: Simplified building model (a=electric equivalent,b=building model).

The estimation of these parameters from the building elements characteristics, although of a very simple model, requires a calculation by a building expert, which makes the commissioning already complex. Therefore, we propose to describe these parameters linguistically, independently on the building size. The proposition will allow even an unskilled practitioner to elaborate the initialization model satisfactorily.

The software POLYSUN2 ([Hub 97]) uses a one-node building model to calculate the dynamic behaviour of a small building (148 m2 heated floor area). One property of this software is precisely the linguistic description of the building characteristics. For each linguistic description, specific values for the parameters (wall structure, window area and thermal characteristics, air change rate, thermal capacity, available heating power) are determined. From all these values, it is possible to derive the three parameters which are the base of the one-node model (see above).

Thermal insulation H0 [W/K]	High 200	Standard 260	Poor 320
Thermal inertia C [MJ/K]	Heavy 57	Standard 47	Light 39
Equivalent area for solar gain collection Ae [m2]	High 31	Standard 23	Low 18

Table 27: Linguistic description of main thermal characteristics of building. The values are extracted from the software POLYSUN2 for a small size building (148 m2 heated floor area).

This table has been elaborated under the following assumptions:

- The "effective" thermal capacity is evaluated by dividing the total thermal capacity of the building by the factor 5 (only one fifth of the thickness of separation elements are used for the thermal storage under the perturbations such as the solar gains).
- The equivalent horizontal area solar gains collection is derived from the vertical equivalent areas and the ratios of monthly irradiation on vertical surfaces to horizontal surface. It can be shown that these ratios are constant for one given orientation and do not vary significantly over Switzerland. An additional factor of 0.7 has been taken into account for the energy transmission of the glazing.

The values of the Table 27 allow the elaboration of a one-node thermal model of the building. Nevertheless, the parameters are representative of a particular building of 148 m2 heating floor area. In order to generalise the parameters, an additional assumption has to be done on the building size. Namely, H0 and Ae are proportional to the outside area of the building, while C is proportional to the building volume. To get size-independent parameters, the parameters H0 and Ae are divided by the building outside area Aext and C by the building volume V. The new parameters a1, a2 and a3 are then defined in the table below:

Thermal insulation a1 [W/m2K]	High 0.80	Standard 1.04	Poor 1.28
Thermal inertia a2 [MJ/m3K]	Heavy 0.15	Standard 0.12	Light 0.10
Equivalent area ratio for solar gain collection a3 [-]	High 0.13	Standard 0.09	Low 0.07

Table 28: Linguistic description of main thermal characteristics of building

Now the parameters are general, but they do not allow the elaboration of a simple nodal network, because we have two additional parameters (Aext and V). In order to relate these

two parameters, one possible way is to use the maximum heating power Pmax, which is available, both because it is needed by the optimal controller and because it corresponds to the heating equipment, chosen by the equipment designer.

According to the Swiss standard [SIA], Pmax is designed for a temperature difference ΔTdim of 28 °C (20 °C inside, -8 °C outside) for the Swiss Plateau:

$$Pmax = H0 \bullet \Delta Tdim \Rightarrow H0 = Pmax / \Delta tdim$$

thus

$$Aext = H0 / a1 = Pmax / (a1 \bullet \Delta Tdim)$$

Another relationship between the variables is needed to solve the system. For that, an additional assumption on the building shape is done, considering a building with the following characteristics: depth = a, length = 2 • a, height = a (a characterises the building size).

From this assumption we get:

$$V = 2 \bullet (Aext / 8)^{1.5} = 2 \bullet (Pmax / (8 \bullet a1 \bullet \Delta Tdim))^{1.5}$$

6.3 Self-Learning ANN Model

The self-learning process allows the ANN building model to adjust continuously to the reality as measured by the controller's sensors. Therefore, the controller can take into account the building evolution due to several factors: for instance the seasonal variation of the air change rate, a change of the users' behaviour relative to the blind handling, or a degradation of the physical characteristics of the building. The self-learning process must conform to the following requirements:

- Progressively "forget" the rather inaccurate initialization of the simple one-node model.
- Keep enough "different" learning examples, in order to avoid convergence problems related to extrapolation.
- Allow the building model to get better when the knowledge of building thermal characteristics becomes deeper.

In order to fulfil all these requirements, we propose to use two distinct example bases, which are updated in a different way as can be seen in see Figure 76.

Global Example Base

The global base contains a uniformly distributed set of examples spread over the whole input variable space. Each input variable is discretized into a certain number of intervals. At the initialization, every possible combination of central values in each interval are input to the one-node building model and the output from the model fed back to the corresponding "cell".

During the normal function of the controller, only the cell corresponding to the current example is updated (a similar procedure already has been used for the ANN modelling of a heat pump, see [Car 94]). In such a way, examples over the whole input space are kept in the global base. For instance, the season-specific behaviour is kept from one year to the

next one, because each season corresponds to different Te and Gv and therefore to different zones in the global example base.

It has to be noted that the measured examples are not rounded off to the corresponding cell but keep their full accuracy. Moreover, some of the cells are replaced rather often, others much less frequently, and some even never, because some situations are more frequent than others.

The initialization through the one-node model is progressively "forgotten" while the examples from the controller's real function are replacing the initial examples, except some zones where the building will normally never be (for instance: Ph = 800 W, Ti = 25 °C). The correct function of the optimal algorithm can also be guaranteed, because all the zones of the input variable space are filled with examples: it avoids therefore the use of the building model in an extrapolated zone.

Temporary Example Base

The "global" example base spread over the whole input space of the model, but with a rather low example density because the discretization is limited by the available computer memory. For instance, it includes only a few example characteristics of the current situation. In order to remedy that problem, a "temporary" example base is also used in parallel; it contains examples from the last 6 weeks. Each time a new example is added (ie every hour), the oldest example is removed from the base (see Figure 76).

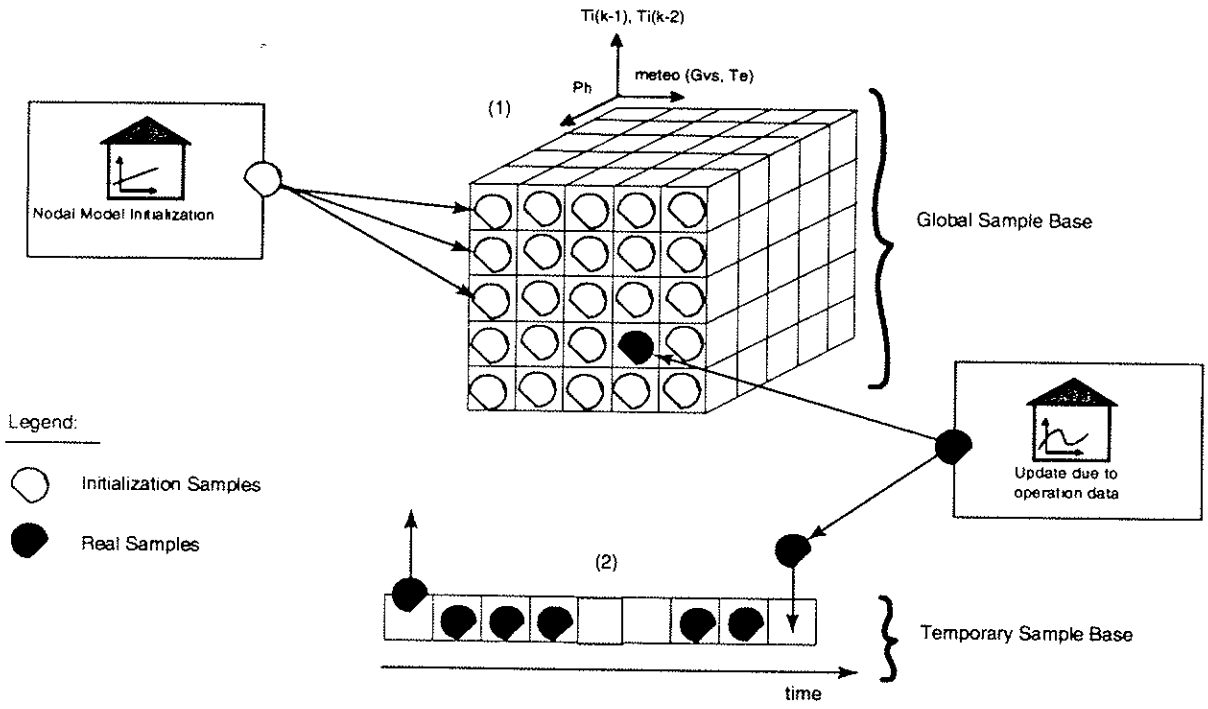

Figure 76: The learning example base is made of two distinct parts. (1) The global base contains a fixed number of examples spread uniformly over the whole input variable space; at the initialization, all examples are filled by the initialization model, then they are updated during the normal function of the controller. (2) The temporary base includes examples from the last 6 weeks of function.

6.4 Simulation Results

In order to evaluate the efficiency of the building model initialization and training, three comparative simulations have been carried out. The goal is to check:

- whether the one-node initialization model allows a satisfactory operation of the controller (during the time period where the ANN has few examples or none)
- the time needed to reach a good performance of the ANN model and
- the saving (energy and comfort) which can be done when using an self-adaptive model.

The simulation are described in the Table 29 below.

	Initial Weights	*Global Example Base*	*Weather Model*	*Building Model*	*Simulation Year*
Initial Building Model	one-node network model	initial	initial (without training)	initial (without training)	1981
Training Building Model	one-node network model	initial, then continuously upgraded	trained	trained	1981
Already Trained Building Model	trained during one year of operation	from one year of operation, then continuously upgraded	trained	trained	1981

Table 29: Description of simulations carried out for evaluation of the initialization and of the self-learning of ANN building model

The results of the simulations are given in the table below.

	Initial Building Model	*Training Building Model*	*Already Trained Building Model*
Simulated Days [days]	212	212	212
Occupation Hours [hours]	1520	1520	1520
Heat delivered to Water [MJ]	1046	1011	988
Heat delivered to Room [MJ]	949	917	896
Direct Solar Gains [MJ]	2575	2575	2575
Potential Solar Gains [MJ]	4612	4612	4612
Artificial Lighting [MJ]	430	430	430
Internal Gains (except Artificial Lighting) [MJ]	547	547	547
Daily Energy Cost, during Occupancy [1/day]	0.02	0.02	0.02
Daily Discomfort Cost, during Occupancy [1/day]	2.07	2.03	2.01

Total daily Cost [1/day]	2.09	2.05	2.04

Table 30: Simulated results (heat and cost) over the heating season 1981-1982. The solar gains are calculated from the blind position and from the blind and window characteristics. The potential solar gains are the solar gains with the blind permanently open. The cumulated cost is calculated separately for the thermal comfort and for the energy.

The Figure 77 shows the monthly heat consumption for the three models. It can be seen that after already two months the consumption of the model currently training catches up the consumption of the already trained model. After that, the monthly consumption are comparable, except in February (this situation is probably due to a rather special weather data during that month, which is not handled in an optimal way by the model because the situation is met for the first time).

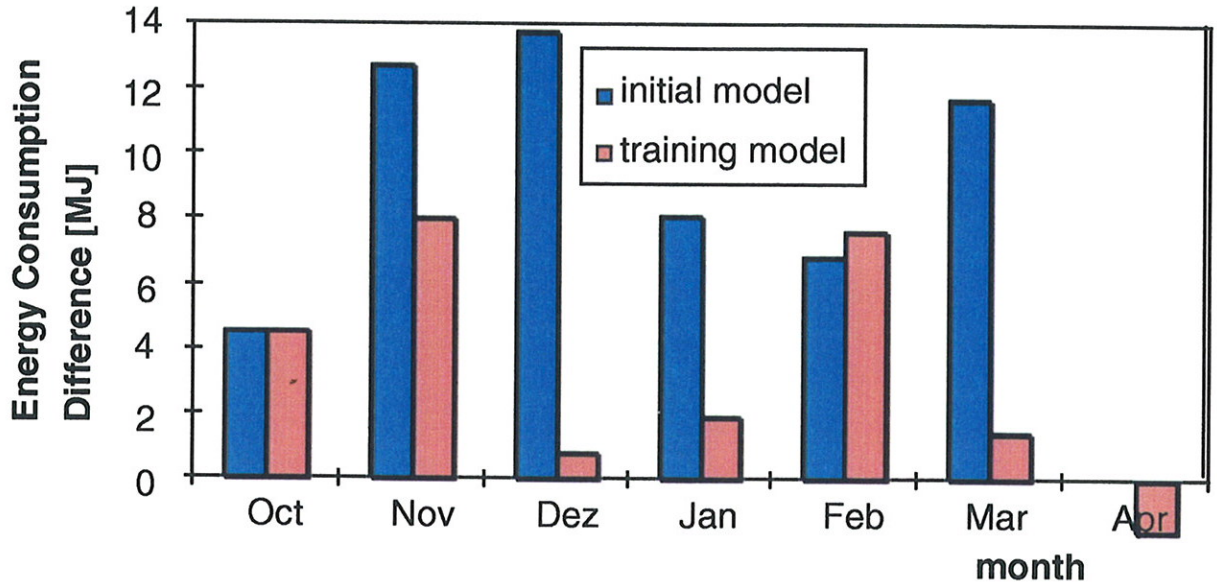

Figure 77: Difference of monthly heat consumption of the initial model and the training model, relative to the already trained model.

Over the whole year, the heating used by the already trained model (988 MJ) is significantly lower than the one used by the initial model (1046 MJ). Moreover, we can do the following statements:

- The initial model allows a satisfactory function of the controller, even without training.
- The training allows a significant reduction of the heat consumption over the whole year (6 %), even more during the mid-season (18 % in November, 13 % in March) when the passive solar gains can yield a very important part of the room heat demand.

When considering thermal comfort, the gain over the whole year is 3 % on the cumulated cost. The Figure 78 shows the monthly average values of the inside temperature during the occupation and the standard deviation around each value for the three building models.

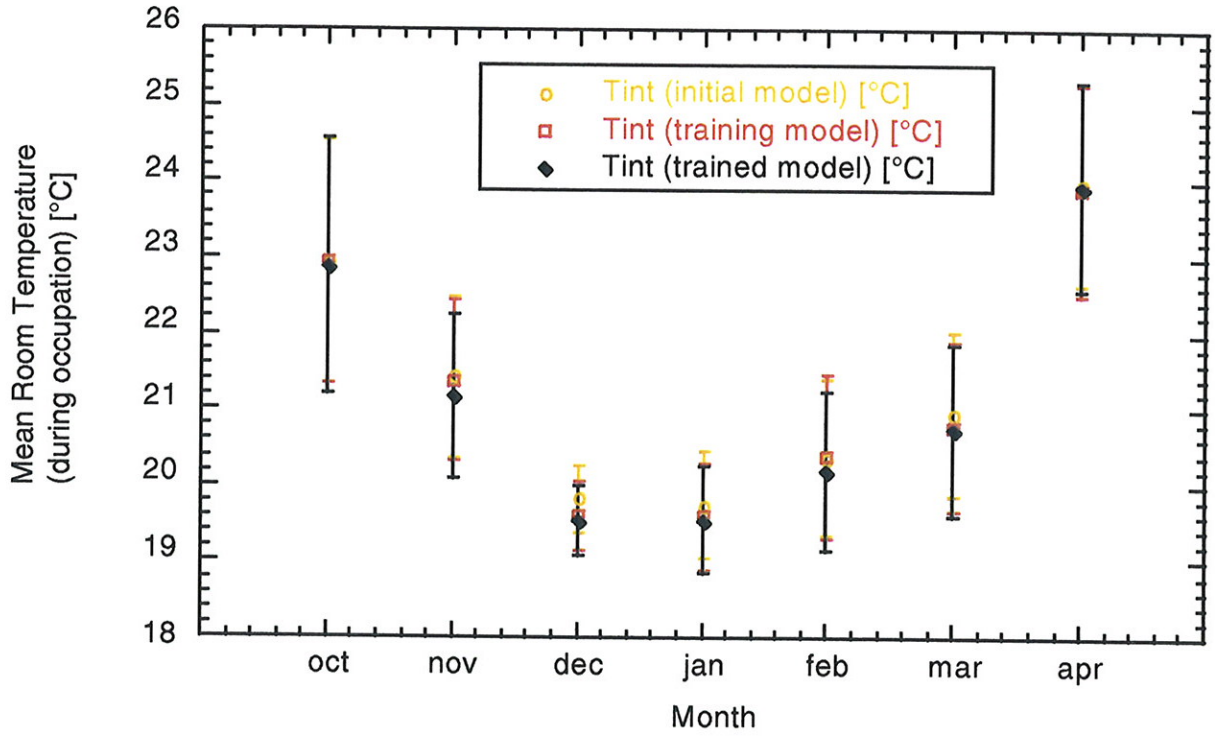

Figure 78: Monthly average inside air temperature and standard deviation (during the room occupancy) for the three building models (initial, training, already trained).

The Figure 78 shows that:

- For October and April, there is no significant difference between the three building models. Indeed, the heat consumption is so low that a small difference in the building behaviour has no influence on the thermal comfort.
- For November, February and March (mid-season), the models with training make the comfort better by reducing the average inside air temperature (less overheating), with similar standard deviations for the inside air temperature (except February for the training model, which has a similar behaviour as the initial model, see remark above).
- For December and January (winter), the average temperature of the models with training are a little lower than the initial model, and a bit under the setpoint temperature. The thermal comfort is therefore a little lower, which explains a part of the energy savings for these months. This difference can be explained by the cost function used in the optimal algorithm: the algorithm will accept a little discomfort resulting from a decrease of the heating consumption. This difference can become a little higher (towards a maximum accepted discomfort) when the model describes the thermal behaviour of the room more accurately.

7. CONCLUSION

7.1 Conclusion

The NEUROBAT research project, Phase I, has shown the interest of using bio-mimetic and neural-fuzzy predictive concepts for the control of technical equipment in buildings. The NEUROBAT project is concerned only by the heating controller, but the basic ideas can be also applied for other technical equipment (cooling, ventilation, artificial lighting, etc.).

The NEUROBAT concept is summarized by Figure 3: two self-learning artificial neural networks (ANN), one for the building model and one for the climate model, allow a prediction of the variables involved in the heating controller (outside temperature, solar radiation, inside temperature) over a 6-hours time horizon. This prediction is used by an optimal control module, which minimises a "cost function" anticipated over that time horizon, by choosing an optimum heating control sequence for the next 6 hours.

The cost function is a very important building block of the controller. It allows to make a compromise between too high energy requirements and a too high thermal discomfort. The cost function used in the NEUROBAT case is simply made of two terms: one taking into account the energy consumption over the time horizon, and one taking into account the thermal discomfort integrated over the same horizon. By giving an important weight to the discomfort term, and emphasising the high thermal discomfort by using an exponential function of the Fanger's PMV (Predicted Mean Vote) deviation from optimal comfort, the user's comfort will remain quite acceptable during the room occupancy (when it is anticipated that no user is present, the corresponding discomfort term is discarded from the cost function).

Both simulation and experimental tests have been carried out. The simulation tests have given a 11 % energy saving over a whole year, when comparing the NEUROBAT controller with a advanced conventional heating controller (using start-stop optimization and heating curve correction with the inside air temperature as well as a control parameters adaptation). The experimental tests have given an energy saving of 20 % for the first winter and mid-season period (heating season 1996-1997) and 13 % for the second heating season (1997-1998, until end of December 1997).

The experimental tests have also shown a good acceptance of the controller by the user, except at the very beginning when there were still some problems (software bugs).

The commissioning of the NEUROBAT heating controller shows also an important advantage of self-adaptive controller, by avoiding the otherwise required involvement of building experts. In the reality, a serious commissioning by good experts is done very rarely, which causes frequent problems including an over-consumption of energy or users' discomfort. A self-commissioning controller can therefore make the controller adaptation to the building and to the users' behaviour much better. It has been shown that the controller function is satisfactory from the beginning on and optimal after two months.

7.2 Outlook

At the completion of the first phase of the NEUROBAT research project, although the project was quite successful, several problems need to be investigated. One important point is the industrialisation of the NEUROBAT controller. Together with one of the industrial partners of the NEUROBAT research project, Phase I, a second project phase of the NEUROBAT project is planned, focusing on the implementation aspects of such a neuro-fuzzy predictive heating controller Nevertheless, other issues need further investigations, for instance:

- The NEUROBAT controller, as realized, is basically a one-room controller. Using the NEUROBAT controller for the heating of a whole building zone (including for instance several apartments or several office room floors) would need a modification of the algorithm in order to take into account a reference room temperatures to give only one heating command.
- The consequences of using a single room control, as an alternative to a central heating control only, needs to be investigated more carefully (sensors and actuators needed, building bus cabling, etc.). The single room control concept still remains a better concept than a common undifferentiated control, but poses some tough requirements.
- A sensitivity analysis should be carried on, relative to various parameters of the controller: for instance, the values used for the commissioning (building and climate).
- During the project, the user could not have any interaction with the heating controller. The interaction with the users, for instance using a button panel available by the user, needs to be implemented and tested.
- In the current state of the practice, the solar sensor might be even too much to include in an actual system. By chance, it can be shown that there is a good correlation between the outside temperature variations and the solar radiation data (typically, a large daily swing in the outside air temperature means that the sky is clear). Therefore, a variant of the NEUROBAT controller without the solar sensor should be nearly as performant as the basic controller.
- The presence sensor is another issue. The NEUROBAT concept requires the knowledge of the user's presence in order to find the optimal command. In the phase 1, we did not consider the self-adaptive behaviour of the controller to a variable time schedule, but instead we supposed that the rooms were occupied with a fixed hourly-weekly time schedule. A self-adaptive presence module could possibly bring further energy saving without impairing the thermal comfort when the users are present. Of course, such a function needs either a presence sensor (IR sensor) or a switch that the users toggles on or off when he/she comes into the room or leaves it (such a system can be seen in a few hotels today).
- The optimal control algorithm, as currently implemented, is quite calculation-intensive and needs important CPU resources. Alternative methods for the dynamic programming, or improvements to the application of the method in our case, should be investigated, in order to be able to run it on less powerful CPU's. The issue will be especially raised if simultaneous control of several rooms need to be handled by only one computer (it would not be reasonable to have one computer for each room).

Some of these issues would be investigated during the NEUROBAT project, phase 2. Other ones should be tackled in other research projects to extend the application of the NEUROBAT control concept.

REFERENCES

[Ast 90] K. J. Aström, B. Wittenmark: computer controller systems, Prentice Hall, 1990

[Bau 94] M. Bauer, Y. Oestreicher, J.-L. Scartezzini: Régulation prévisionnelle appliquée à une installation solaire active, Rapport final OFEN, Série de publications du CUEPE, Université de Genève, 1994

[Bau 95] M.Bauer, M.El-Khoury, N.Morel, R.Höhener: Prestudy of the NEUROBAT Project, BEW-Report, LESO, EPFL, 1995

[Bau 96] M. Bauer, J. Geiginger, W. Hegetschweiler, G. Sejkora, N. Morel, P. Wurmsdobler: DELTA, a blind controller using fuzzy logic, final OFEN Report, LESO, EPFL, 1996

[Bau 97] M. Bauer, J.L. Scartezzini: A simplified correlation method accounting for heating and cooling loads in energy-efficient buildings, Energy and Buildings, 27, 147-154, 1998

[Bau 98] M. Bauer: Gestion biomimétique de l'énergie dans le bâtiment, Thèse, Ecole polytechnique fédérale de Lausanne, 1998

[Bel 96] J. Belzer, C. Naef: Entwicklung einer BO-fördernden Benutzeroberfläche von Heizungsregelungsgeräten, Schlussbericht DIANE C3, ETH, Zürich, 1996

[Ber 76] D. Bertzekas: Dynamic programming and stochastic control, Academic press, New York, USA, 1976

[Car 94] A. Carrière, A. Cela, Y. Hamam: Thermal systems simulation using neural network, CISS - First Joint Conference of International Simulation Societies Proceedings, 371-376, Zürich, 1994

[Com 91] R. Compagnon, J. M. Fürbringer, M. Jakob, C. A. Roulet: Mesures d'échanges d'air entre les locaux et avec l'extérieur, Rapport final projet NEFF 339.2, Laboratoire d'énergie solaire et de physique du bâtiment, Ecole polytechnique fédérale de Lausanne, 1991

[Cun 88] Y. Le Cun, J. S. Denker, S. A. Solla: Optimal Brain Damage, Advances in neural information processing systems, 2, 598-605, IEEE Conference on Neural Information Processing Systems, 1988

[Cur 94] P.S. Curtiss, J.F. Kreider: Energy Management in Central HVAC Plants Using Neural Networks, ASHRAE Transactions, Vol.100-°1, 1994

[Dou 95] A.I.Dounis, M.J.Santamouris, C.C.Lefas, A.Argiriou: Design of a Fuzzy Set Environment Comfort System, Energy and Buildings, 22, 81-87, 1995

[Duf 74] J. A. Duffie, W. A. Beckman: Solar Energy Thermal Process, John Wiley & Sons, 1974

[Fan 81] P.O. Fanger: Thermal comfort, R.E. Krieger, Malabor, USA, 1981

[Gau 97] Alain Gauthreau, Prévision d'ensoleillement à court terme, INSA-IRISA, Département Informatique, F-35043 Rennes Cedex, CISBAT 1997, Lausanne

[GER 84] GER-IRCOSE: Commande stochastique, rapport d'activité annexe G, Valbonne, 1984

[Gom 96] J.B Gomm, D. Williams, J.T. Evans, S.K. Doherty, P.J.G. Lisboa: Enhancing the non-linear modelling capabilities of MLP neural networks using spread encoding, Fuzzy Sets and Systems, 79, 113-126, 1996

[GRE 85] GRES/LESO-PB/EPFL: LESO, Dossier systèmes, rapport technique, projet NEFF 110, EPFL, Lausanne, 1985

[Hag 94] M. T. Hagan, M.B. Manhaj: Training feedforward Networks with the Marquardt algorithm, IEEE Transactions on Neural Networks, 5, 989-993, 1994

[Ham 94] S. Hammarsten: Lumped parameter models, system identification applied to building performance data, 67-90, Joint Reasearch Center, european commission, 1994

[Has 95] B. Hassibi, D. G. Stork: Second order derivatives for network pruning, optimal brain surgeon, Advances in neural information processing systems, 164-171, Denver, Colorado, 1995

[Hay 94] S. Haykin: Neural Networks, a comprehensive foundation, Prentice Hall, 1994

[Hep 94] Simon Hepworth: Hybrid Neural Control of Heat Exchangers in HVAC Plant, PhD Thesis of The Oxford Queens College, Michaelmas 1994

[Hub 97] C. Huber, S. van Velsen, U. Frei: Polysun 2.0, CISBAT 97, 440, EPFL, 1997

[Kra 98] J.Krauss, M.Bauer, M.El-Khoury, N.Morel: Neuronaler Regler in der Klimatechnik, INFRASTRUCTA, Basel, 1998

[Kre 94] J.F.Kreider, A.Rabl: Neural Networks applied to Building Energy Studies, Mc Graw-Hill, Boston, 1994

[Lan 94] Landys&Gyr: Presence detector for ceiling mounting QPA 82.2, Technical description no 5483e, Zug, 1994

[Lut 95] P. Lute, D. van Paassen: Optimal indoor temperature control using a predictor, IEEE Control Systems, 4-9, 1995

[Mat 97] Mathworks: MATLAB, a high performance numeric computation and visualization software, http:/www.mathworks.com, 1997

[Met 96] MeteoTest: Meteonorm 95, v2.0, BEW, Berne, 1996

[Nat 97] National Instruments: Labview, a graphical programming for instrumentation, http:/www.natinst.com, 1997

[Nor 94] U. Norlen: Estimating thermal parameters of a homogeneous slab, System identification applied to building performance data, 213-230, Joint Reasearch Center, european commission, 1994

[Nyg 90] A. M. Nygard: Predictive thermal control of building systems, Thèse, Ecole polytechnique fédérale de Lausanne, 1990

[Par 87] P. Parent: Optimal control theory applied to dwelling heating system, IRCOSE, Agence française pour la maitrise de l'énergie, 1987

[Rab 94] A. Rabl: Application of parameter identification in buildings - an overview, System identification applied to building performance data, 67-90, Joint Reasearch Center, european commission, 1994

[Rey 85] D. Rey: Développement et étude des performances d'une régulation prévisionnelle appliquée à l'énergie solaire passive, Travail de diplôme, dpt de Mathématique, EPFL, Lausanne, 1985

[Ric 94] V. Richalet: LADY, An identification method based on a modal state-space model, System identification applied to building performance data, 277-285, Joint Research Center, european commission, 1994

[Ros 86] M. M. Rosset: Gestion thermique optimale d'un bâtiment, Thèse, Université de Paris-sud, Centre d'Orsay, 1986

[Sau 96] Sauter: Régulateur de chauffage QRK 201, Manuel Technique, SAUTER S.A., Bâle, 1996

[Sca 91] J.L. Scartezzini, F. Bochud, M. Nygard: Applying stochastic methods to building thermal design and control, Final Report, LESO-PB, EPFL, Lausanne, 1991

[Sca 97] J.-L.Scartezzini, S.Citherlet, M.Bauer: Régulation prévisionelle de Chauffage par Téléréseau, Rapport Projet, LESO, EPFL, Lausanne, 1997

[SIA 83] SIA: Recommandation SIA 384/2, Puissance thermique à installer dans les bâtiments, Société suisse des ingénieurs et des architectes, Zürich, 1983

[Tan 94] M.Tanaka, J.Ye, T.Tanino: Identification of Non-linear Systems using Fuzzy Logic and Genetic Algorithms, IFAC System Identification, 265-270, Denmark, 1994

[Unb 87] H.Unbehauen: Regelungstechnik: Zustandsregelung, digitale Regelung und nichtlineare Regelsysteme, Vieweg Verlag, 1987

[Vis 93] J.-C. Visier, V. Paillassa, A. Marti, M.-H. Foucard: La commande optimale, un outil d'aide à la définition de stratégies de gestion, Journées RCT 93 (Régulation - Commande - Télégestion), 97-107, Sophia Antipolis, 1993

[VNR 96] VNR: Système d'acquisition de données V4.00, VNR électronique SA, Lausanne, 1996

[Zum 95] Zumtobel: Manual of the Luxmate system, Zumtobel Licht, Dornbirn, 1995